07

UTILIZATION OF ERTS-1 DATA TO MONITOR AND CLASSIFY EUTROPHICATION OF INLAND LAKES

Dr. Robert H. Rogers
Bendix Aerospace Systems Division
3300 Plymouth Road
Ann Arbor, Michigan 48107

Dr. V. Elliot Smith
Cranbrook Institute of Science
500 Lone Pine Road
Bloomfield Hills, Michigan 48103

November 1974
Final Report

Prepared for

GODDARD SPACE FLIGHT CENTER

Greenbelt, Maryland 20771

1598 A

TECHNICAL REPORT STANDARD TITLE PAGE

1. Report No.	2. Government Accession No.	3. Recipient's Catalog No.
4. Title and Subtitle Utilization of ERTS-1 Data to Monitor and Classify Eutrophication of Inland Lakes		5. Report Date November 1974
		6. Performing Organization Code
7. Author(s) Robert H. Rogers (Bendix), V. Elliott Smith (Cranbrook Institute of Science)		8. Performing Organization Report No. BSR 4168
9. Performing Organization Name and Address Bendix Aerospace Systems Division 3300 Plymouth Road Ann Arbor, Michigan 48107		10. Work Unit No.
		11. Contract or Grant No. NAS 521810
12. Sponsoring Agency Name and Address Goddard Space Flight Center Greenbelt, Maryland 20771		13. Type of Report and Period Covered Final Type III Report Sept 1972–Nov 1974
		14. Sponsoring Agency Code

15. Supplementary Notes

The Co-investigator, Elliott Smith, is a staff member at the Cranbrook Institute of Science in Bloomfield Hills, Michigan.

16. Abstract

Methodology and techniques were developed for using ERTS-1 data to monitor the state and progress of eutrophication in inland lakes of Michigan. Water quality in six test lakes was studied coincidentally with ERTS passes during spring and summer of 1973. Ground radiometry was used to find absolute reflectance and make atmospheric corrections to ERTS CCT data. Deep water and bottom features were classified and mapped by machine processing of CCT. Geometrically correct map overlays (color coded) of lakes and their watershed areas were prepared at several scales by similar methods. Positive correlations of ERTS data and ground measurements of water color and turbidity were demonstrated. The feasibility of using ERTS watershed maps as an aid to forecasting nutrient loadings to lakes was shown.

17. Key Words (Selected by Author(s))	18. Distribution Statement

19. Security Classif. (of this report)	20. Security Classif. (of this page)	21. No. of Pages	22. Price*

PRECEDING PAGE BLANK NOT FILMED

ORIGINAL PAGE IS OF POOR QUALITY

PREFACE

OBJECTIVES OF THE PROGRAM

The objective of this experiment is to demonstrate the feasibility of ERTS in measuring the state of eutrophication of inland lakes as a broad survey monitor. Specific objectives are:

a. Determine the effectiveness of ERTS in resolving small lakes and lake features, as a function of their size, shape, depth, color, and shore definition.

b. Determine differences in the color and reflectivity of lakes by analysis of multispectral data from ERTS, aircraft, and ground monitors.

c. Correct ERTS data for solar and atmospheric effects so that resulting measurements are directly comparable with ground measurements.

d. Describe physical, chemical, and biological variables which influence water color and turbidity within lakes.

e. Correlate these color-related variables with the general trophic condition of each lake, considering additional water quality indicators.

f. Classify and map land use and cover in lake watersheds to provide a basis for predicting further eutrophication in lakes.

g. Evaluate ERTS-1 as a broad survey monitor of eutrophication (its extent and rate) in inland lakes.

SCOPE OF WORK

The final scope of the project was much greater than originally planned. Techniques were demonstrated for mapping lake watershed features as well as for detecting parameters of lake water quality. The experiment examined the utility of ERTS monitoring as an aid to forecasting the trophic quality of lakes in addition to assessing its current status.

CONCLUSIONS

Techniques were developed for using ERTS-1 to monitor eutrophication in inland lakes of Oakland County, Michigan. Water turbidity and color, phytoplankton, chlorophyll, and nutrients were surveyed in six lakes (40 to 1280 acres) concurrently with ERTS passes. Lakes were characterized by ground truth according to trophic level and enrichment potential. Lake and watershed features of one acre or larger were detected in ERTS bulk imagery. Some definition of shallow areas and deep water masses were noted in density-sliced imagery, particularly in Bands 4 and 5. Bands 6 and 7 were best for defining land-water boundaries and surface vegetation.

Removal of atmospheric parameters (atmospheric attenuation, and scattering from atmosphere) from ERTS radiance measurements permitted the absolute reflectance of lakes to be determined. The atmospheric parameters were derived from ground measurements with the Radiant Power Measuring Instrument (RPMI) developed by NASA for ERTS ground truth. Direct spot-reflectance measurements of the lakes were obtained with the RPMI for comparison with spacecraft measurements. The reflectance derived from spacecraft data show that: in Band 4, deep water reflectance ranges from 3 to 5.5%; in Band 5, it was 0.3 to 2.3%. Band 6 and band 7 values were near zero. Shallow water reflectance ranged up to 9% in Band 4.

ERTS measurements correlated with water turbidity and transparency. In general, expected relationships were observed: i.e., the intensity of reflectance, particularly in Band 5, varied directly with turbidity (and inversely with transparency). The ratio of ERTS Band 4 to 5 (4/5) measurements also correlated with suspended matter. Surface phenomena such as algal scums were readily detected in ERTS Bands 6 and 7.

Processing of ERTS tapes yielded an automatic classification of deep and shallow water which corresponded well with the actual bathymetry of test lakes. Further classification of deep waters resulted in a partial separation of lakes based on turbidity, i.e., a difference of 0.8 and 1.9 mg/liter particulate concentration (dry weight) was discriminated in ERTS decision imagery.

Other target categories of land use mapped by computer techniques from ERTS tapes included wetlands (swamps), untended grass, tended grass, trees, barren earth, and urban areas. Classification accuracy was better than 90% for all categories. Geometric corrections were applied to the classified ERTS data tape to produce color-coded map overlays at scales of from 1:24,000 to 1:250,000. These geometrically corrected map overlays, one for each target category, were drawn by a pen under computer control. The overlays placed over an AMS map of the same scale immediately provide target locations. A number of new lakes were mapped for the first time. The maps and data were produced from ERTS tapes at a tenth of the cost of conventional techniques.

A technique was developed for storing and retrieving from a computer data bank the classified map of Oakland County as produced from ERTS. The user interacts with the data bank to obtain within lake watersheds the area covered, in square kilometers, by each land-use category. This technique was successfully demonstrated by establishing correlations between watershed land-use and lake water quality, as indicated by a total and fecal coliform bacteria counts. These computer procedures are basic elements for determining those land-use factors and sources of nutrients that accelerate eutrophication in lakes and reservoirs.

The maps and data generated from the ERTS spacecraft can be used to monitor seasonal changes in lake features and in watershed factors that affect eutrophication rates. Repetitive use of these techniques will serve to alert planners to potential losses in water quality.

RECOMMENDATIONS

A program is recommended that would extend the results of this investigation from the demonstration stage to the operational support of agencies involved in ongoing water quality programs. In addition to firming-up correlations between ERTS measurements and water quality parameters, the program would prove the cost benefits of using ERTS for the surveillance and control of lake eutrophication on an operational basis.

CONTENTS

CONTENTS (CONT.)

ILLUSTRATIONS

ILLUSTRATIONS (CONT.)

ILLUSTRATIONS (CONT.)

TABLES

1. INTRODUCTION

The feasibility of using ERTS-1 to monitor and classify the level and rate of eutrophication in inland lakes has been examined. In scope this investigation was limited to the development of methods for collecting ground truth data, for ERTS data processing and for the preparation of such ERTS data products as would be required for operational use of ERTS-1 in eutrophication surveillance. The report describes techniques developed for measuring the color and absolute (%) reflectance of deep waters. Correlations with concurrent water quality measurements are discussed. The automatic classification of lakes into deep and shallow waters was demonstrated. By similar methods lake watersheds were classified into several land use/cover categories, the drainage from which affects to varying degrees the trophic potential of lakes. Automatic area tabulation of these categories within watershed boundaries was carried out. Color-coded map overlays were prepared from ERTS data at several scales to demonstrate the direct comparison of classified imagery with lake and ground features. Additional methods and approaches were recommended for related operational use of ERTS.

The results show that this methodology will be useful for periodic monitoring of high trophic levels in small lakes where urban development of watersheds can cause rapid and severe changes in water quality. More importantly, by monitoring quantitative changes in watershed land use, ERTS can provide planners with a basis for anticipating water quality problems. It is clear that comparable lake and watershed monitoring on the ground without ERTS support is far more expensive and time consuming.

2. BACKGROUND

2.1 STATEMENT OF THE PROBLEM

This study addresses the continuing problem of monitoring the rate and progress of eutrophication in inland lakes. By nature eutrophication is a long term process, developing usually in the course of years. Generally, small increments of trophic change are superimposed on the large seasonal changes that all temperate lakes undergo. Many of the accepted indicators of water quality, such as nutrient and biomass levels, are affected by both trophic and seasonal changes. Fortunately, ERTS-1 is best suited for monitoring these long-term events. Though its effectiveness is limited by cloud cover, ERTS can be expected to furnish repetitive coverage of most areas from season to season, if not from month to month.

Measurements of deep water color and reflectance are important in evaluating the trophic status of lakes. In principle, eutrophication is accompanied by increases in the magnitude of back-scattered (upwelling) light and changes in water color. The first is due to increasing numbers of suspended particles; the latter is influenced by solutes as well. Although these relationships are complex and not yet well-defined, there is still a need to explore the sensitivity of ERTS to such changes. Water color and reflectance are transient phenomena in themselves, but they vary in each lake according to yearly cycles that change with trophic structure.

Algal blooms and surface scums are even more transient events that may or may not be recorded by an occasional ERTS pass. To the degree that they are, the intensity, frequency and composition of blooms may be considered as indicators of trophic status.

Bathymetry and bottom cover are conservative features of lakes that require monitoring on a year to year basis. Sediment character and bottom vegetation patterns change with trophic quality. Indirectly, the remote detection of bottom detail in relation to depth can be used as a measure of water clarity.

Finally, remote monitoring of trophic processes should provide data that is useful as a basis not only for assessing current conditions but for anticipating future changes as well. The latter can come only from a consideration of land use and cover in the individual lake watershed. Many other studies have already shown the feasibility of monitoring from ERTS the types of land use features that bear directly on the quality of drainage entering lakes. Such information, when used to forecast water quality trends, is more valuable to managers and planners than are assessments of current lake quality alone.

The following (Table 1) summarizes the general types of lake features of importance in eutrophication monitoring. This report further describes the development of ERTS methodology necessary for these types of monitoring.

Table 1. Lake Features Desirable to Monitor From ERTS on Seasonal/Annual Basis

Type of Feature/Reflectance	Information Yield
Deep Water	Water turbidity and color, productivity
Surface Phenomena	Algal scums, floating plants
Bottom Plants	Macrophyte growth patterns
Shallow Water	Lake Bathymetry, sedimentation rates
Lake Watersheds	Land use categories, runoff potentials, nutrient sources

2.2 REVIEW OF RELATED WORK

The optical properties of water (transmissivity, color, and reflectivity) are influenced by suspended matter, both particulate and dissolved. This fact is the qualitative basis for remote sensing of water quality. Much recent work in this field has been directed toward defining the quantitative relationships that are involved. The ultimate success of these efforts will determine the degree to which remote sensing can supplement or replace water quality monitoring at ground level.

Not even pure water appears colorless to an overhead observer since it scatters blue light and absorbs light strongly at the red end of the visible spectrum (James and Birge, 1938). Natural waters are never pure, however, and their coloration is highly variable as a result of numerous physical, chemical, and biological factors (Hutchinson, 1957). In a lake or other water body these factors combine in a highly complex way to produce an overall color and reflectance, which contain much information about water quality. This "light of the water" or upwelling light is a modified component of the total incident light that is back-scattered by water molecules and larger particles. Superimposed on this "internal" reflectance is specular or surface reflectance. Unfortunately, although the latter may account for most of the reflected light, it usually contains no information about water quality. McNeil and Thomson (1974) and Jerlov (1968) provide thorough discussions of this phenomenon, which has great significance to remote sensing.

Generally, an increase in the trophic state of natural waters results in more organic matter in suspension and a shift in water color toward longer wavelengths. The relative magnitude of upwelling light, particularly at longer wavelengths, also increases. Examples of these effects in ocean waters are seen in Figure 1. Much earlier, Juday and Birge (1933) had showed such a qualitative relationship between organic carbon content and water color in Wisconsin lakes (Figure 2).

Although a color standard for drinking water exists (Water Quality Criteria, 1968), there is so far none that relates water color to specified levels of eutrophication in fresh waters. The development of such a standard would be a difficult but not impossible task for lakes within a given geographical setting: i.e., the midwestern glacial lakes. However, that is beyond the scope of this experiment. Suffice to say that accurate discrimination of water color and reflectance is essential to remote sensing of lake trophic levels. Although the ERTS spectral bands are broad, several investigators have reported successful monitoring or discrimination of turbidity and water color with ERTS (Pluhowski, 1973; Coker et al., 1973; Bowker et al., 1973; Klemas et al., 1973; Scherz et al., 1973; Yarger et al., 1973).

In terms of ERTS spectral bands the effect of increasing eutrophication on water color is seen as a decrease in the ratio of band 4 to band 5 reflectance. In qualitative terms this amounts to an increase in the "brown-ness" of water (Jerlov, 1968). Clearly, sufficient turbidity must be present and consequent scattering must occur before such changes in water color would be detectable by ERTS. One purpose of the present study has been to define this threshold of color change detection.

Land use/cover mapping with ERTS has been undertaken in other studies but evidently not in relation to the prediction of trophic change in lakes. In principle, the nutrient content of land runoff (storm water) is related to human activity in lake watersheds. In other words, in any given area the proportions of urban development, bare earth, rangeland, forested land, etc., in each watershed are statistically related to the quality of surface drainage entering a lake. Land use/cover affects both the nutrient content and volume of runoff (slope being constant). At present the quantitative relationships between land use/cover and enrichment potential of drainage are being investigated by Hetling (1973) and others. Recent reviews by Likens and Bormann (1974) and Schindler et al. (1974) emphasize the importance of considering nutrient transport from specific watersheds to aquatic ecosystems when estimating eutrophication rates and potentials. The utility of ERTS, as reported here, is that it provides a unique means of mapping watershed features spatially, qualitatively and quantitatively.

Figure 1 Correlations of Organic Content and Spectra of Upwelling Light for Ocean Waters

(a) (from Jerlov, 1968)

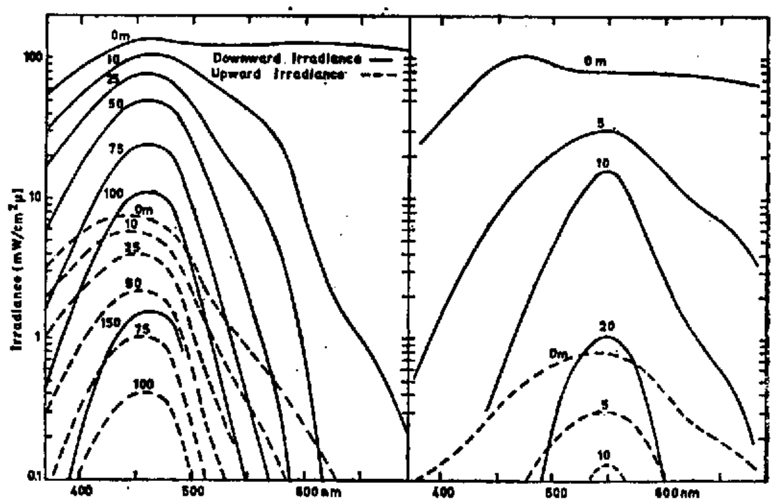

Fig.53. Comparison between spectral distribution of downward and upward irradiance for solar elevation of 55–60°. Left: Sargasso Sea ("Dana" expedition, 1966). Right: Baltic Sea (after AHLQUIST, 1965).

(b) (from Clarke, <u>et</u> <u>al</u>., 1970)

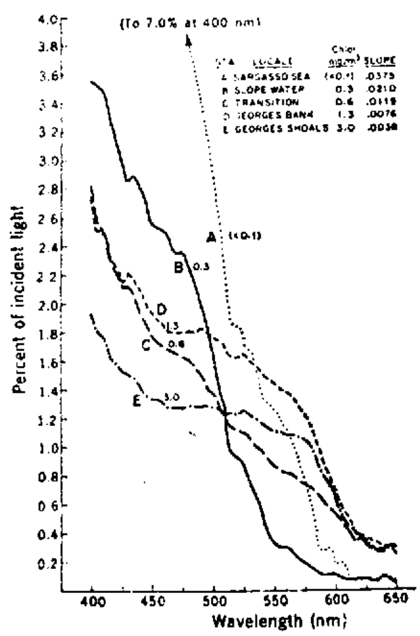

Fig. 4. Spectra of backscattered light measured from the aircraft at 305 m on 27 August 1968 at the following stations (Fig. 2) and times (all E.D.T.): Station A, 1238 hours; Station B, 1421 hours; Station C, 1428.5 hours; Station D, 1445 hours; Station E, 1315 hours. The spectrometer with polarizing filter was mounted at 53° tilt and directed away from the sun. Concentrations of chlorophyll a were measured from shipboard as follows: on 27 August, Station A, 1238 hours; on 28 August, Station B, 0600 hours; Station C, 0730 hours; Station D, 1230 hours.

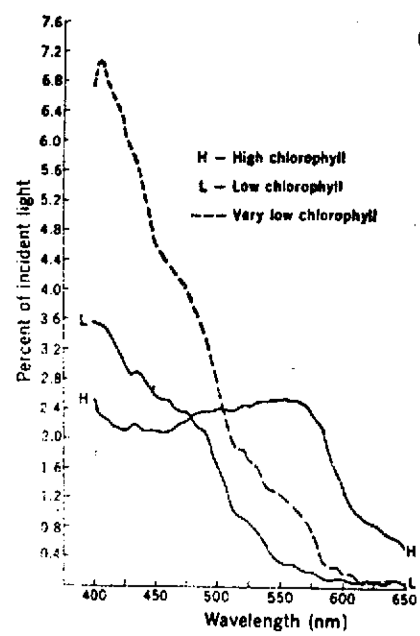

Fig. 3. Data from the high and low chlorophyll curves plotted as percentage of the incident light and compared with data taken on the same day from an area with very low chlorophyll concentration south of the Gulf Stream.

Figure 2 Correlation of Water Color with Organic Carbon (from Juday and Birge, 1933: pp. 232-233) Based on a Sample of 530 Wisconsin Lakes and Ponds

The relation between the color of the surface waters of the lakes in northeastern Wisconsin and the amount of organic carbon in them. The lakes are separated into groups on the basis of their brown color in comparison with the platinum-cobalt standard; the maximum, minimum and mean quantities of organic carbon are indicated in milligrams per liter of water for the various color groups, as well as the number of lakes in each group. The lakes are grouped by color ranges of 10 up to 69, but the number in the various 10 groups above this color is so small that they have been combined into larger color groups in order to obtain a fair mean.

Color	Number of lakes	Organic Carbon		
		Maximum	Minimum	Mean
0	56	4.5	1.2	3.0
1—9	57	6.4	1.7	3.6
0—9	113	6.4	1.2	3.3
10—19	101	12.5	2.1	4.6
20—29	77	12.2	2.2	5.7
30—39	46	15.0	3.9	7.7
40—49	23	12.5	4.9	8.3
50—59	27	12.3	5.3	9.2
60—69	22	13.0	4.0	10.3
70—99	44	16.6	7.5	12.1
100—129	40	22.4	6.0	14.3
130—159	15	19.6	12.3	16.0
160—199	9	24.8	14.5	17.1
200—340	12	25.8	13.5	21.4

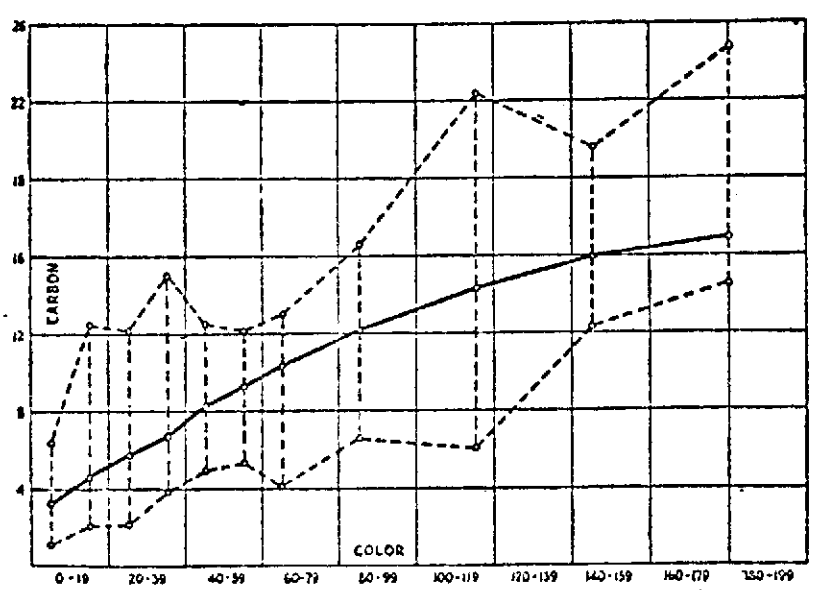

The relation between the color of the water and its organic carbon content. The upper curve shown by a broken line represents the maximum amounts of organic carbon found in the various color groups; the lower broken line curve shows the minimum amounts of organic carbon. The solid line curve between them indicates the mean quantities of organic carbon in the various color groups.

2.3 OBJECTIVES OF THE STUDY

The general objective of this experiment, as stated in the original proposal (MMC 598), was to explore the feasibility of using ERTS-1 to monitor and classify the state of eutrophication, or enrichment, of inland lakes. Implicit in this objective is the idea that ERTS surveillance would supplement, rather than replace, more conventional types of water quality monitoring on the ground and even remote sensing from aircraft.

The specific objectives proposed in 1972 were to:

a. Determine the minimum size of inland lakes detected by ERTS when considering factors of color, size, shape, and shore definition.

b. Determine correlation of surface color to various indices of eutrophication for preparing charts of eutrophication versus surface color. Such indices are algal count, Secchi disc transparency, leptopel (detrital) content, macrophyte extent, phosphates, etc.

c. Determine if algal blooms are detectable by ERTS when they occur and color the surface of small inland lakes. Algal blooms are an indicator of enrichment.

d. Determine if changes in leptopel (suspended particulate) level are detectable by ERTS. This is another measure of eutrophication that can be related to ERTS.

e. Determine the feasibility of establishing classification of levels of inland lake eutrophication by either lake, pond, and swamp taxonomies or by individual indicators such as surface color, transparency, leptopel level, and appearance of algal blooms.

At the midpoint of the program (Rogers and Smith, 1973; Interim Report, August 1973), it was necessary to evaluate these objectives in light of our progress, findings and the results of other studies. At that point an extension of the objectives seemed in order. Accordingly, they were restated as a more logical series of steps that we felt must be taken to fulfill the general purpose of this investigation. These were to:

a. Determine the effectiveness of ERTS in resolving small lakes and lake features, as a function of their size, shape, depth, color, and shore definition.

b. Detect differences in the color and reflectivity of lakes by analysis of multispectral data from ERTS, aircraft, and ground monitors.

c. Correct ERTS data for solar and atmospheric effects so that resulting measurements are directly comparable with ground measurements.

d. Describe physical, chemical, and biological variables which influence water color and turbidity within lakes.

e. Correlate these color-related variables with the general trophic condition of each lake, considering additional water quality indicators.

f. Evaluate ERTS-1 as a broad survey monitor of eutrophication (its extent and rate) in inland lakes.

Still later in the program we realized the importance of classifying and mapping lake watersheds as a basis for predicting the further eutrophication of lakes. In this role ERTS provides unique information and data products that can be of great value to planners in safe-guarding lake quality in future years. Thus, watershed mapping became an important objective late in the program.

Finally, it became increasingly clear that ERTS, because of its 18-day period, is better suited to monitor the more conservative features of small lakes than transient phenomena such as algal blooms, turbidity changes, etc. Our objectives were modified to allow for that inherent limitation of the ERTS system.

3. STUDY SITE

3.1 TEST AREA

The study area designated for this investigation is within Oakland County in southeastern Michigan (Figures 3 and 4). The county includes the northwestern suburbs of Detroit, the city of Pontiac and numerous smaller municipalities. It also contains some 400 natural lakes surrounded by urban and suburban development, which toward the north grade into farmland, pastures and some undeveloped areas. Urbanization, particularly in the southeastern quarter, has been rapid: the county's population has doubled during every decade since 1940 (Doxiadis, 1966). Shoreline development around lakes will continue at a rapid pace since this will always be considered choice property with high recreational value.

The lakes of Oakland County were formed some 8,000 – 9,000 years ago from remnants of retreating glaciers following the Wisconsonian glacial stage (Blodgett, 1971). Blocks of ice imbedded in glacial till or outwash soils were left behind to melt and form "kettles," or lakes, usually with no discrete inlet or outlet. Most of the Oakland County lakes lie within a morainal belt crossing the county from southwest to northeast (Figure 5). The terrain is mostly low hills (i.e., moraine) in the northwestern half descending to flat land (old lake bed) toward the southeast. The elevation varies from 175 m. to 400 m. above sea level. Soils in the lake watersheds are sands, gravels, silts and clays occurring either as unsorted till in moraines or as highly sorted deposits in outwash areas.

Kettle lakes in this and other glacial settings can be regarded as collecting basins for all materials that have eroded from the surrounding land since their formation. Additions of mineral and organic materials to the lakes are now seen in all stages of their ultimate conversion to swamps and bogs. Where the sedimentation rate has equalled the rate of material input, only gradual enrichment or "eutrophication" of the water column has occurred since glacial times. However, when input rates have greatly exceeded losses to the bottom (as now occurs frequently), extreme cases of eutrophication have been the result. The condition of lakes in Oakland County varies from mesotrophic (moderately enriched) to hypereutrophic (highly enriched). Since most of these lakes are roughly of the same age (8,000 – 9,000 years), their various aging rates are a complex function of nutrient input and sedimentation rates, lake volume and, sometimes, exchange with ground-waters.

Figure 3 Location of the Test Area in Southeastern Michigan. Area Covered by ERTS Scene Shown in Figure 4 is Noted by Dotted Lines

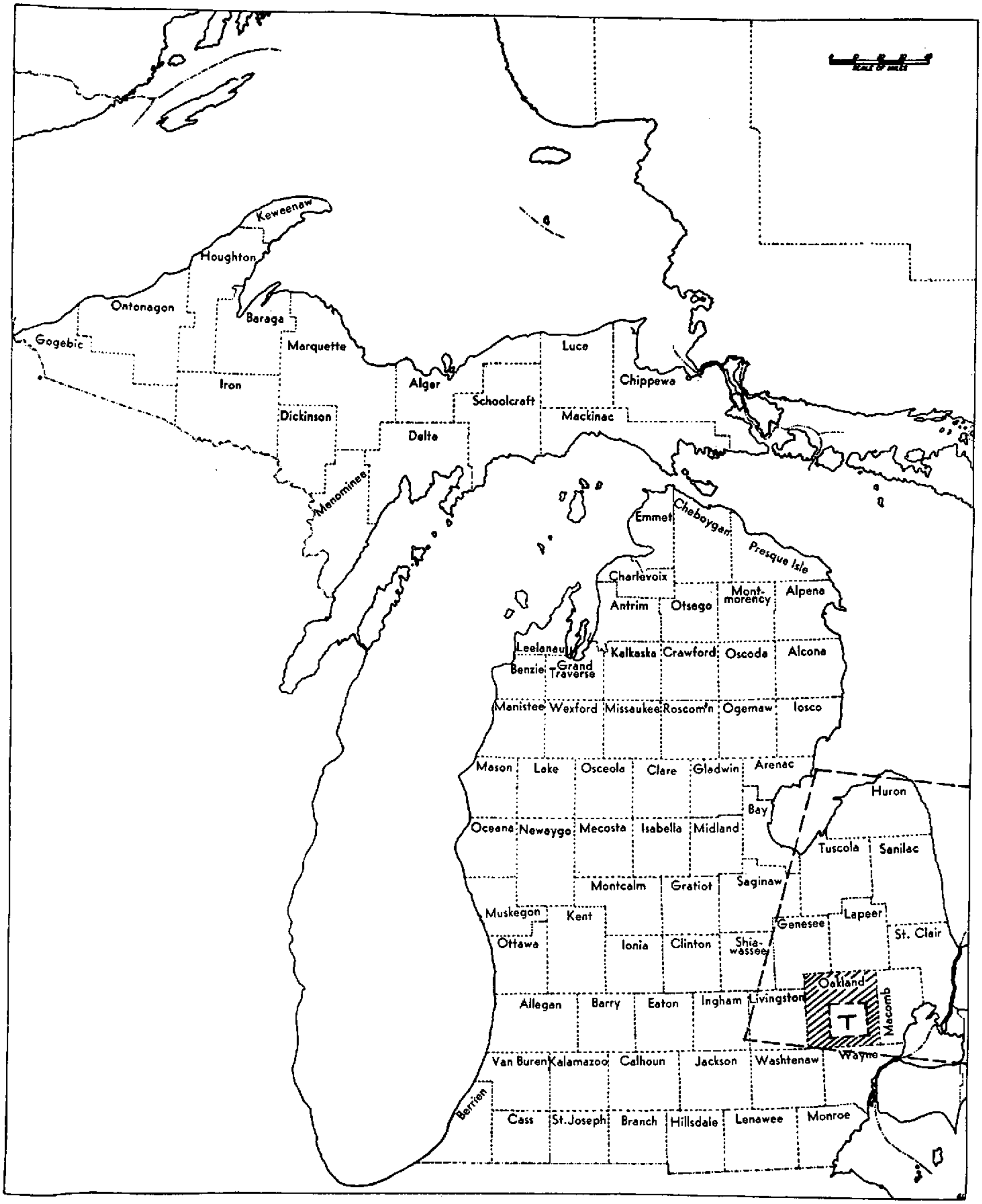

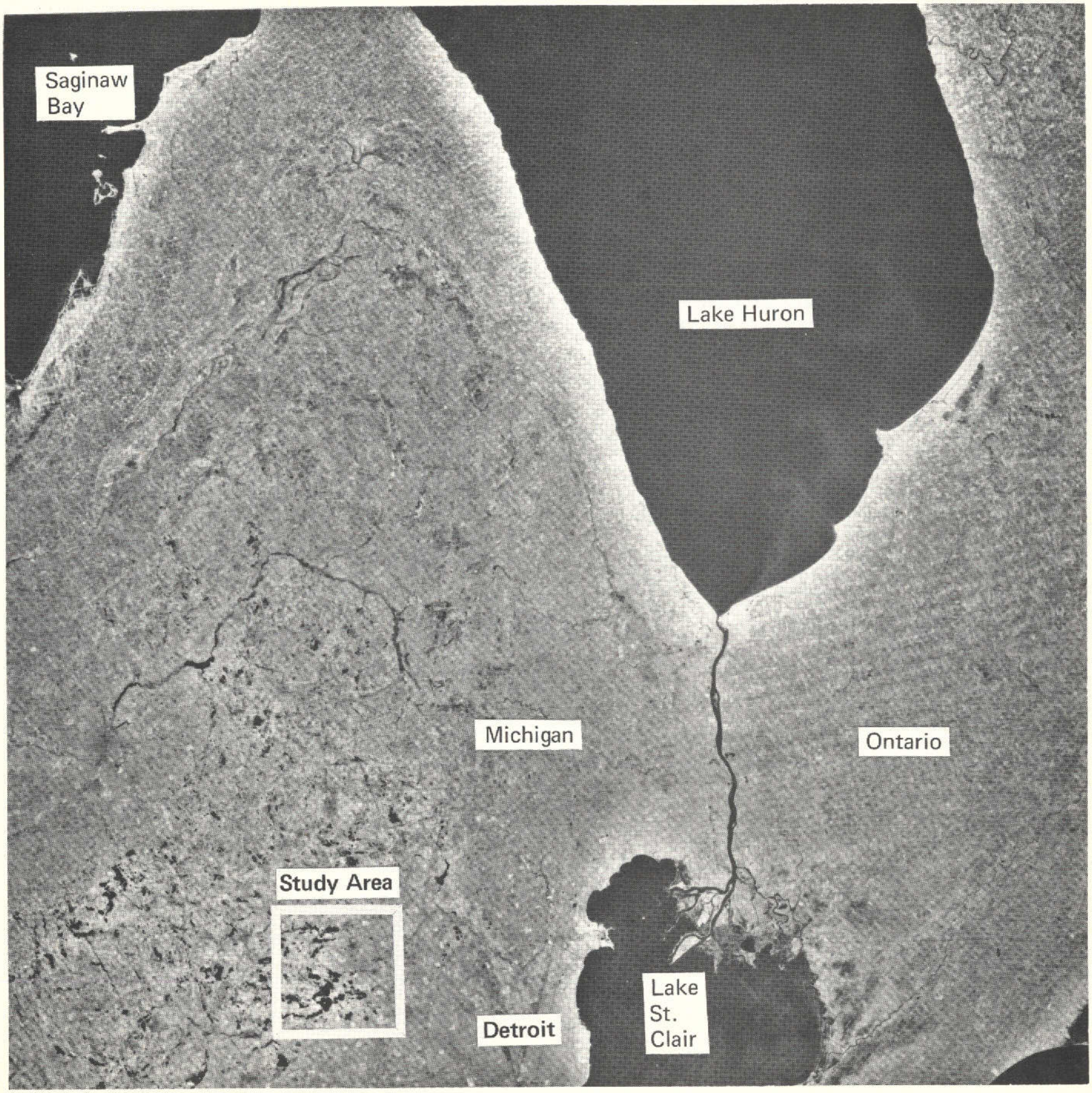

11798C-7

Figure 4. ERTS Band 7 Scene Recorded on March 27, 1973, (ID No. 1247-15474) with Location of Study Area Shown

Figure 5. Topographic Map of Oakland County, Michigan (Oakland County Planning Commission, 1966). Contour interval is 50 feet.

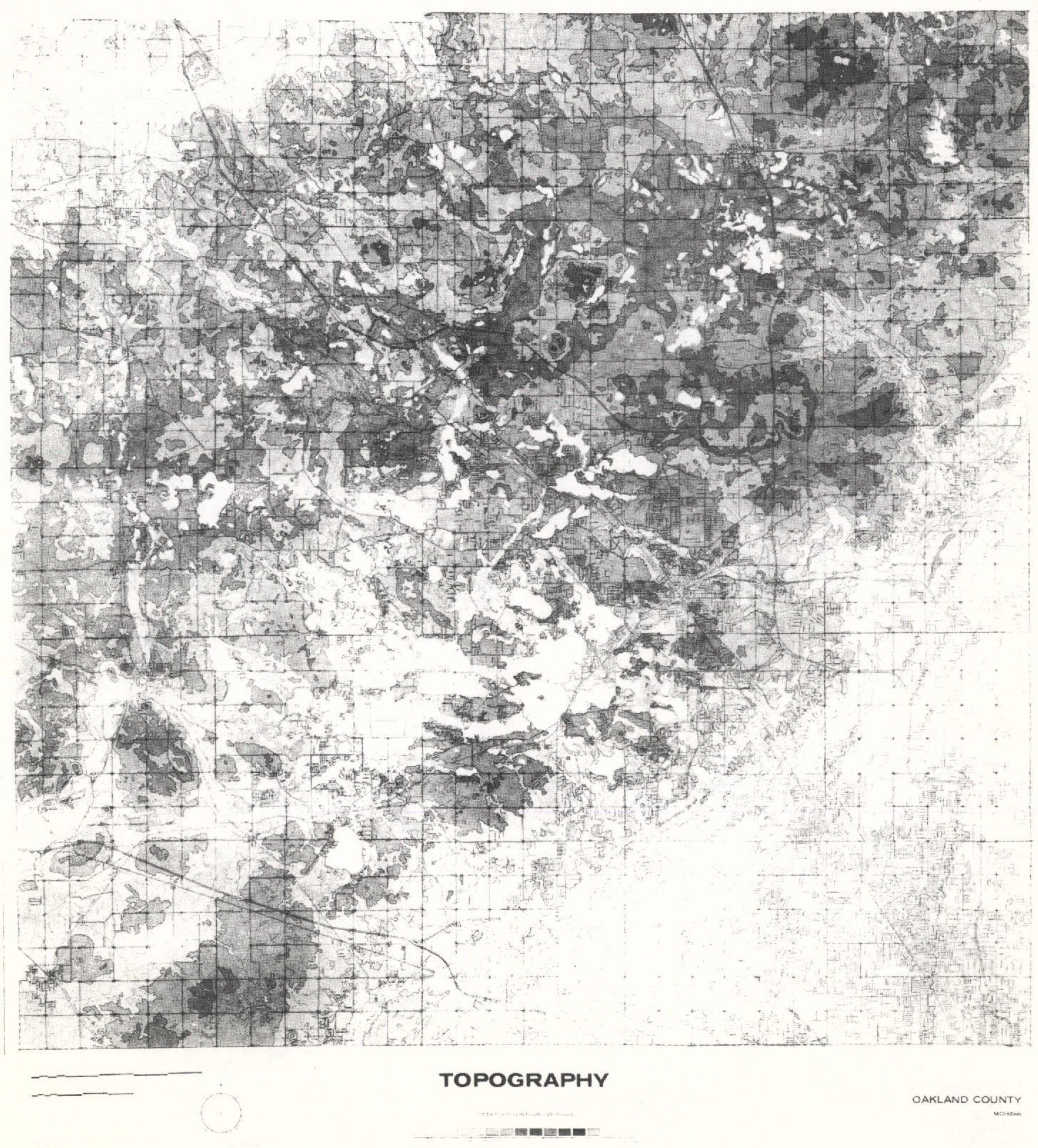

3.2 TEST LAKES

The six test lakes were chosen to represent a range of size and water quality. The bathymetry of test lakes is shown in Figures 6 – 11. Here, shallow waters are mapped as they appeared in 1964 aerial photographs (U.S. Department of Agriculture). The two categories of "dark" and "light" bottom represent various combinations of depth and bottom cover. Generally speaking, the darker areas are beds of aquatic plants (submerged) and the lighter areas are sand or marl sediments. These patterns in Orchard and Cass Lakes were substantially the same in 1973 aerial photographs (NASA).

As will be explained later, sub-areas or "training sets" were chosen within these lakes for computer classification (categorization) of deep and shallow water.

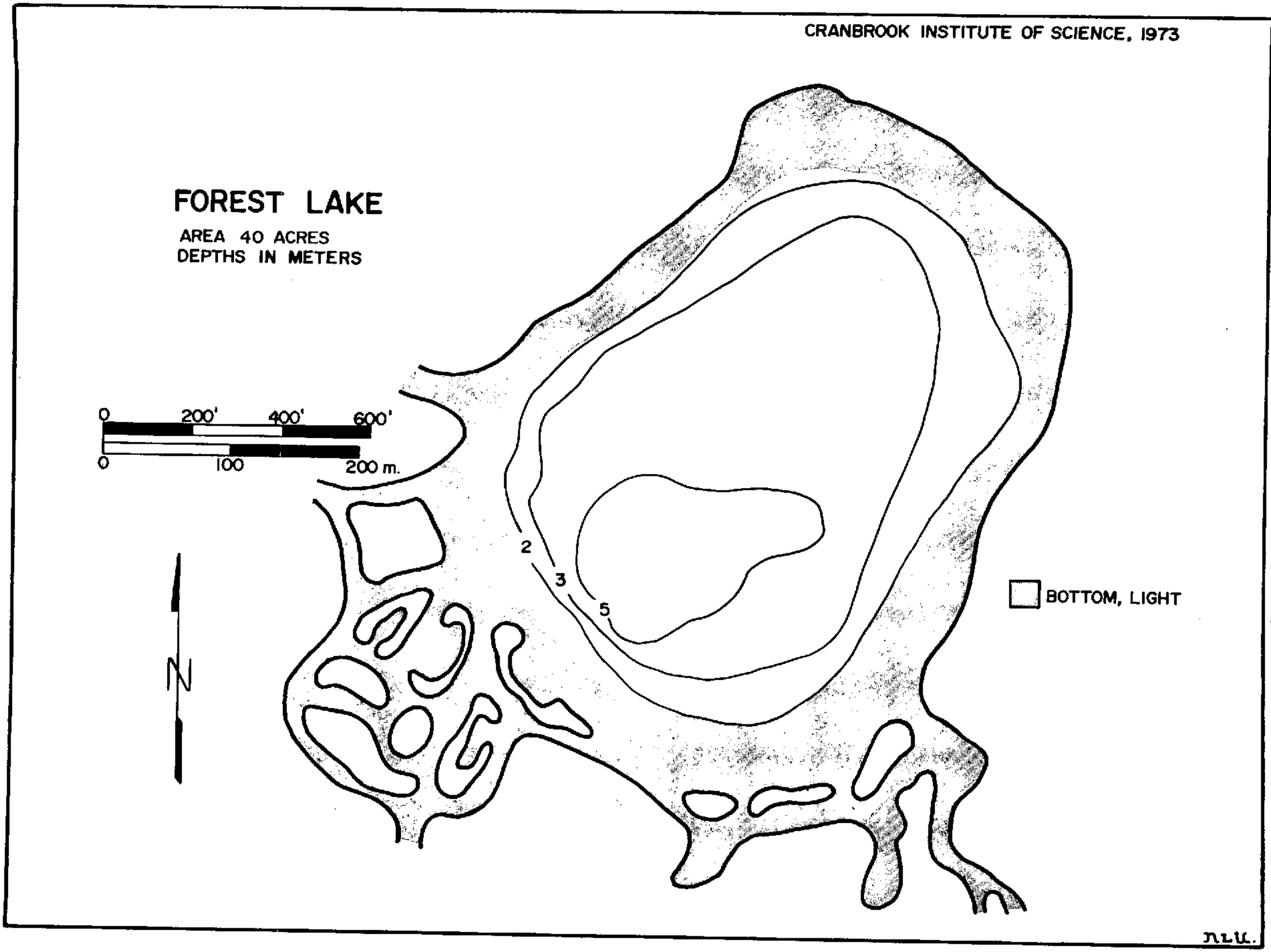

Figure 6. Forest Lake Bathymetry

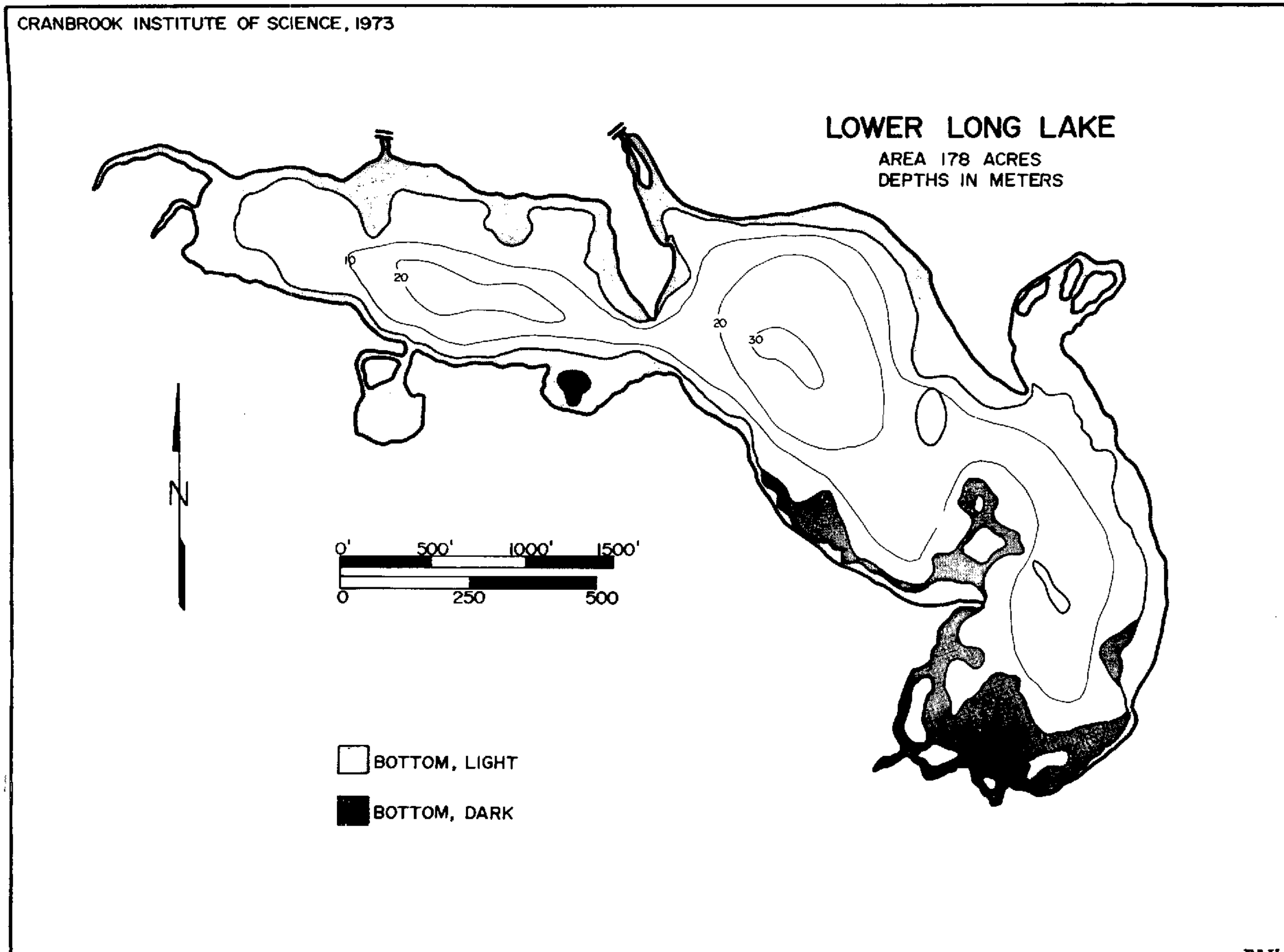

Figure 7. Lower Long Lake Bathymetry

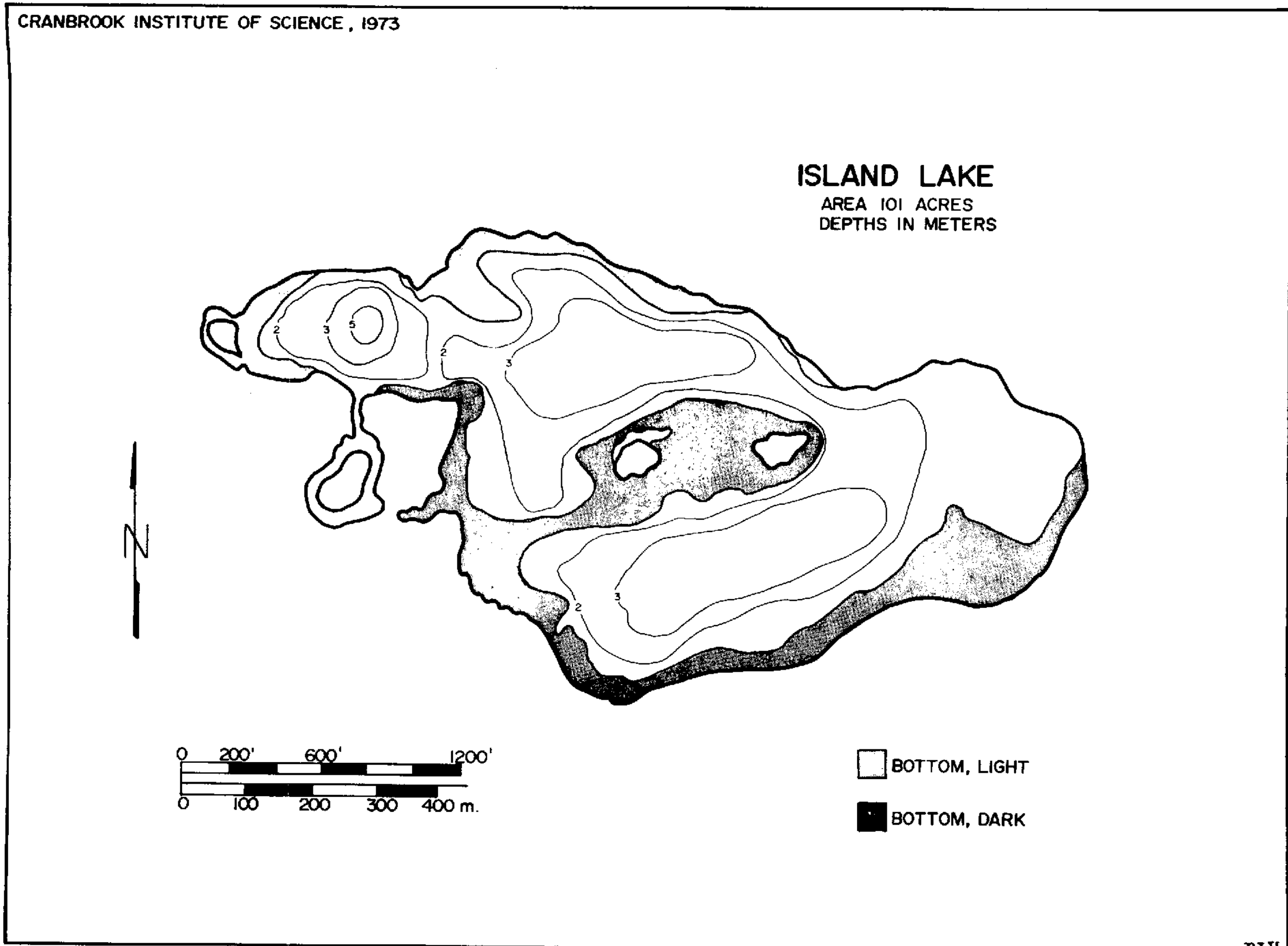

Figure 8. Island Lake Bathymetry

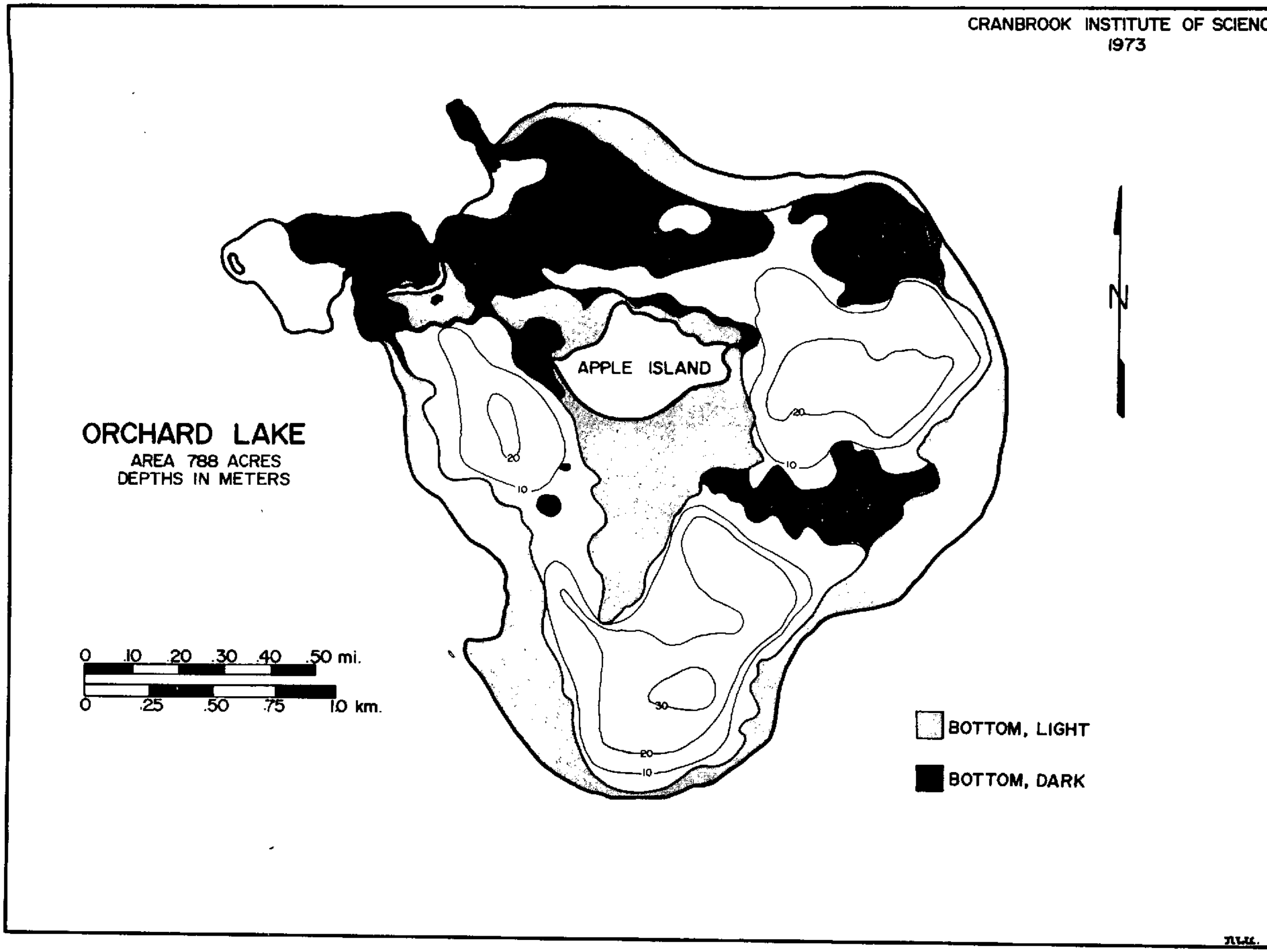

Figure 9. Orchard Lake Bathymetry

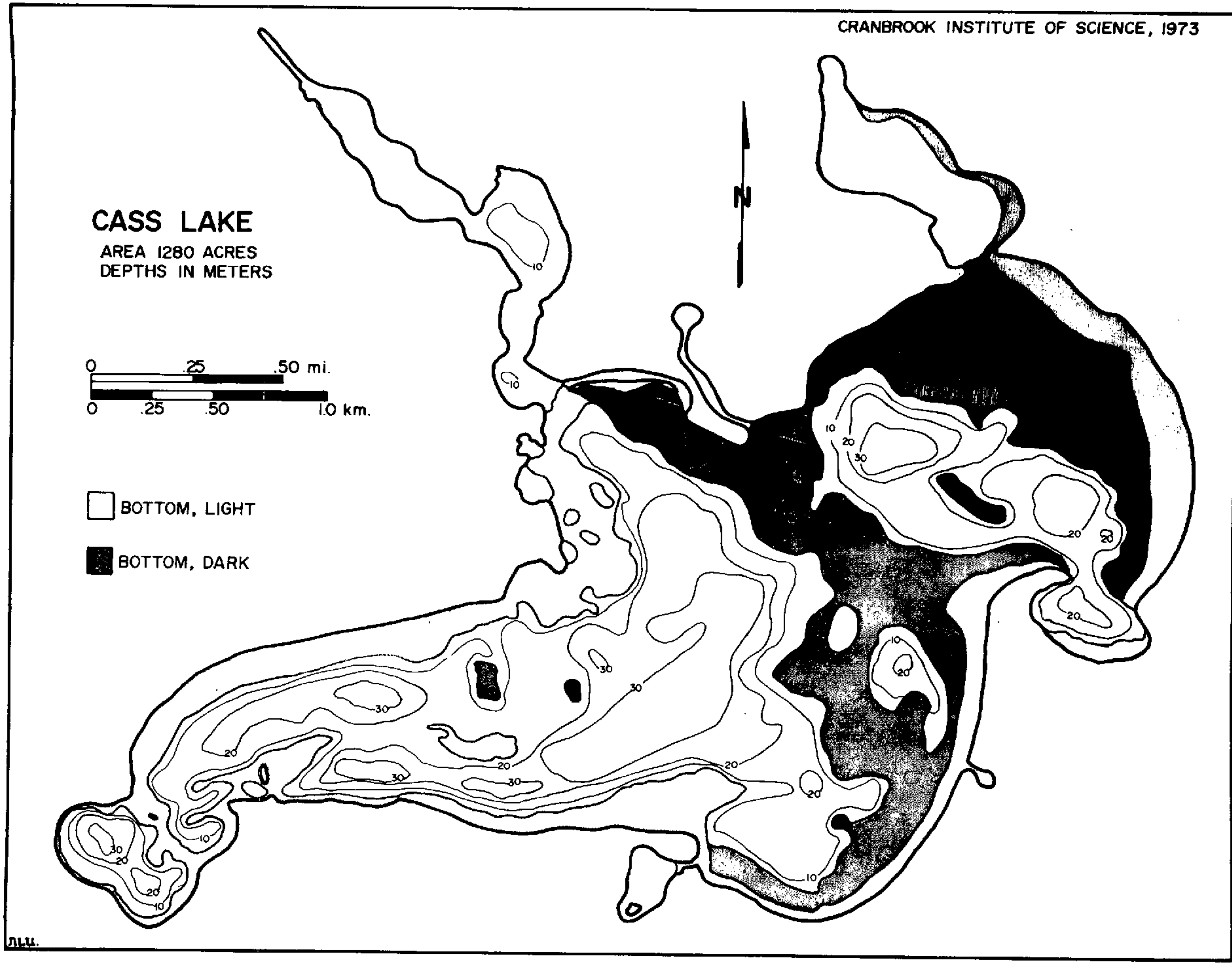

Figure 10. Cass Lake Bathymetry

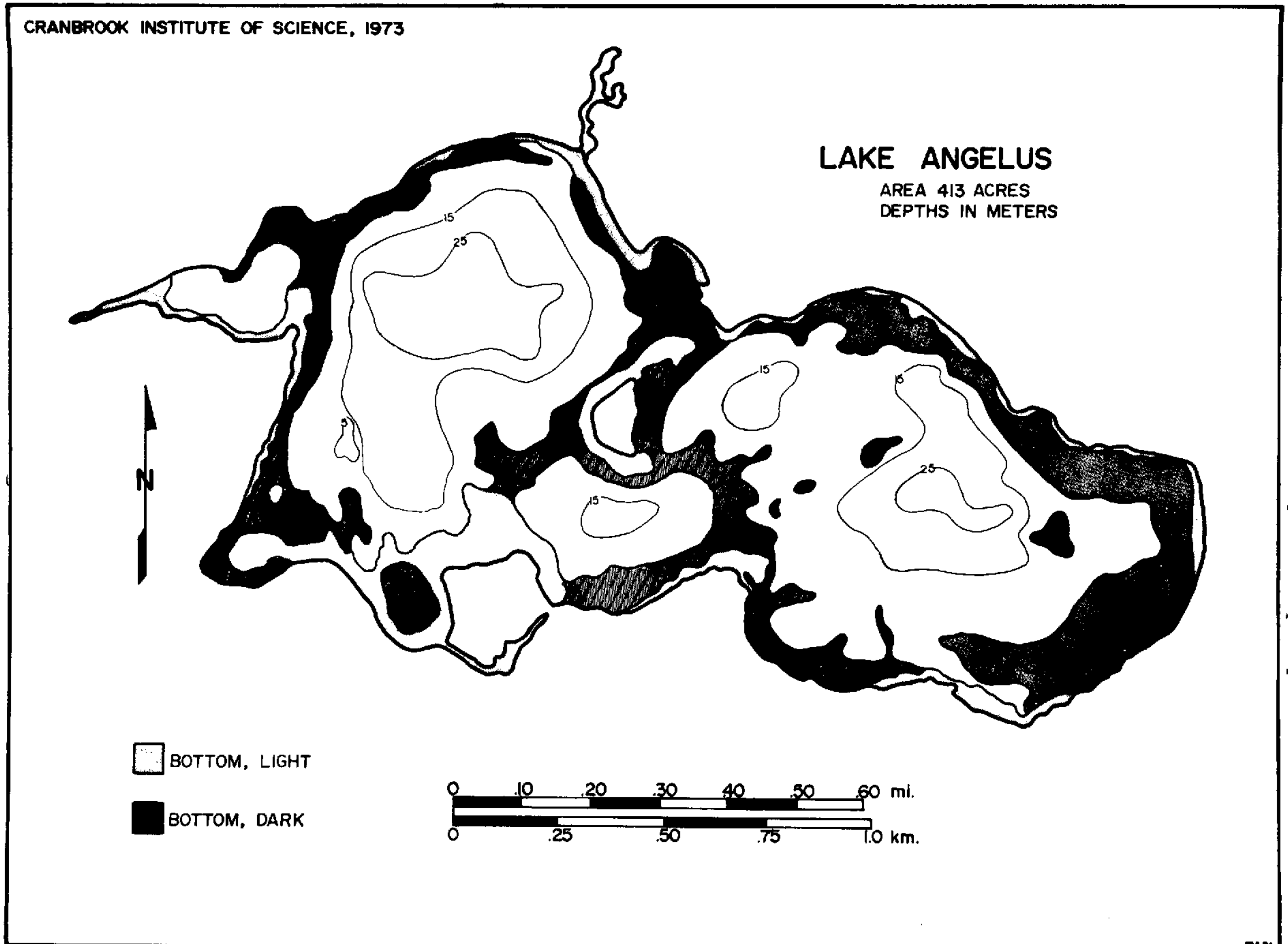

Figure 11. Lake Angelus Bathymetry

4. APPROACH AND METHODOLOGY

4.1 PLAN OF OPERATION

The approach involved several stages of data collection and analysis:

a. Testing of water quality in the six study lakes coincident with ERTS passes.

b. Radiometric measurements of water and atmospheric parameters coincident with ERTS passes.

c. Preliminary study of ERTS photographic (bulk) imagery for lake and watershed features.

d. Detailed analysis of ERTS computer compatible tapes (CCTs) for reflectances and spectral signatures of lake and watershed features.

e. Preparation of classified imagery, map overlays and other ERTS data products.

f. Comparison and correlation of ERTS data and ground truth.

g. Evaluation of the ERTS system as a tool for monitoring lake eutrophication.

At the outset it was not expected that the bulk imagery would yield much useful information about water quality owing to the small size of the test lakes and the subtle differences in their trophic condition. Moreover, only two scenes of the area, both with considerable cloud cover, were available during the first seven months of the project. Nevertheless, the bulk images were examined in some detail for gross lake features, but no machine processing of the digital tapes was attempted. Microdensitometry of the photographs was not feasible due to atmospheric haze. The first ERTS scene suitable for processing was recorded on March 27, 1973. The ground truth program commenced on that date.

4.2 GROUND TRUTH METHODS

This part of the program was chiefly the responsibility of the Cranbrook Institute of Science as a subcontractor to Bendix Aerospace Systems Division.

4.2.1 FIELD MEASUREMENTS AND SAMPLING

Collection of field data and water samples was accomplished usually within a time frame of two hours before and after the ERTS pass. Water temperature, color and transparency were measured from a small boat at two deep-water stations on each lake. Samples (4 liters) for laboratory analysis were taken from just below the surface in cleaned polypropylene (Nalgene) bottles.

Water color estimation using Forel-Ule standards was done with the aid of a unique viewing device developed for this project. The construction and use of this viewer are described in Section 5.1.3.

Radiometric measurements of deep water in situ and of reflectance standards were made with a Radiant Power Measuring Instrument (RPMI) from the same boat. The RPMI, described by Rogers et al., (1974), measures radiance from the water in same bands as ERTS. Other radiometry of atmospheric parameters was done on a golf course adjacent to Forest Lake with the instrument tripod-mounted.

Supplemental data on water quality (temperature-dissolved oxygen profiles) were collected twice during the project to provide further insight into the trophic condition of test lakes.

Other ground truth activities involved inspection of test sites chosen to represent categories of watershed land use/cover. Additional measurements of water quality and radiometry were made on other lakes in Oakland County and in northern Michigan; this was done for purposes of comparison to the test lakes and for observation of trophic conditions that did not occur on the test lakes.

4.2.2 LABORATORY ANALYSIS OF WATER SAMPLES

Water samples were kept in the dark under refrigeration until analyzed, usually within 48 hours. All work was carried out in the facilities of Cranbrook Institute of Science and Oakland University. The following parameters were measured by the methods indicated.

a. Total algae (cells/ml): enumerated by microscopic study of cleared filters, according to Millipore Corporation Publication AB 310 (1974) and Palmer (1962).

b. Particulate carbon (mg/l): determined spectrophotometrically after wet oxidation, according to Strickland and Parsons (1968).

c. Particulate chlorophyll and carotenoids (mg/l): determined spectrophotometrically after acetone-methanol extraction, according to Strickland and Parsons (1968).

d. Suspended particulates, total and inorganic (mg/l): determined gravimetrically, before and after ashing, according to Standard Methods (1971).

e. Dissolved nitrate-nitrite (mg/l): determined spectrophotometrically as the nitroferrocyanide complex, according to Strickland and Parsons (1968).

f. Dissolved ortho-phosphate (mg/l): determined spectrophotometrically as the ammonium molybdate complex, according to Strickland and Parsons (1968).

4.2.3 WATER QUALITY DATA ANALYSIS

The water quality factors monitored in the test lakes are among those most commonly associated with the eutrophication process. In other words, lake enrichment (eutrophication) is generally accompanied by increases in the concentrations of particulate solids of all kinds, including algae (with chlorophyll) and organic carbon; these result in increased turbidity and discoloration, and decreased transparency (Secchi depth). With hyper-eutrophication comes periodic excesses of dissolved nutrients, such as nitrate-nitrite and ortho-phosphates.

An early objective in this study was to determine whether seasonal changes in the water quality of test lakes were detectable by ERTS as reflectance or color changes. Generally speaking, differences or changes in water quality were judged to be "significant" if transparency, color or turbidity differed by a factor of two or more. Certainly, variations of this scale must be detectable if ERTS monitoring is to be worthwhile. If this proved feasible, the next step planned was to correlate specific trophic levels with ranges of water reflectance and color measured by ERTS.

The definition of "trophic level" is difficult, but some authors have reduced it to a relative value by means of various weighted equations of water quality factors. However, no such classification of trophic levels was attempted in this work for reasons that will be made apparent. Suffice to say that no such "trophic index" standard is universally accepted. Moreover, it is self-evident that no such index can be better correlated to ERTS data than can one or more of its component factors of turbidity, color, etc. when considered separately.

Consequently, the approach here was to compare ERTS measurements independently to each water quality factor. For example, we attempted to classify the test lakes from ERTS data at a time when they varied widely in transparency (Secchi depth) or color (Forel-Ule number). In another approach, the same ERTS and ground measurements were analyzed by means of regression equations of the form:

$$E = a_o + a_1(P_1) + a_2(P_2) + a_3(P_3) \ldots . a_x(P_x)$$

where E is the ERTS measurement, and P_n is the water quality parameter measurement. The equation is solved for coefficients a_n, whose value and sign indicate the relative degree of correlation between ERTS and ground measurements.

4.3 ERTS BULK IMAGERY ANALYSIS

Single-band bulk images (9 x 9 inch, black and white positive transparencies) were examined on a light table with a binocular microscope and hand lenses (10x). The object was to find out how the resolution of lakes and lake features varied with size, shape, surface cover, surroundings and orientation with respect to scan lines.

4.4 ERTS CCT ANALYSIS

Computer software, techniques, and procedures used to transform ERTS CCTs into land-use maps and data were developed in the Bendix Earth Resources Data Center. The elements of this center include a Digital Equipment Corporation PDP-11/15 computer with 32 K-words of core memory, two 1.5 M-word disk packs, two nine-track 800-bit-per-inch tape transports, a line printer, a card reader, and a teletype unit. Other units are a color moving-window computer-refreshed display; a glow-modulator film recorder; and a computer-controlled Gerber plotter.

The data processing steps used to transform ERTS CCTs into land-use map overlays and data are briefly summarized in the following paragraphs.

Analysis

The first processing step is to locate the CCT coordinates, in terms of resolution element number and scan-line count number, of those areas that best typify the land-use/water target categories of interest, the "training areas".

This function was performed by techniques that included transforming a single channel of data to 70-mm film and to a gray-scaled computer line-printer printout, and by simply viewing data on the color-coded moving-window display. The last technique was found to be the fastest way of locating the training areas. Once the target of interest is located on the display, its coordinates are designated to the computer by placing a rectangular cursor over the desired area and assigning a training area designation, category code, and color code. Several training areas are picked for each category. The color code is used in later playback of the tapes when the computer-categorized data is displayed in the designated colors.

The ERTS spectral measurements within the training area boundaries are edited by the computer from the computer compatible tape (CCT) and processed to obtain a numerical description to represent the "spectral characteristics" (computer processing coefficients) of each land-water category. To test the computer's capability to use these spectral characteristics, they are first applied to categorize data from known areas. The processed results are viewed on the TV monitor, and output in the form of accuracy tables. Selection of training areas, generation of accuracy tables, and evaluation of processing results using computer printouts and the TV monitor are iterative operations.

Produce Decision Data Products

When satisfied with the accuracy of the decision processing, the processing coefficients are placed into the computer disk file and are ready to process the full ERTS CCT or portions of the CCT defined by the investigator. Decision products, produced for this study, included printouts giving the area covered by each land/water category, decision imagery, and decision map overlays.

The processing coefficients are first applied to categorize that portion of the CCT covering the study area. This first step in the decision processing resulted in a new or categorized CCT, wherein each ERTS spatial element is represented by a code designating one of the land-use/water categories. This first step also results in a computer-generated area measurement table.

Area Measurement Table - The area measurement table provides a quantitative measure of the amount of land that falls within a particular category in terms of square kilometers, acres, and as a percent of the total area processed.

Categorized Imagery - The categorized tape produced from decision processing was also used to generate 70-mm imagery wherein each image shows a single land/water category at a scale of 1:1,000,000. In this case a color-code is used to designate each land-water category. Categorized imagery is produced rapidly and provides an immediate overview of the processed scene. The imagery was particularly useful for comparing results of decision processing with ground truth to confirm classification accuracy.

Categorized Map Overlays - To produce land-use classifications that will directly relate to a map, the categorized CCTs is submitted to a second stage of processing. In this stage, a new tape is generated that has data corrected for Earth rotation and that is formatted to be compatible for driving the Gerber plotter. This tape, when played back by the computer, causes a geometrically-corrected map of a specified target category to be drawn on film at a map scale selected by the operator. The operator has an option of obtaining either boundary line drawings which enclose a select land/water category or filled-in boundaries. The film, when removed from the plotter and photographically processed, provides transparent overlays which can be used directly, or processed further to produce color-coded land-use overlays.

5. RESULTS AND DISCUSSION

5.1 WATER QUALITY AND COLOR MEASUREMENTS

5.1.1 WATER QUALITY VARIATION IN TEST LAKES

Seasonal variations in the test lakes during spring-fall, 1973 are compared in Figures 12 - 15 with respect to four parameters: water transparency, color, particulate carbon, and total particulates. These variables have a direct bearing on water color and reflectance as monitored by ERTS. The figures indicate that on any particular date the lakes may be arranged into categories according to color, turbidity, etc. For example, on March 27 and June 7 water quality factors in the test lakes were distributed as shown in Figures 16 and 17, respectively. Here the values are grouped into classes which are arbitrary but represent differences in water quality that are significant. Although it is quite possible for six lakes of identical trophic condition to differ this much on any given day, the same values taken as averages would indicate important differences among the lakes in their degree of eutrophication. To be feasible as a monitoring tool, ERTS must detect differences of this general magnitude. It was hoped that a classification of the lakes from ERTS data (reflectances values) would confirm one or more of these natural groupings (Figures 16 and 17) with some degree of sensitivity.

5.1.2 TROPHIC CONDITION OF TEST LAKES

Other data besides those already given indicate the general trophic state of test lakes. Vertical profiles of temperature and dissolved oxygen (Figure 18) were measured on September 12, 1973. These show the depletion of oxygen with depth, resulting from organic decay. The extent to which the hypolimnion (or zone below the thermocline) is depleted during the summer stagnation period is one measure of the lake's enrichment level and productivity in surface waters in proportion to its depth and volume.

After consideration of all of the data in the Figures 12 - 18, the test lakes were arranged in the following hierarchy of increasing eutrophication levels:

Orchard (mesotrophic)
Lower Long
Angelus
Cass
Forest
Island (eutrophic)

Figure 12 Variation of Transparency (Mean of 2 stations) in Test Lakes in 1973.

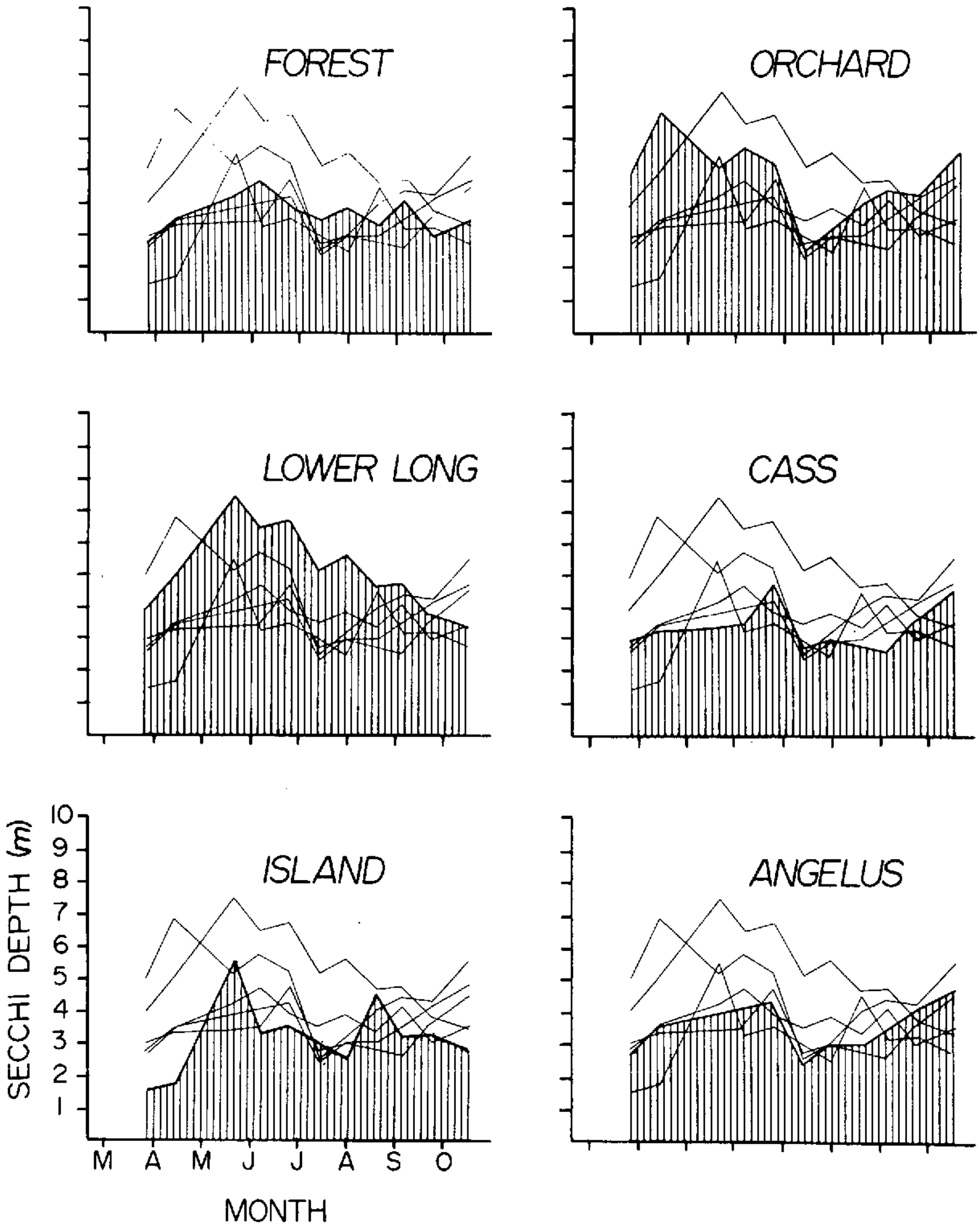

Figure 13 Variation of Apparent Color (Mean of 2 stations) in Test Lakes in 1973.

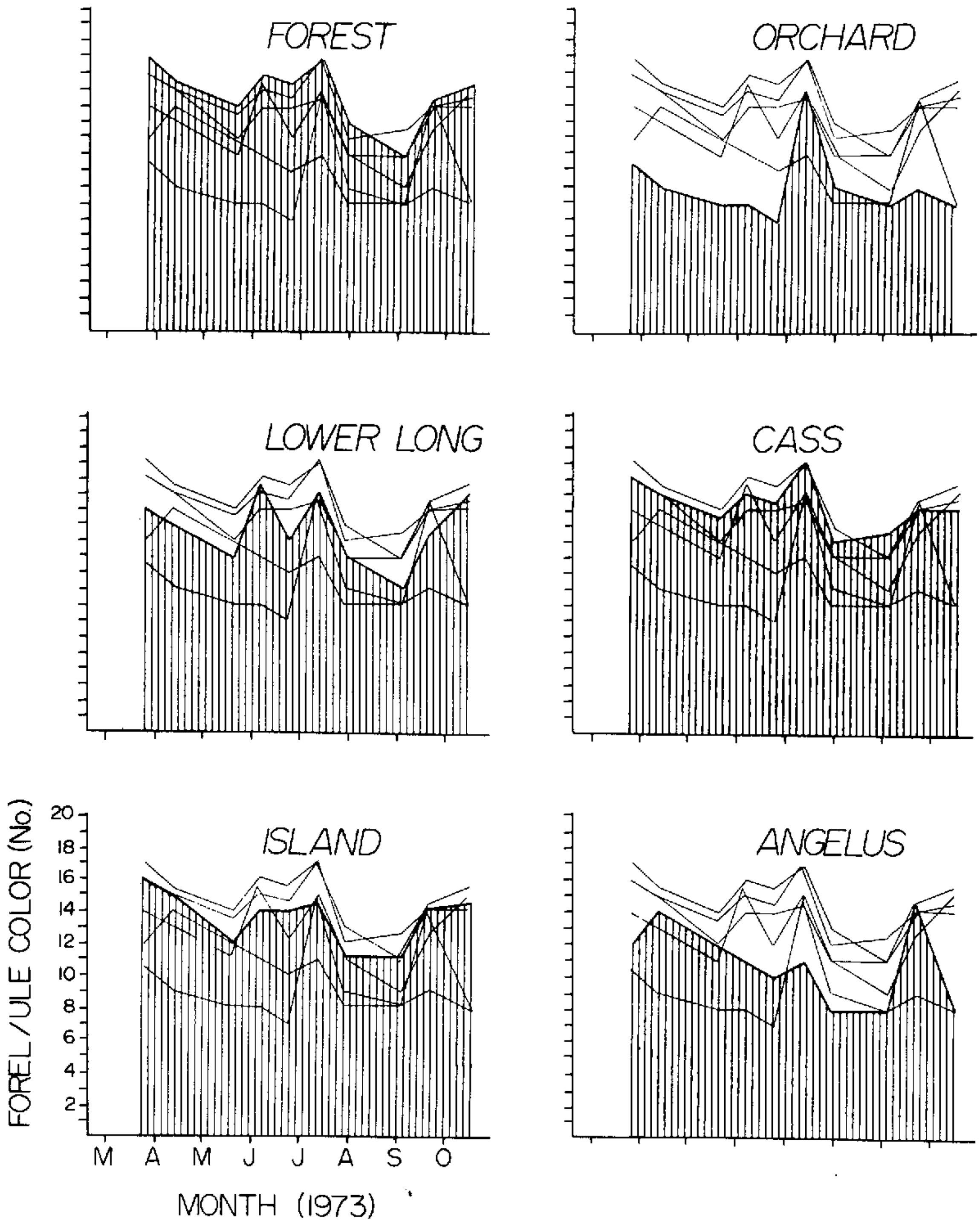

Figure 14 Variation of Suspended Particulate Carbon (Mean of 2 stations) in Test Lakes in 1973.

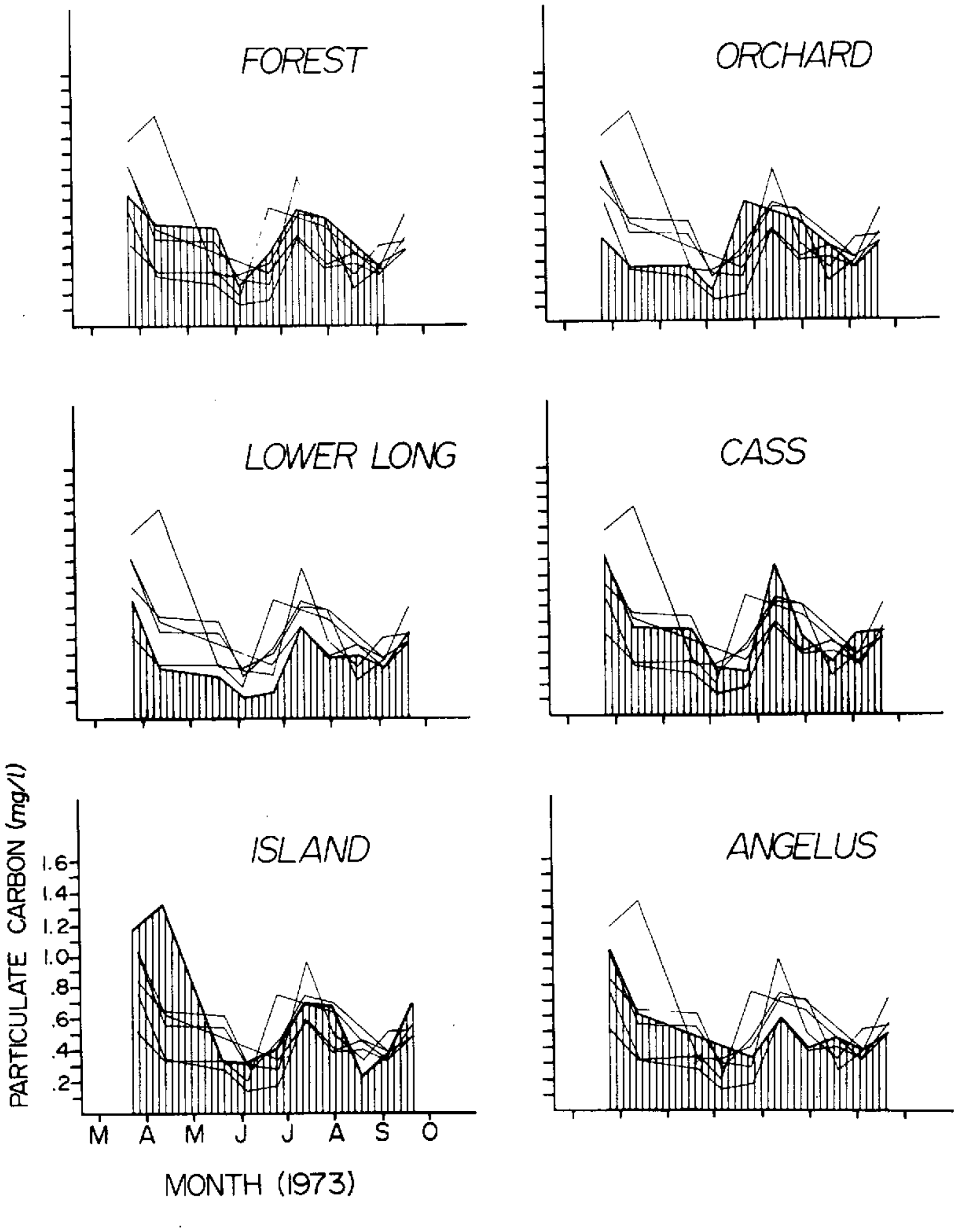

Figure 15 Variation of Suspended Total Particulates (Dry weight; mean of 2 stations) in Test Lakes in 1973.

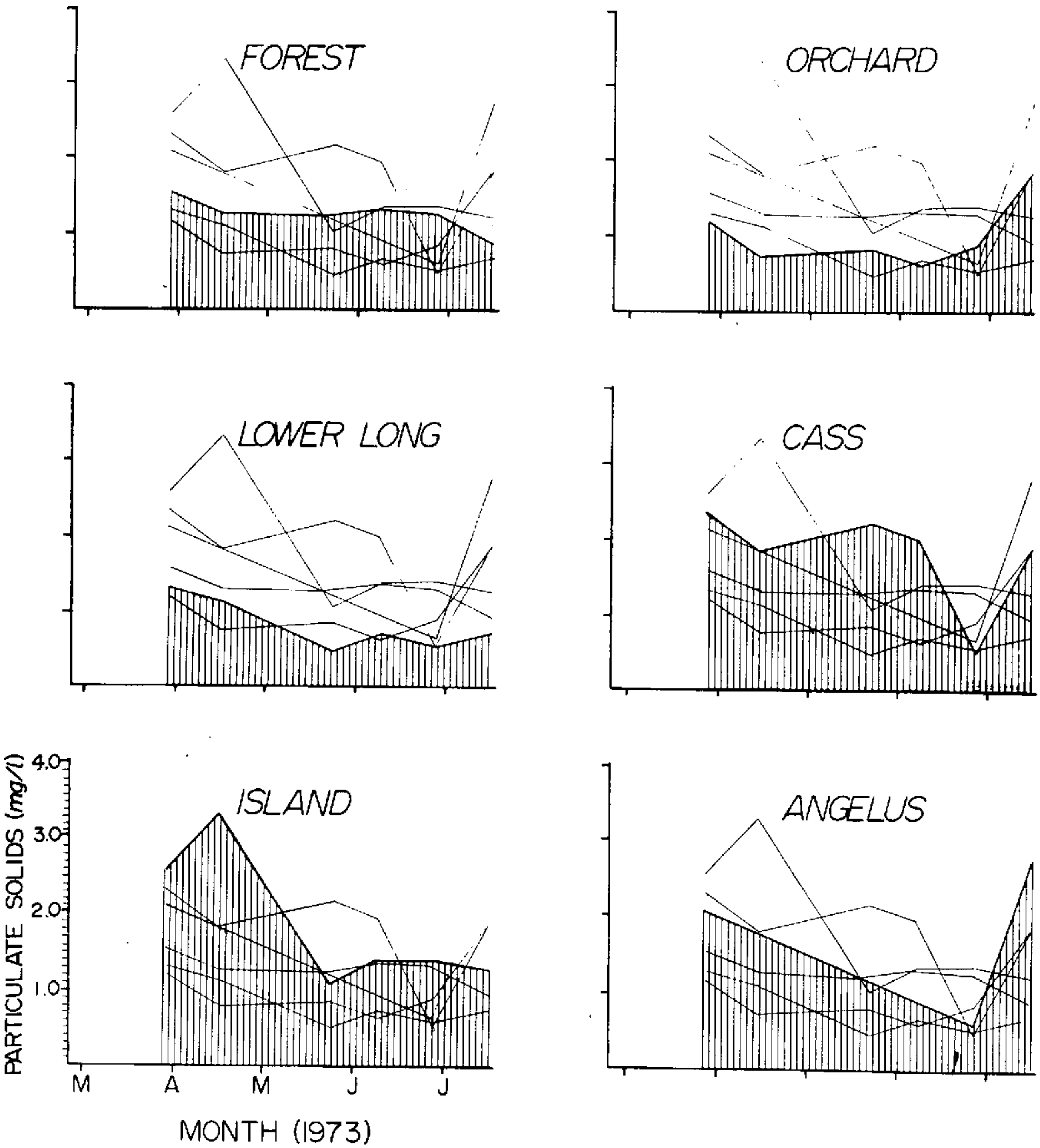

Figure 16 Arbitrary Classification of Lakes (March 27, 1973) Based on Water Quality Measurements.

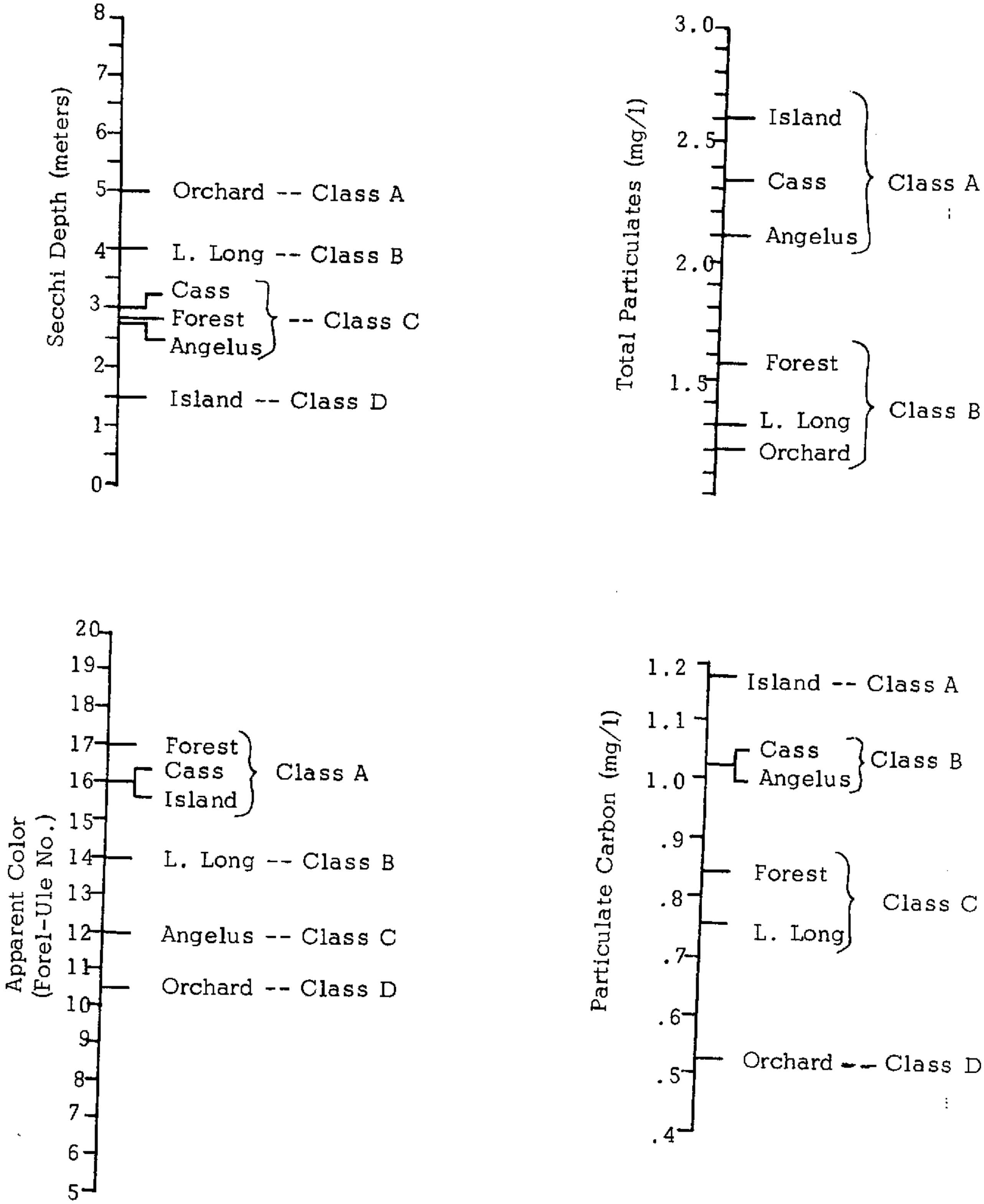

Figure 17 Arbitrary Classification of Lakes (June 7, 1973) Based on Water Quality Measurements.*

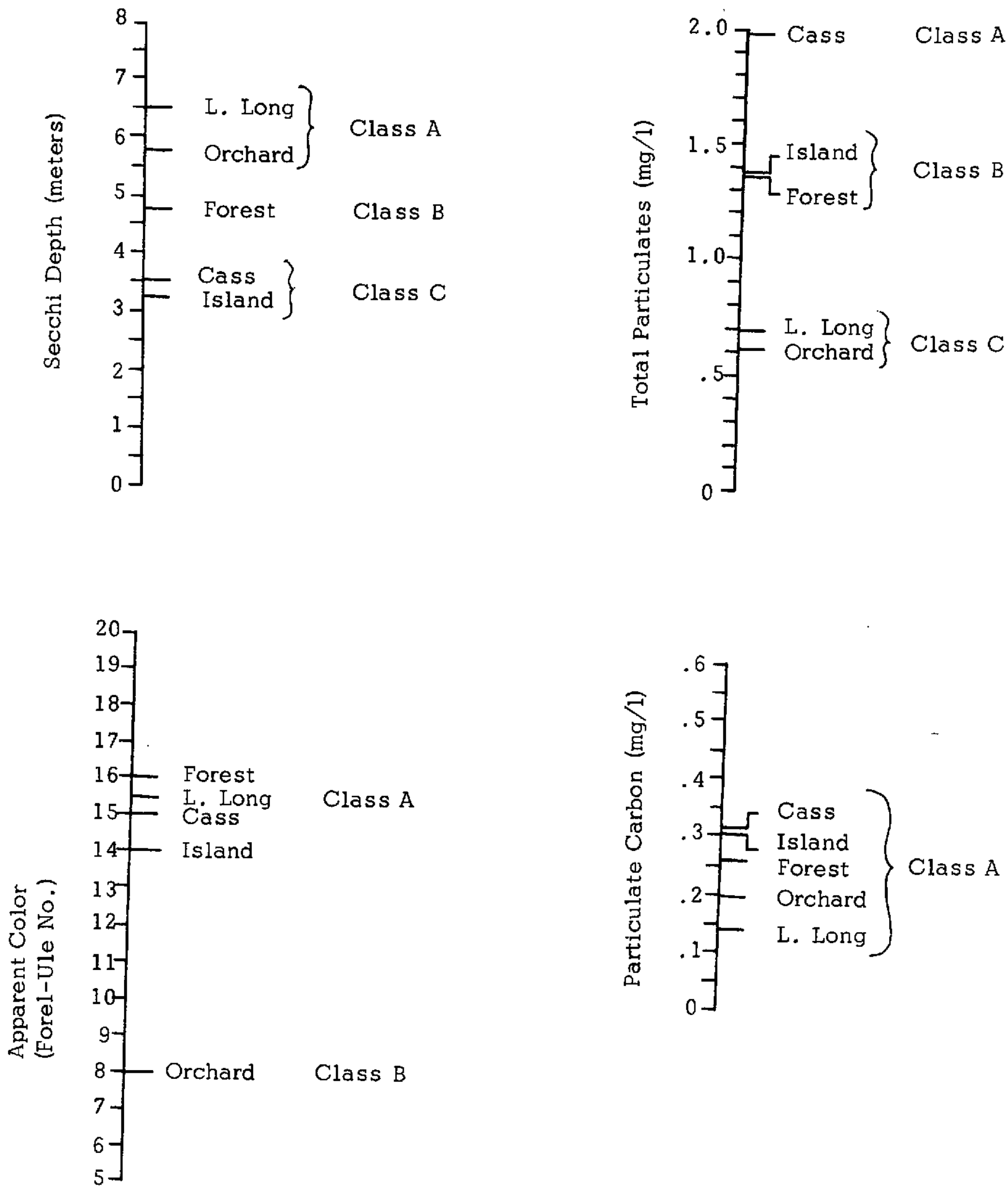

*(No data for Lake Angelus)

Figure 18 Temperature-Dissolved Oxygen Profiles in Test Lakes on September 12, 1973.

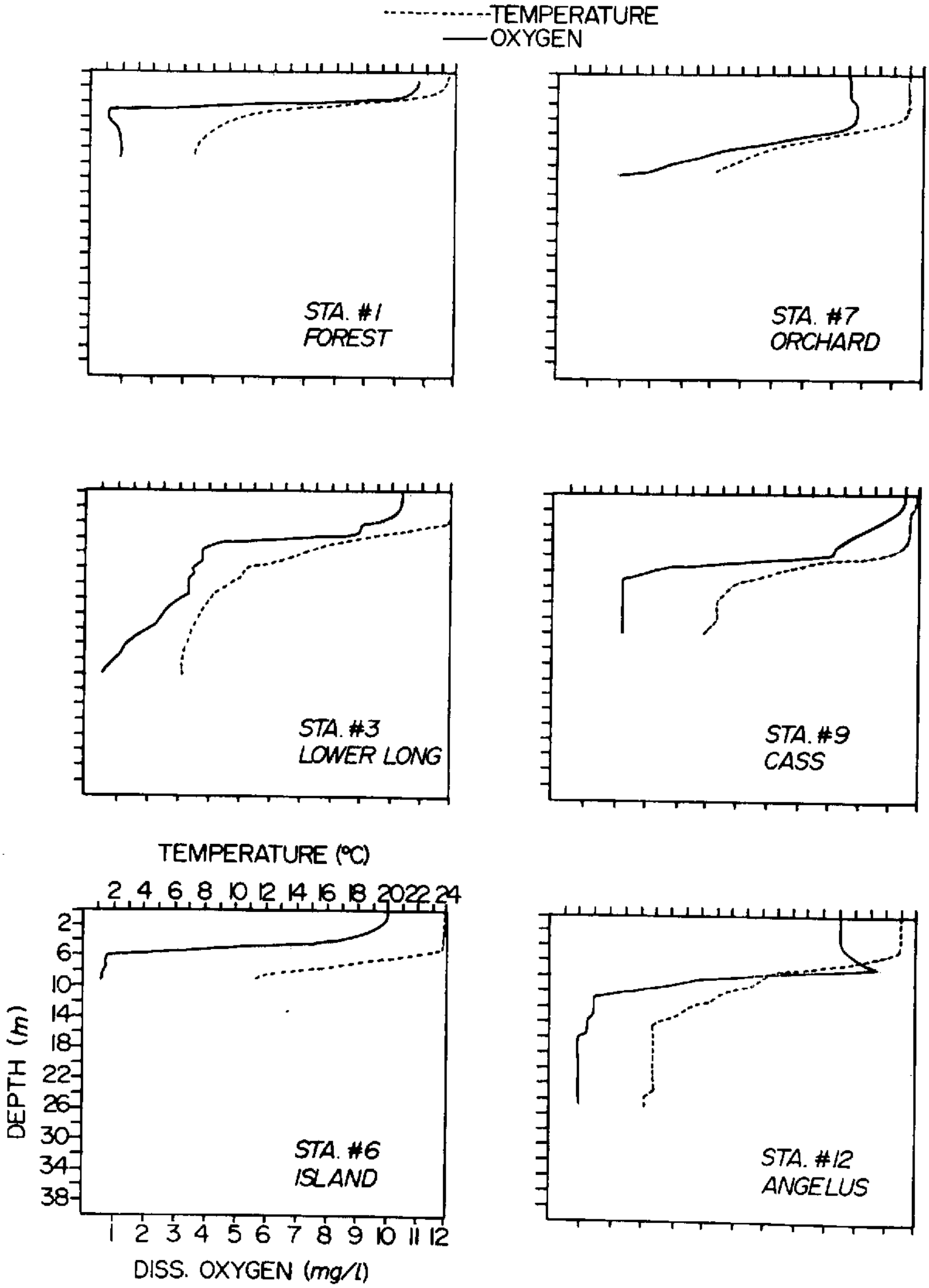

Given these limited data and the confusion that still exists in the literature about what distinguishes mesotrophic from eutrophic conditions, it is not reasonable to specify each lake's exact position in this general hierarchy. However, it is meaningful to compare individual measurements of reflectance (ERTS) and water quality factors, including water color in situ.

5.1.3 WATER COLOR ESTIMATION

Estimation or measurement of water color is an important part of any water quality monitoring concerned with trophic levels or organic production. Much of the biology and chemistry of natural water is manifested in water color. Plant and animal cells, their particulate remains (seston or leptopel), and their soluble residues (the "yellow stuff" or humic acids of fresh and salt waters) all contribute to water color directly. Consequently, water color is highly variable and responsive to trophic changes, especially in small, urban lakes. Color is also the principal water quality factor that is measureable by multispectral remote sensors. It is important that any measurements of water color by ERTS be relatable to some expression for the color in situ. There must be assurance that the increments of color change in lakes, as recorded by ERTS, represent comparable changes observed at ground level. Therefore, a rather detailed consideration of water color and its estimation in situ is warranted in this study.

Ideally, the determination of water color should be objective, sensitive, and repeatable. It should also be sufficiently convenient for use in the field (preferably in a small boat) if large numbers of routine observations are to be made. One consideration in developing ground-truth techniques for ERTS studies is that the methods and tools should be widely available, so that new methods may be applied easily by other investigators on lakes throughout the world.

Simple observations of water color without reference to any standards, even if done by an experienced person, are likely to be unreliable since they depend heavily on elements of color recognition and memory. Human abilities vary widely with respect to both. On one hand it is undoubtedly true that the classification of trophic levels based on fine distinctions of color will require precise instruments such as scanning spectroradiometers. On the other hand, visual comparisons of water with color standards have long been accepted as the simplest means of estimating lake and ocean colors in situ. Under proper conditions the normal human eye is sensitive to spectral shifts on the order of only a few nannometers (Optical Society of America, 1953).

The two most common types of water color standards are the following:

a. Platinum-Cobalt Standards

Hazen (1892) first developed a series of water color standards composed of varying concentrations of potassium chloroplatinate and cobalt chloride in dilute hydrochloric acid. On a scale of 1, 000, each unit is comparable to 1 ppm of chloroplatinate ion. This mixture forms a stable solution of pale yellow to brown color. In common use, the standards and sample water are compared in long glass tubes by transmitted light. Alternatively, color class discs are substituted for the liquid standards. Although accepted widely in water analysis practice (Standard Methods, 1971), the platinum standard has serious drawbacks. Even small amounts of turbidity increase the "apparent" color of water samples (removal of particles by lengthy centrifugation is recommended for estimation of "true color"). Second, lake color may vary greatly with depth, especially below the epilimnion. Thus, a small sample is scarcely representative of the entire photic zone. Third, the yellow-brown component of color in lakes is pH dependent and somewhat unstable to sunlight. Therefore, transport of samples or even dilution in the field, for color matching purposes, may introduce errors. Finally, from the standpoint of correlating water color with ERTS, it is inadvisable to gauge lake color based on samples removed from the natural environment of transmitted, scattered, and reflected light. These variables and others contribute to the apparent color of lakes as recorded by remote sensors. For the reasons above, the platinum-cobalt standards were not used in the present study.

b. Forel-Ule Standards

Forel (1889) devised a series of blue to green water color standards, which was extended by Ule (1892) to include yellow to reddish-brown colors. The combined scale, still widely used, consists of 22 different proportions of cuprammonium sulfate (blue), potassium chromate (yellow), and cobalt ammonium sulfate (red-brown), combined as in Figure 19a.

The color ratios are also shown graphically in Figure 19b. Units of the Forel-Ule scale do not correspond to any quantitative measure of ions, however. The solutions, normally contained in sealed glass

Figure 19 (a) Composition of Forel-Ule standards (according to Hutchinson, 1957).

Solution*	I	II	III	IV	V	VI	VII	VIII	IX	X
1	100	98	95	91	86	80	73	65	56	46
2	0	2	5	9	14	20	27	35	44	54
3	0	0	0	0	0	0	0	0	0	0
Color	Blue		Greenish blue		Bluish green			Green		

Solution*	XI	XII	XIII	XIV	XV	XVI	XVII	XVIII	XIX	XX	XXI	XXII
1	35	35	35	35	35	35	35	35	35	35	35	35
2	65	60	55	50	45	40	35	30	25	20	15	10
3	0	5	10	15	20	25	30	35	40	45	50	55
Color	Greenish yellow					Yellow				Brown		

* Solution 1 = 0.5 g. $CuSO_4 \cdot 5H_2O$ + 5 ml. strong NH_4OH + to 100 ml. H_2O
2 = 0.5 g. $K_2CrO_4 \cdot 5H_2O$ + 5 ml. strong NH_4OH + to 100 ml. H_2O
3 = 0.5 g. $CoSO_4 \cdot 7H_2O$ + 5 ml. strong NH_4OH + to 100 ml. H_2O

(b) Proportions of color components in Forel-Ule standards.

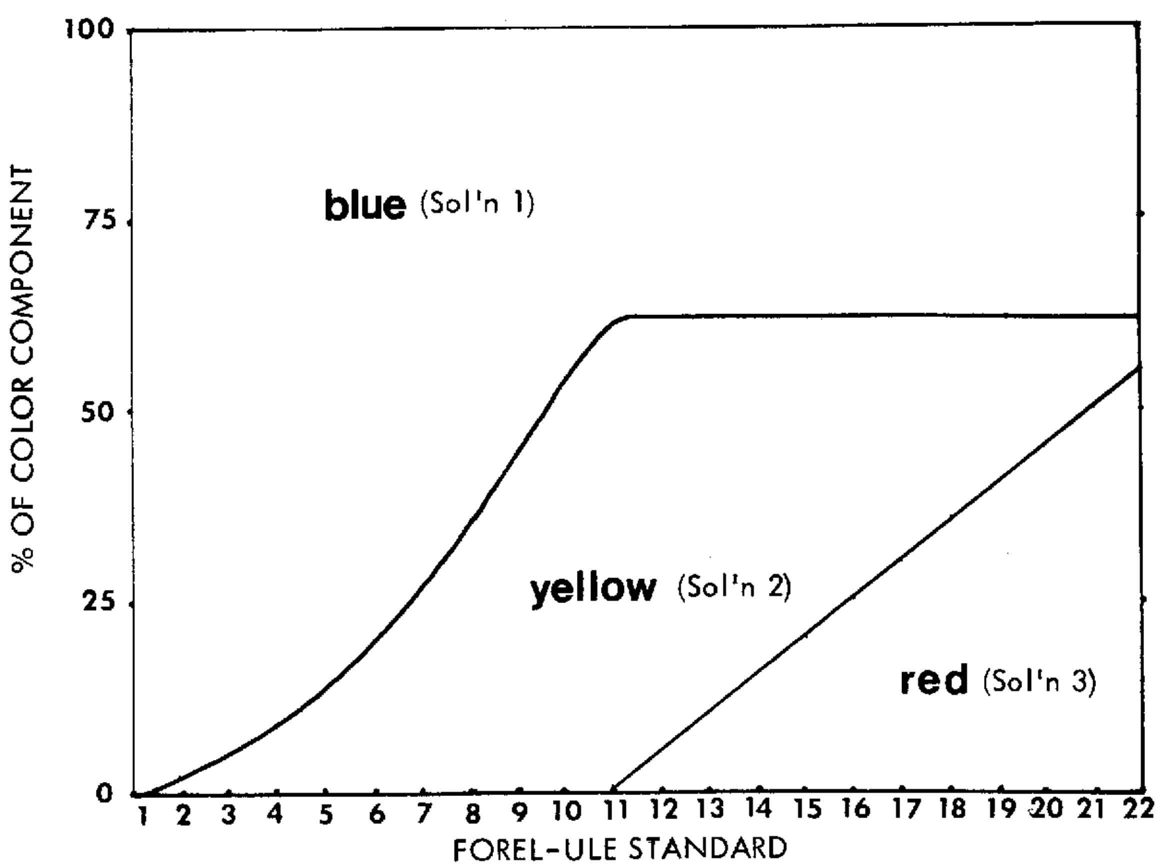

vials (13mm O. D.), are stable and form a series of routhly equal gradations in color. Though arbitrary, the scale was designed to furnish an empirical standard of actual water colors as viewed downward from the surface, whether with or without a submerged, white disc as background.

LaMotte Chemical Company of Chestertown, Maryland, manufactured some of the Forel-Ule standards used in this work. Their instructions for field use are as follows:

1. Immerse the Secchi disk with the white side up. Lower the disk to a total depth of one meter below the water's surface. Avoid direct light reflection.

2. Insert the distilled water ampoules in the blank holes in the comparator (a plastic holder with windows covered by a white diffusion filter).

3. Hold the comparator at arm's length so as to view both the Secchi disk and the Forel-Ule scale.

4. Compare the color as seen through the blank hole in the comparator with the color of the water as viewed over the Secchi disk.

5. The value in the comparator that most nearly matches the color of the water is taken as the value for that sampling location. Record this value.

As prescribed, this method is unworkable and leads to faulty estimates of water color. After considerable experimentation, we found that a far more effective method requires the use of a special viewing tube which allows a side-by-side comparison of the standards and water color. The standards are viewed in a mirror by transmitted sky light and the upwelling light ("light of the water") is viewed through the glass bottom of the tube. No Secchi disc is used. Seen in this manner, the standard colors compare favorably in saturation and brightness to those of the deep water illuminated by the same daylight. The observer has little difficulty making the best choice of a matching standard. The design of this viewer is shown in Figure 20.

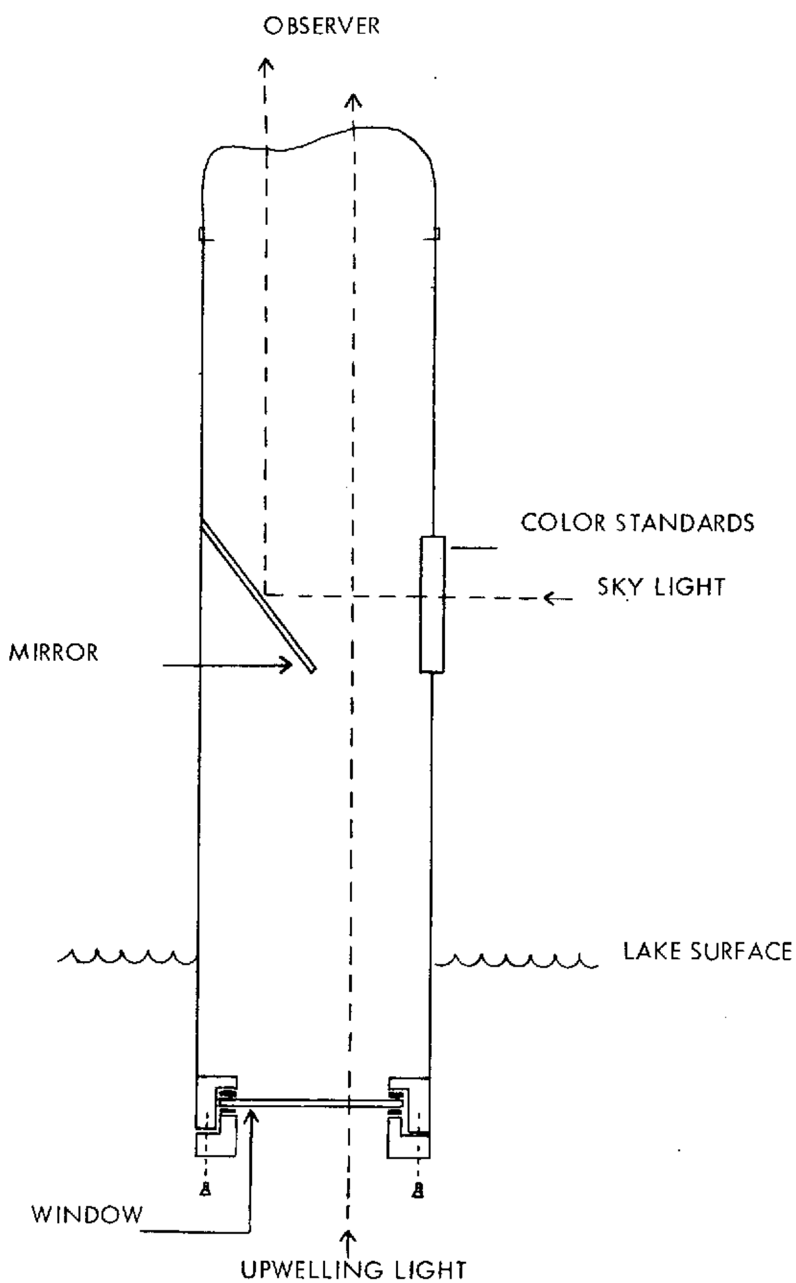

b. Operational Diagram of Water Color Viewing Device

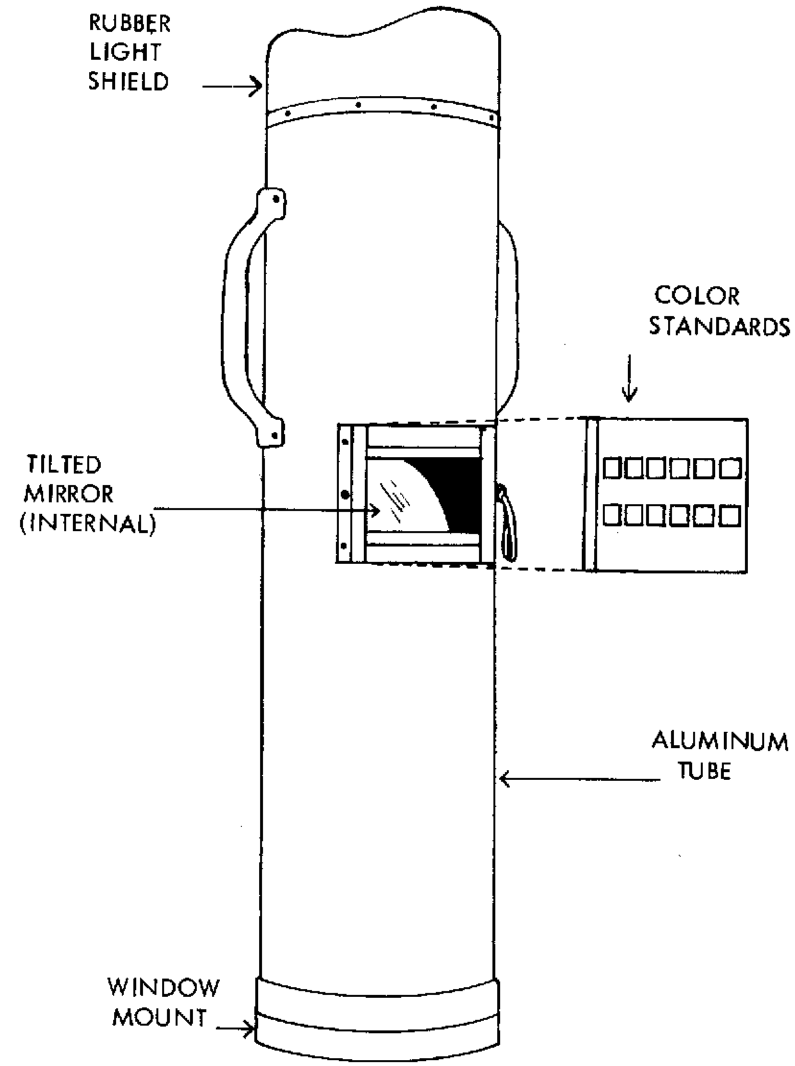

a. Design of Water Color Viewing Device (Used with Forel-Ule Standards for Estimating Water Color *in situ*)

5.1.4 SPECTRAL ANALYSIS OF FOREL-ULE STANDARDS

The inorganic contents of the Forel-Ule standard bear no relation to the largely organic substances that produce color in natural waters. Even so, the obvious similarity between the standard and water colors suggests that their reflectance or transmittance spectra are similar. Any such relationship becomes important when one considers that the ratios of reflectance between ERTS spectral bands might be useful in characterizing the colors of lakes and of water color standards. As the dominant color (λ max) of water shifts by uniform steps toward longer wavelengths (i.e., green to brown to red), the transmittance or reflectance ratios of band 4 to band 5 should decrease in some correspondingly regular fashion. Similarly, if the Forel-Ule scale is composed of even hue increments, the same correlation should apply. Since Forel-Ule standards are used here to characterize lake colors in situ, we decided to define each of their spectral curves with respect to the ratios of total transmittance within three of the ERTS MSS bands; band 4, band 5, and band 6. At the time, no means were available to obtain reflectance curves of these solutions in the 400 to 800 nm range. The standards were prepared according to Hutchinson (1957).

Transmittance (% T) curves of the three component solutions, read on a Zeiss recording spectophotometer, are shown in Figure 21. Transmittance curves of the 22 standards, composed of the three solutions as defined by Hutchinson, are shown in Figures 22 through 26. The areas under each curve within the first three "ERTS bands" (assuming rectangular bandpass characteristics) were measured with a planimeter. Using these values, we determined certain transmittance ratios using the "ERTS band" regions of each curve; band 4 (0.5 to 0.6 μm), band 5 (0.6 to 0.7 μm), and band 6 (0.7 to 0.8 μm). The results are given in Table 2. The point of this exercise was to see whether these "ERTS band" ratios for Forel-Ule standards resembled the corresponding reflectance ratios for lake waters matching these standards. This comparison is discussed later in connection with the data in Table 3.

The band ratios, as determined above by measuring the area under Forel-Ule transmittance curves, were also determined experimentally in the field, using a clear sky background and reading the transmittance through each of the 22 standards with the RPMI. The RPMI records radiance and irradiance in the same bands as ERTS. This was done to examine the "ratio technique" further as a means of characterizing the spectral shift of standards from blue to red-brown. The results of both methods are compared in Figure 27.

Figure 21 Transmittance (%) of Forel-Ule Component Solutions

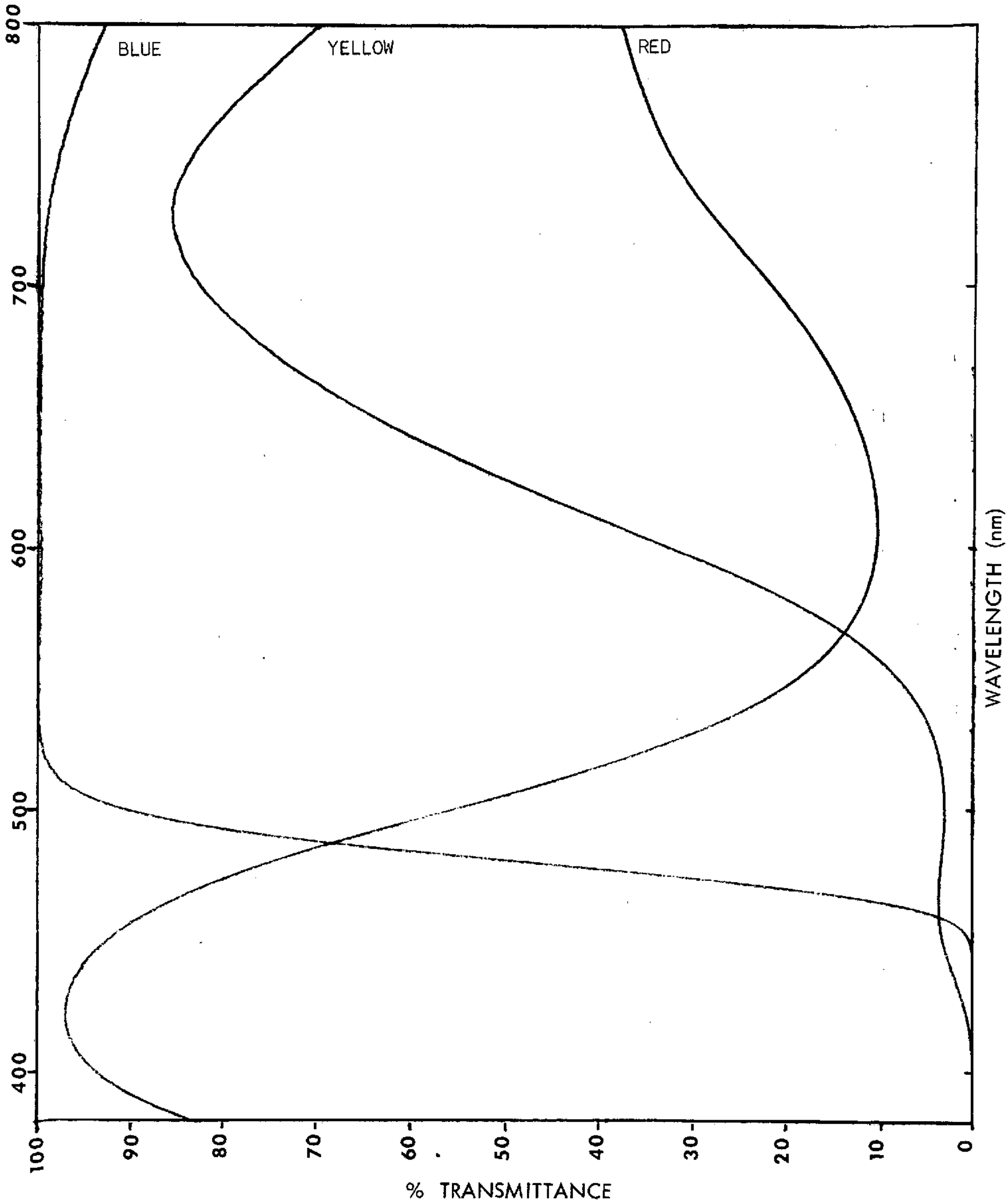

Figure 22 Transmittance (%) of Forel-Ule Standards

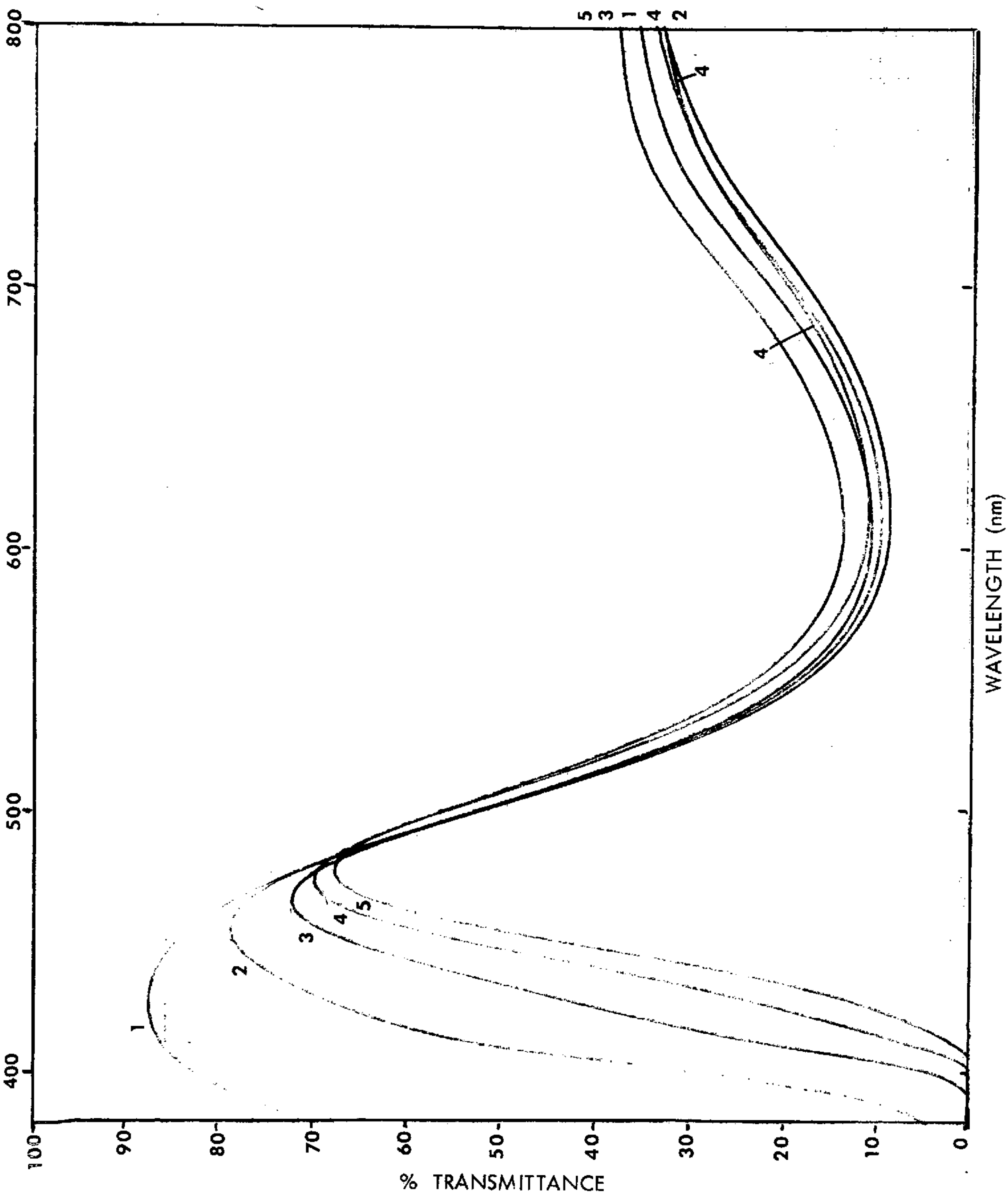

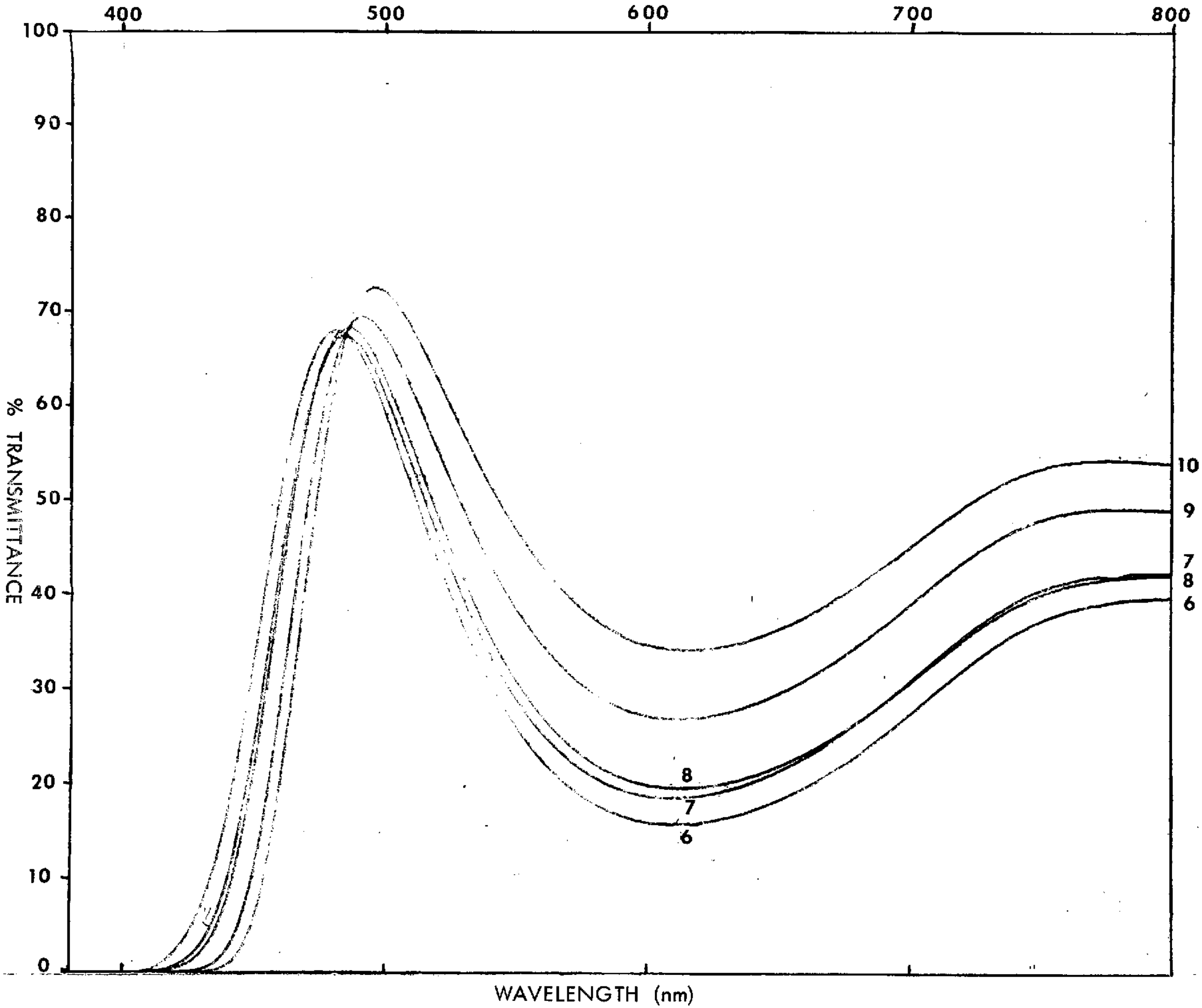

Figure 23 Transmittance (%) of Forel-Ule Standards

Figure 24 Transmittance (%) of Forel-Ule Standards

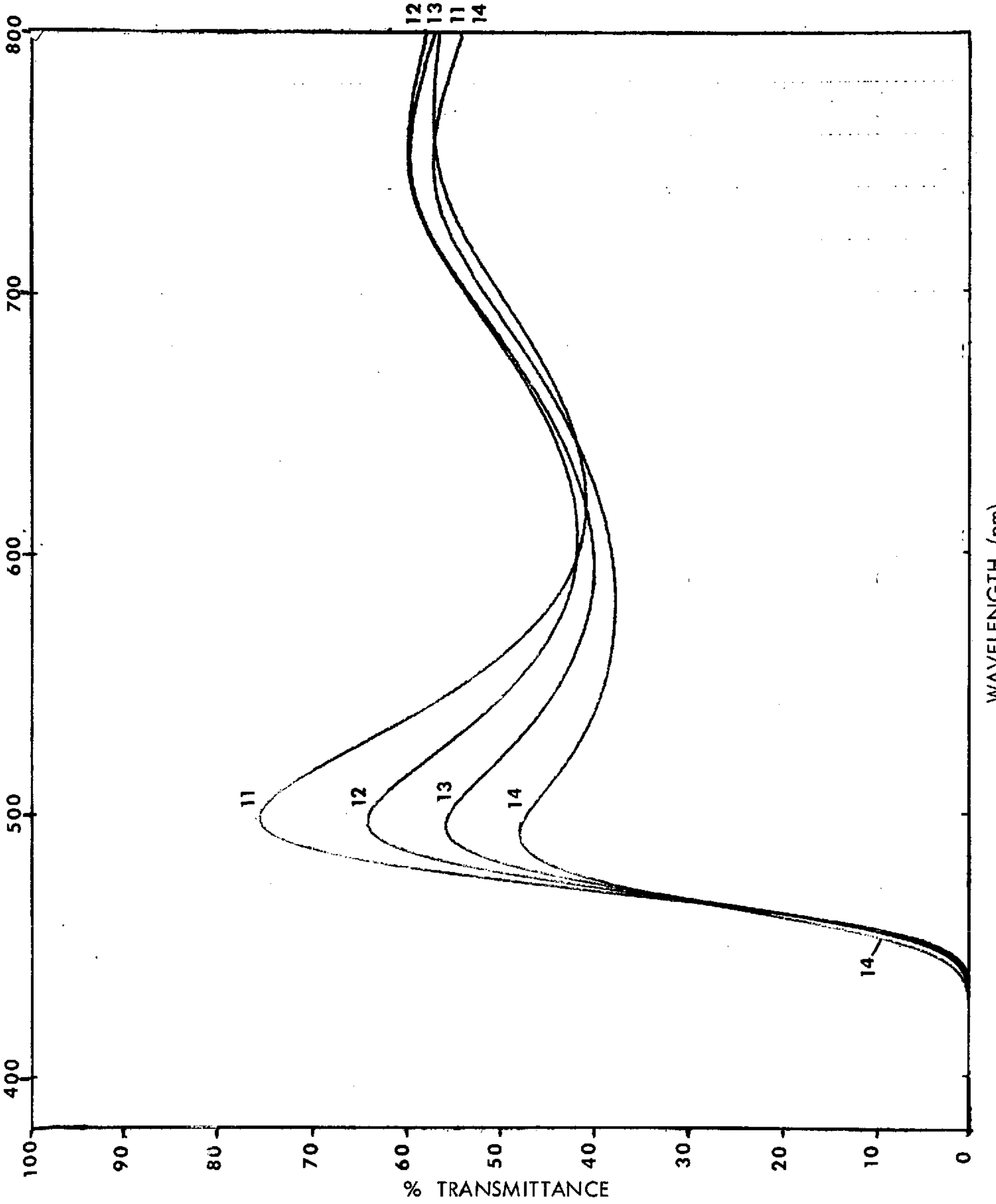

Figure 25 Transmittance (%) of Forel-Ule Standards

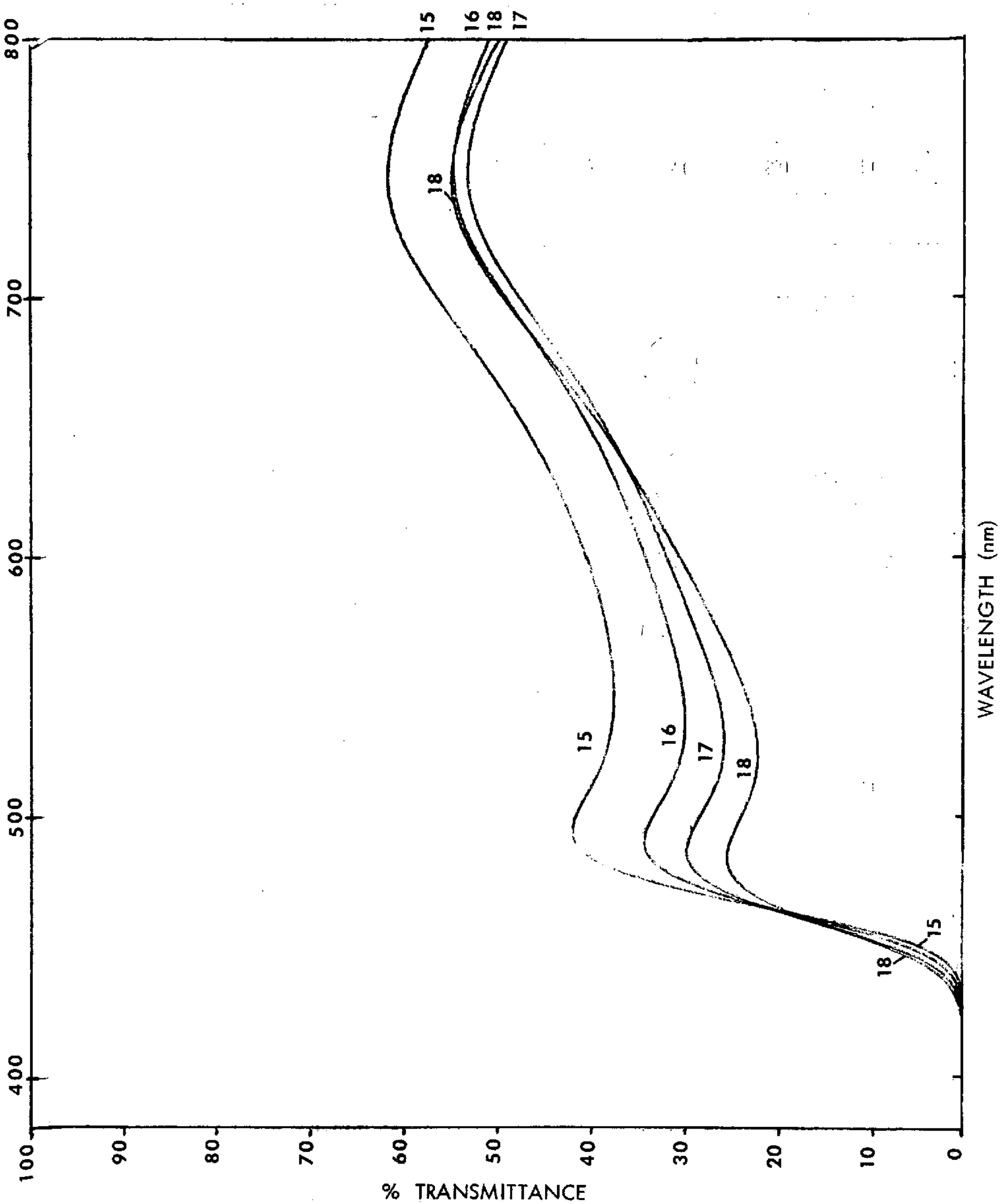

Figure 26 Transmittance (%) of Forel-Ule Standards

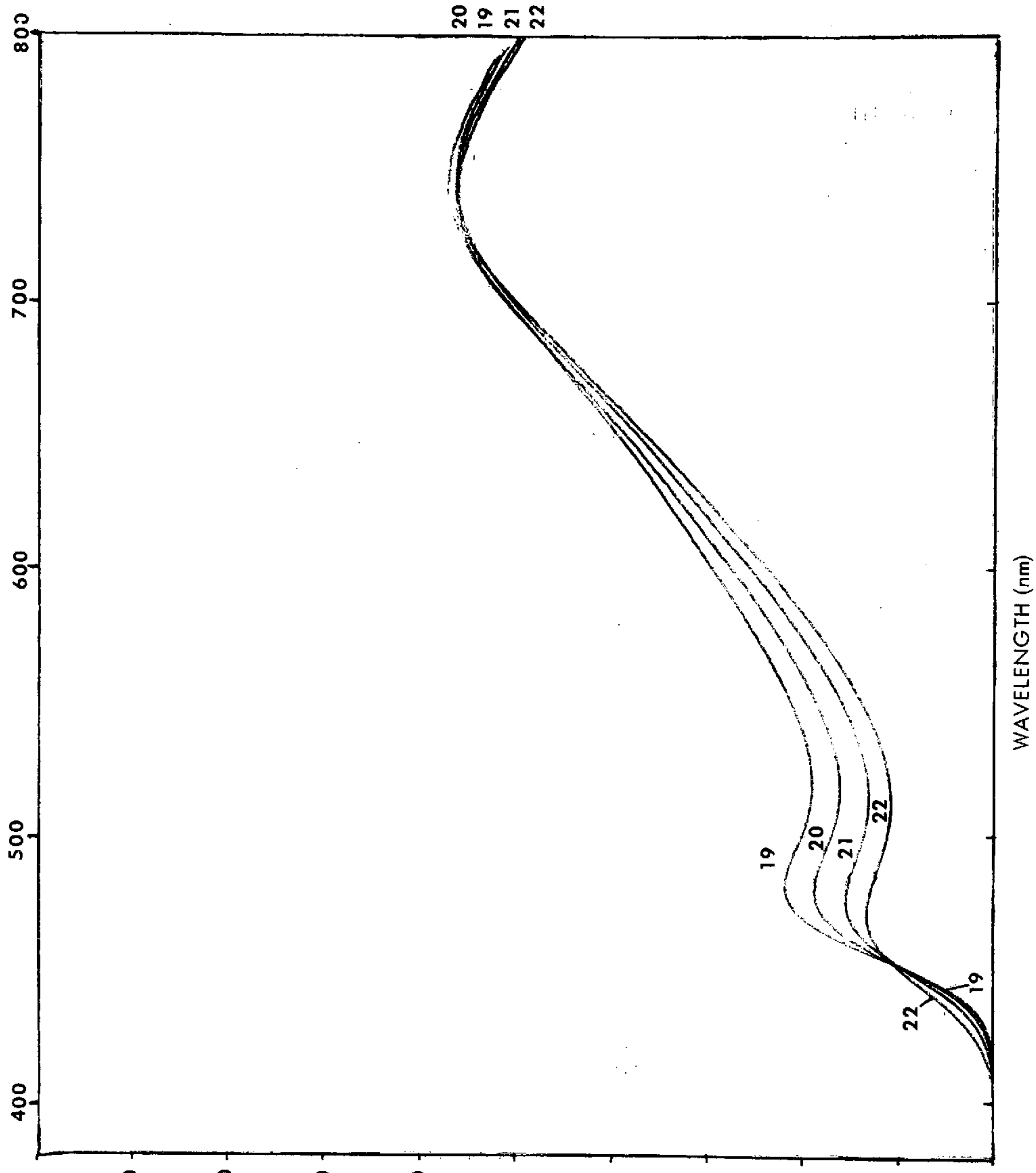

Table 2. Percent transmittance (integrated by planimeter) within ERTS bands 4, 5, and 6. Ratios of band transmittance.

Forel-Ule #	ERTS SPECTRAL BANDS 4	5	6	BAND RATIOS 4/5	4/6
1	.228	.127	.279	1.795	.817
2	.221	.113	.270	1.956	.819
3	.235	.144	.309	1.632	.761
4	.258	.135	.282	1.911	.915
5	.277	1.70	.343	1.629	.808
6	.296	.200	.358	1.480	.827
7	.318	.233	.396	1.365	.803
8	.357	.240	.391	1.488	.913
9	.408	.312	.454	1.308	.899
10	.496	.383	.511	1.295	.971
11	.565	.435	.539	1.299	1.048
12	.514	.447	.592	1.150	.868
13	.433	.443	.591	.977	.733
14	.406	.440	.550	.923	.738
15	.387	.482	.596	.803	.649
16	.312	.408	.532	.765	.586
17	.280	.383	.501	.731	.559
18	.250	.392	.538	.638	.465
19	.226	.402	.534	.562	.423
20	.199	.396	.552	.503	.361
21	.174	.381	.542	.457	.321
22	.152	.371	.532	.410	.286

Figure 27 Comparison of % transmittance of color standards within ERTS bands 4 and 5. Planimeter measurement of area under T-curves (———) ; direct RFMI measurement of standards (-----).

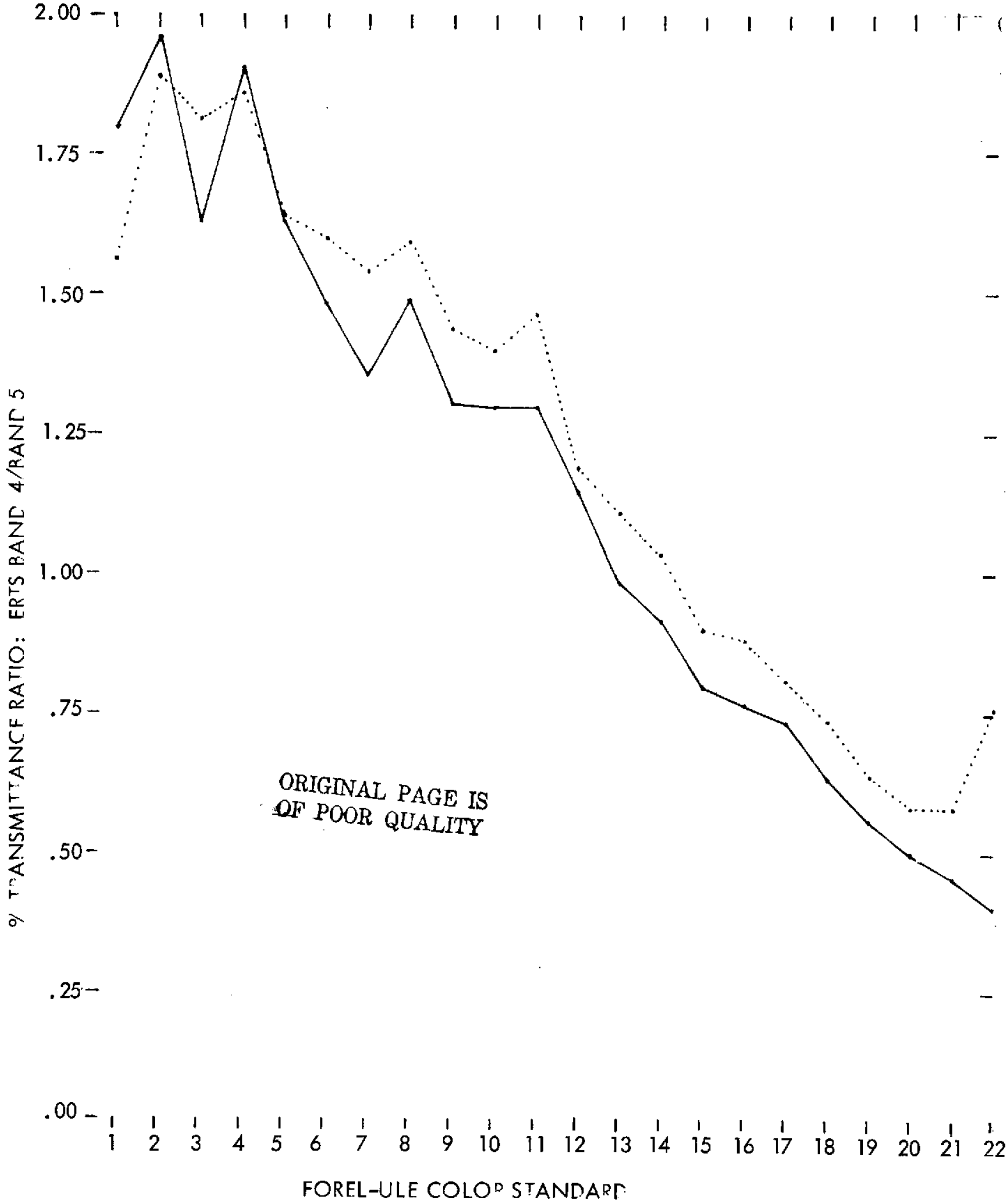

5.1.5 TRANSLATION OF FOREL-ULE COLOR ESTIMATES TO THE CIE SYSTEM

A second method was developed to compare the Forel-Ule expression for water color with reflectance measurements made by ERTS or similar multispectral sensors. Transmittance curves of the standards have been converted to tristimulus values in the CIE system of color specification. The 22 standards were then plotted in the CIE chromaticity diagram, as shown in Figure 28. Lines drawn from the illuminant or neutral point through these loci intersect the boundary line, indicating the "dominant wavelength" value for each standard. The percentage-distance that each standard point is displaced from the neutral point toward the boundary line is the "excitation purity." These values, summarized in Table 3, indicate that the color differences between standards are fairly constant, although standards 7 and 15 are somewhat anomalous with respect to the others.

We have also attempted to translate ERTS measurements of reflectance into CIE coordinates by analysis of the transmission spectra of the ERTS bandpass filters. ERTS bandpass characteristics are plotted in Hugh's report (1972). This step would permit a direct comparison of lake colors recorded (as band ratios) by ERTS with those estimated using Forel-Ule standards on the ground. In practice, however, some of the CIE values derived from ERTS data by this computer program were unrealistic: i.e., with a negative sign. Clearly there are atmospheric or other corrections that must be considered. Work will continue on this problem. At any rate it is important that ERTS data be evaluated in terms of, not only percent of reflectance in each band, but of a universal standard of color that these combined values represent. The CIE specification would then become an expression of the ERTS spectral "signature."

5.2 DETECTION OF LAKE FEATURES IN ERTS BULK IMAGERY

Visual study of the single-band, photographic (bulk) imagery yielded only limited information about lake features as noted in Table 4. Under the best atmospheric conditions, the subtle variations in lake water and bottom reflectance were detectable to some degree in bands 4 (500 - 600 nm) and 5 (600 - 700 nm). No microdensitometry was attempted due to the small size and generally low reflectance of test lakes. Land-water boundaries were best seen in bands 6 (700 - 800 nm) or 7 (800 - 1100 nm).

Figure 28 Forel-Ule Standard Colors Plotted on CIE Chromaticity Diagram, I. C. L. Illuminant C

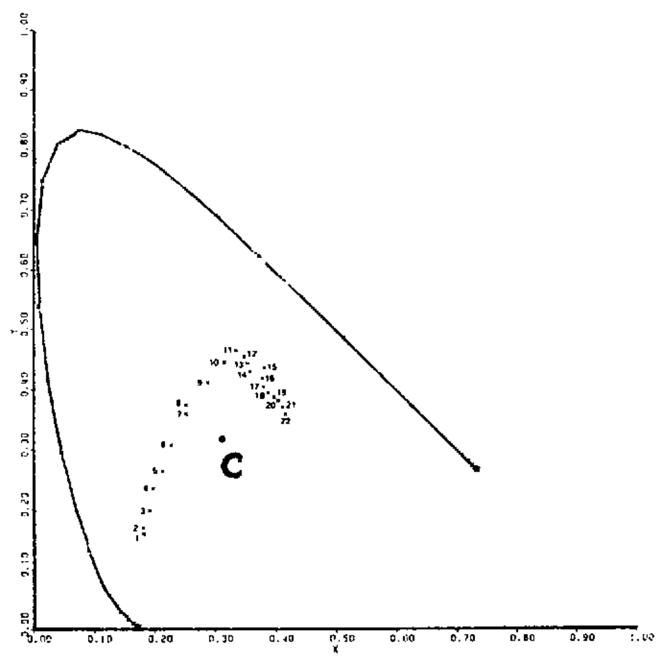

Table 3. CIE color specification of Forel-Ule standards.

Forel-Ule Standard	CIE Coordinates X	CIE Coordinates Y	Dominant Wavelength (Hue)	Excitation Purity (Saturation)	Luminous Reflectance (Brightness)
1	.202	.238	482	.49	(Not Determined)
2	.203	.259	484	.46	
3	.218	.298	488	.36	
4	.233	.353	497	.27	
5	.250	.386	506.5	.20	
6	.274	.435	530	.25	
7	.309	.499	550	.49	
8	.306	.483	550.5	.45	
9	.346	.512	558	.63	
10	.374	.524	563	.73	
11	.394	.526	566	.79	
12	.403	.514	568	.78	
13	.405	.503	568.5	.76	
14	.407	.488	570	.72	
15	.426	.485	572.5	.77	
16	.419	.470	572.5	.71	
17	.418	.455	573.5	.67	
18	.420	.440	575.5	.62	
19	.425	.428	578	.61	
20	.427	.419	579	.59	
21	.429	.400	582.5	.55	
22	.427	.380	585.5	.50	

Table 4. Named Lakes Visible in ERTS-1 Image of Band 7 September 28, 1972 (ID No. 1067-15463) of 50 Square Mile Portion of the Test Area.

Lake Name	Area (Acres)	Max. Depth (Feet)	Shore Length (Miles)	Lake Shape	Shape Fit: Image/Map
Cass	1280	123	11.5	Elliptical	Good
Orchard	788	110	5.7	Circular	Good
Union	465	102	4.0	Elliptical	Good
Sylvan	458	---	4.7	Triang. - Square	Good
Pine	395	90	4.3	Elliptical	Good
Elizabeth	363	90	3.3	Rectang.	Good
Upper Straits	323	96	5.5	Elongate	Good
Walnut	232	101	3.2	Square	Good
Lower Long	178	95	3.7	Elongate	Good
Middle Straits	171	55	4.1	Elongate	Good
Green	166	---	3.0	Elongate	Good
Upper Long	108	---	2.5	Elongate	Good
Island	101	35	2.0	Triang.	Good
Square	94	67	1.4	Square	Good
Crescent	90.4	40	2.3	Elongate	Fair
Hammond	85	---	1.5	Circular	Good
Otter	81	---	1.8	Elliptical	Poor
Crystal	51	---	2.2	Elongate	Good
Forest	40	55	0.8	Circular	Good
Turtle	37	65	1.4	Elliptical	Good
Orange	37	---	1.1	Elliptical	Good
Wabeek	25	---	0.9	Rectang.	Good
Geneva	19.2	---	0.8	Elliptical	Good
Darby	16.5	---	0.7	Square	Good
Simpson	13.2	---	0.5	Elliptical	Fair
Crawford	13.0	---	0.5	Elliptical	Good
Morse	13.0	---	0.9	Rectang.	Fair
Mirror	11.0	25	0.5	Elliptical	Fair
Sodon	10	19	0.4	Circular	Fair
Landers	9.6	---	0.6	Rectang.	Good
Scotch	9.3	---	0.6	Elliptical	Good
Dawson's Mill Pond	8	---	1.1	Elongate	Poor
Fiddle	7.5	---	0.6	Elongate	Poor
Cross	7.3	---	0.6	Elliptical	Good
Dow	6.5	---	0.4	Square	Poor
Mud	6.2	---	0.5	Rectang.	Fair
Egg	5.6	---	0.3	Elliptical	Fair
Haines	5.5	---	0.4	Triang.	Fair

Identification of the smallest lakes (1 – 5 acres) was best in Bands 6 and 7. Shape, orientation and physical surroundings of the lakes did not significantly effect their identification. Identification also was not greatly improved in enlargements of the imagery produced directly from the CCTs. In summary, the information contained in bulk imagery was adequate to identify test lakes by size and shape, but not adequate to classify lakes by color and reflectance characteristics.

5.3 LAKE REFLECTANCE MEASUREMENTS

5.3.1 REFLECTANCE DISCRIMINATION IN BULK IMAGERY

It is well known by now that various gray levels, corresponding to high concentrations of water turbidity, are readily seen in ERTS bulk imagery; that is especially true in bands 4 (0.5 to 0.6 μm) and 5 (0.6 to 0.7 μm). Less turbid waters, such as in the test lakes, appear essentially black in all four bands of bulk imagery. Photographic imagery (70 mm) was also produced from CCTs at Bendix and was enlarged several times to emphasize details of water reflectance in test lakes. Very little structure was visible, however. We inferred from this that microdensitometry would have very limited value as a method of discriminating water quality differences among the test lakes, except during rare periods of extreme turbidity. The technique of "density slicing" the digitized data in ERTS CCTs is a much better means of distinguishing any minor differences in relative reflectance between lakes in one scene. This approach is described below in Section 5.3.3.

5.3.2 DETERMINATION OF ABSOLUTE REFLECTANCE

As a prelude to comparison of lake reflectances, an important step was to convert the digital levels from ERTS CCTs to absolute (%) reflectance values. This was accomplished using the Radiant Power Measuring Instrument (RPMI) and techniques developed by NASA Experiment MMC 655 and described in the appendix and summarized below.

Atmospheric Equation Model

The absolute reflectance of lake water, ρ, has obtained from ERTS radiance measurements, L, recorded on CCTs by the computer application of the equation

$$\rho = \frac{(L - L_A) \cdot \pi}{\tau (H_o \tau^m \cos Z + H_{SKY})} .$$

where the solar and atmospheric parameters beam transmittance τ ; path radiance, L_A; and direct-beam solar irradiance above the atmosphere, H_o;

are derived from RPMI measurements obtained by field teams deployed during ERTS overflight. The sun zenith angle Z was available in the ERTS CCT header information and was measured with the RPMI. The RPMI, the procedure for obtaining the atmospheric parameters, and the use of these parameters in the computer processing of ERTS data are discussed in detail in the appendix.

Transfer Calibration

Color panels, whose reflectance is known in each ERTS band, were used as points of reference to determine, by "transfer calibration", the reflectance of unknown surfaces. Since the RPMI's output is linear with reflectance, the procedure was, simply, to aim the RPMI at the calibration panel(s) as in Figure 1D of the appendix, note the meter indication, aim the RPMI at the target of unknown reflectance, and again note the meter indication. A straight-line extrapolation transforms the meter indication obtained from the unknown target to a reflectance value.

Figure 29 is a plot of the RPMI meter indication versus the reflectance of four cardboard panels, denoted A, B, C, and D. The absolute reflectance of the panels was known for each ERTS band and the plot of panel reflectance against meter shows a desired linear relationship. On July 13, 1973, the reflectance of Forest Lake water was obtained from a boat using this method, as illustrated in Figure 30. RPMI readings for this case were made one meter about the panels and lake surface.

Figure 29 Plot of reflectance (%) vs. RPMI readings for reference panels A-D.

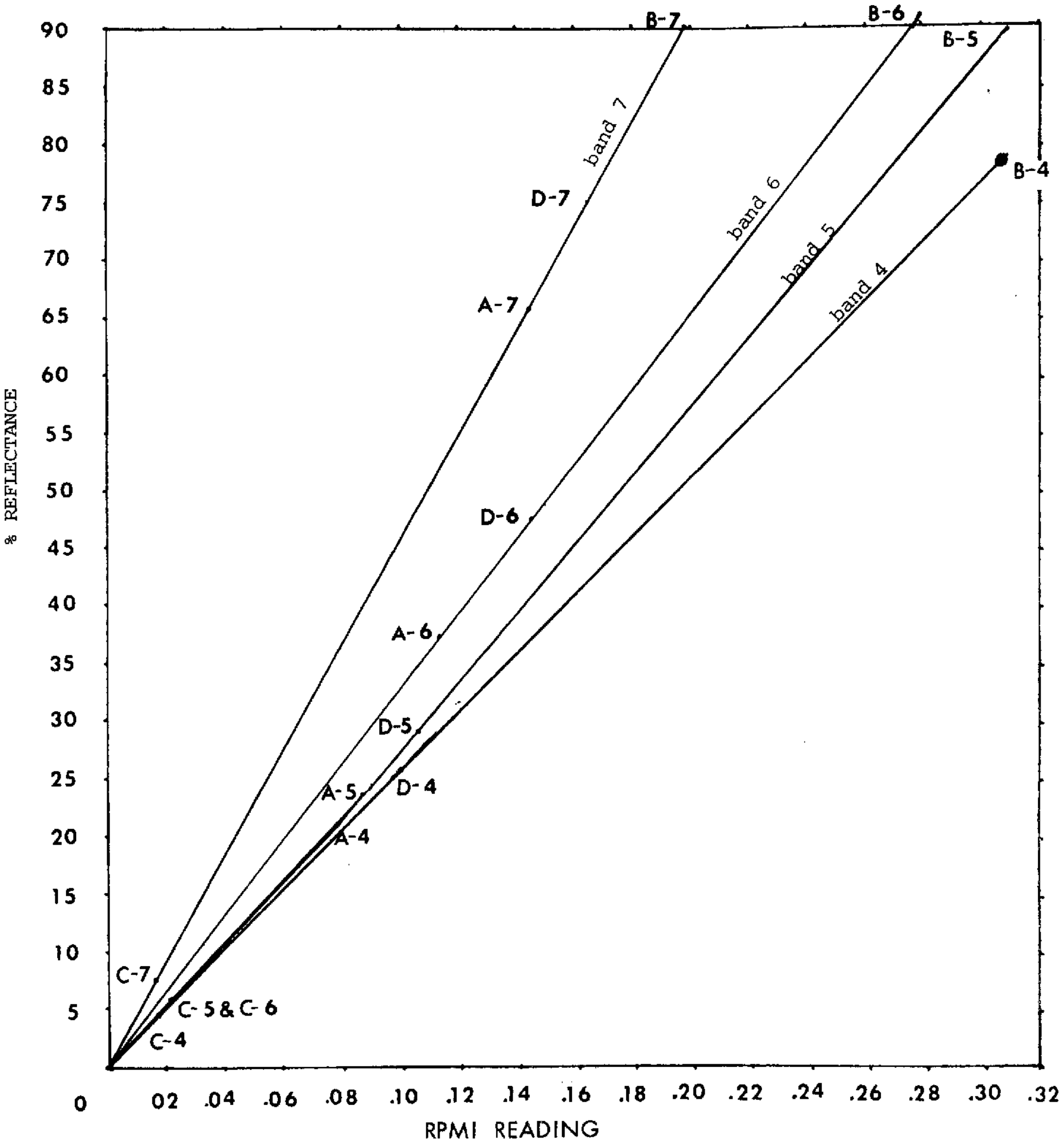

Figure 30 Transfer calibration method of determining unknown reflectance (of water) based on that of reference panels.

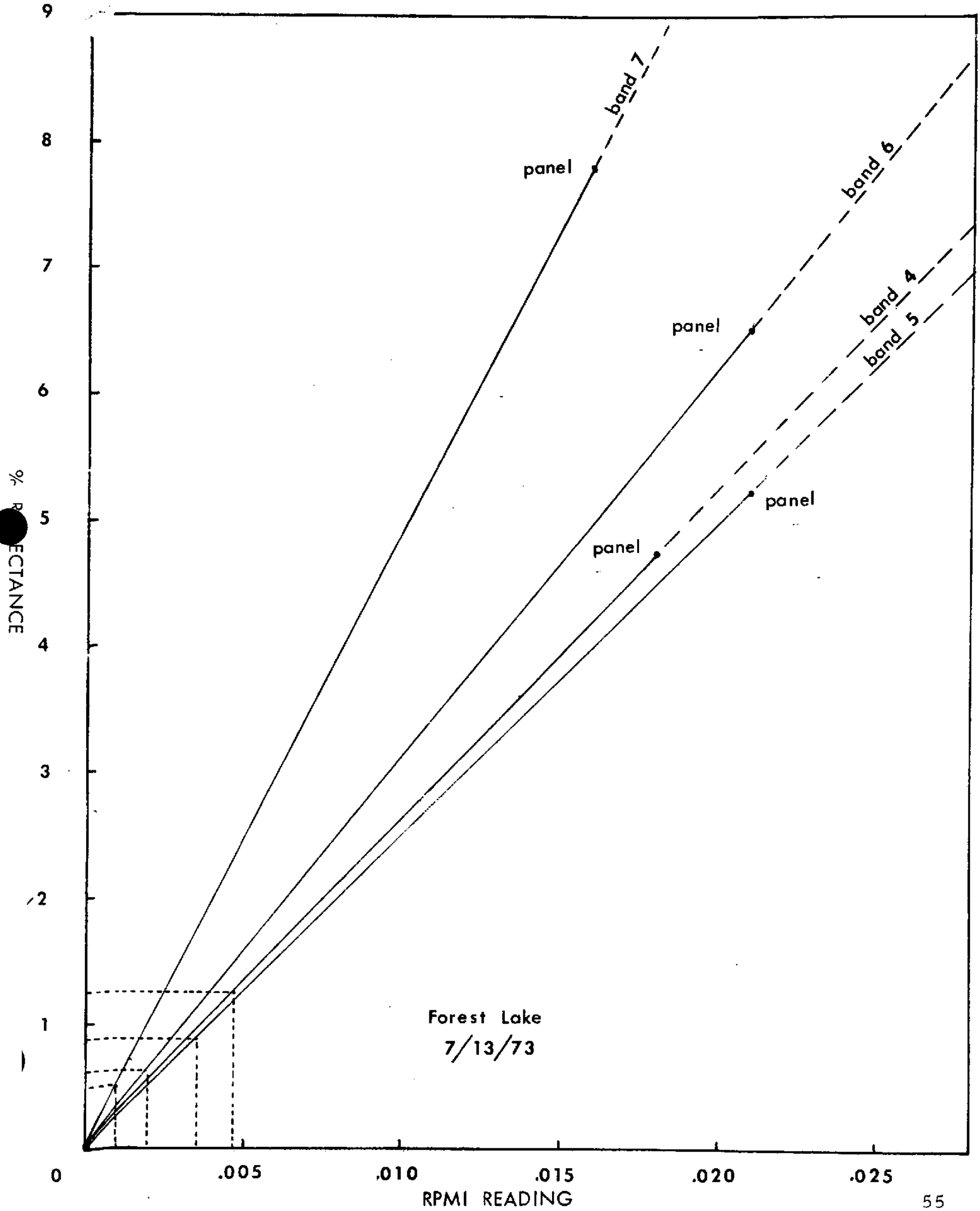

5.3.3 DENSITY SLICING OF CCT REFLECTANCE LEVELS

Screening of ERTS CCTs for water reflectance (digital) levels was carried out on a color-coded TV monitor. To facilitate viewing, the ERTS band having the best target background contrast was chosen and displayed. (The signal range of interest within this band is generally sub-divided into 16 parts and displayed in 16 distinctive colors, i.e., color-sliced. The investigator can specify the signal amplitude and range into which the 16 colors are assigned.) As an example, Figure 31 shows three bands of the study area CCT for March 27, 1973, as displayed on the monitor and compared to an aerial photograph (NASA, C-130) of the same date. In the band 4 and 5 images it is apparent that reflectance varies at least in the shallow water zones of Orchard and Cass Lakes. A close-up of the band 4 display (Figure 32) shows this more clearly and reveals some reflectance structure in the deep-water areas as well. "Banding" effects are also evident among scan lines in Cass Lake (upper center).

As described in Section 5.3.2, absolute (%) reflectance was determined (using RPMI data) for all digital levels within the boundaries of test lakes. For example, Figure 33 shows a band 4 printout of Orchard Lake data in which various symbols represent ranges of percent reflectance measured by ERTS. In this scene (March 27) deep water reflectances in Orchard Lake ranged from 3.1% to 5.5%, and those of shallow water from 5.9% to 8.7%. A total of six reflectance levels are recognizable. The importance of deriving absolute reflectance is that these measurements can be compared from scene to scene since they are corrected for atmospheric differences.

5.4 CLASSIFICATION OF LAKE REFLECTANCE DATA

5.4.1 DECISION PROCESSING OF CCT TO CLASSIFY WATER AND BOTTOM REFLECTANCE

The general technique of decision processing of ERTS CCTs as developed by Bendix is described in Section 4.4 Initially, a classification of land and surface water was carried out to test the procedure. The resulting printout of picture elements comprising the land-water boundary resembled

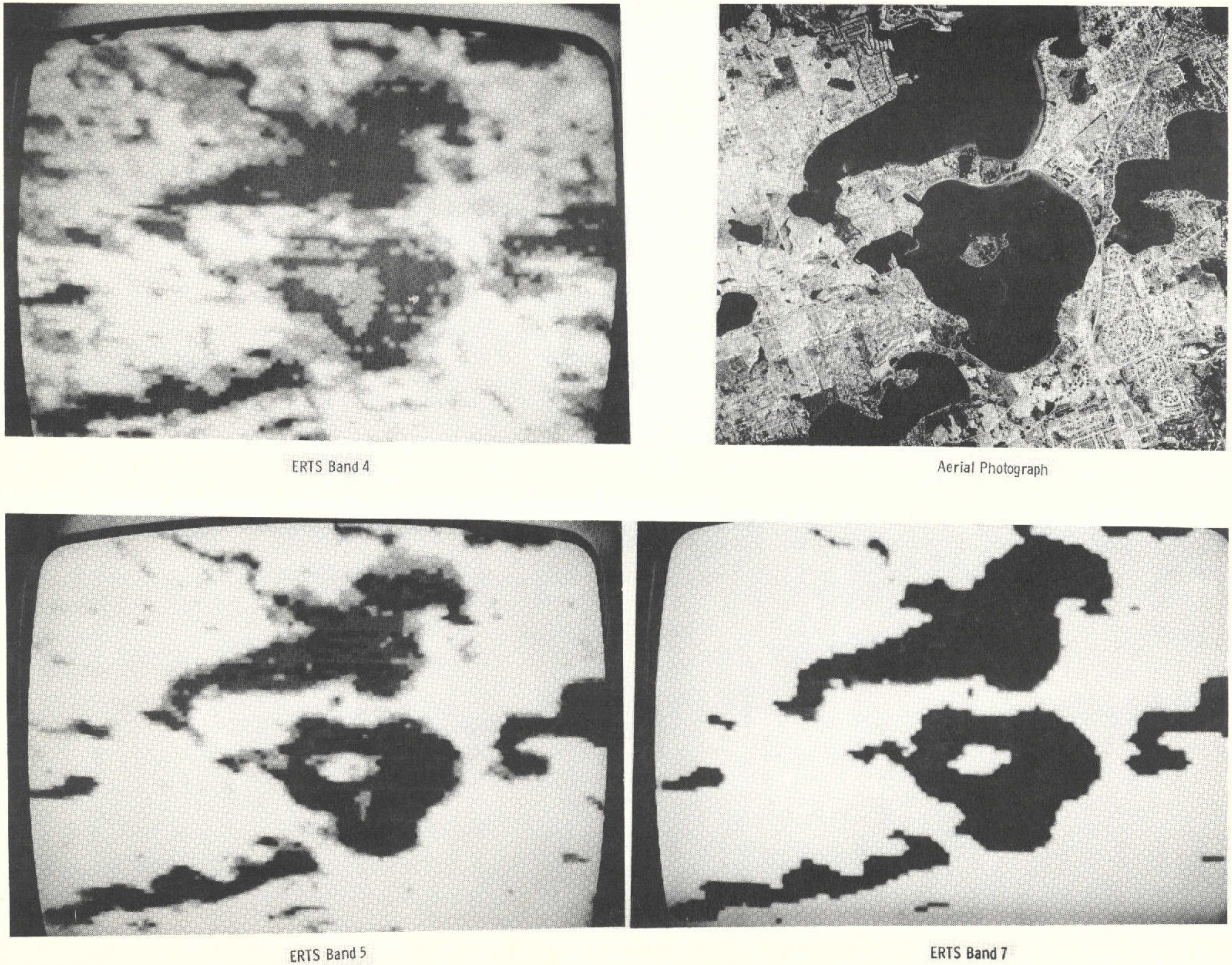

Figure 31 Comparison of Orchard and Cass Lakes Using Color Reflectance Displays and Aerial Photograph. ERTS Imagery of March 27. 1973 (ID No. 1247-15474).

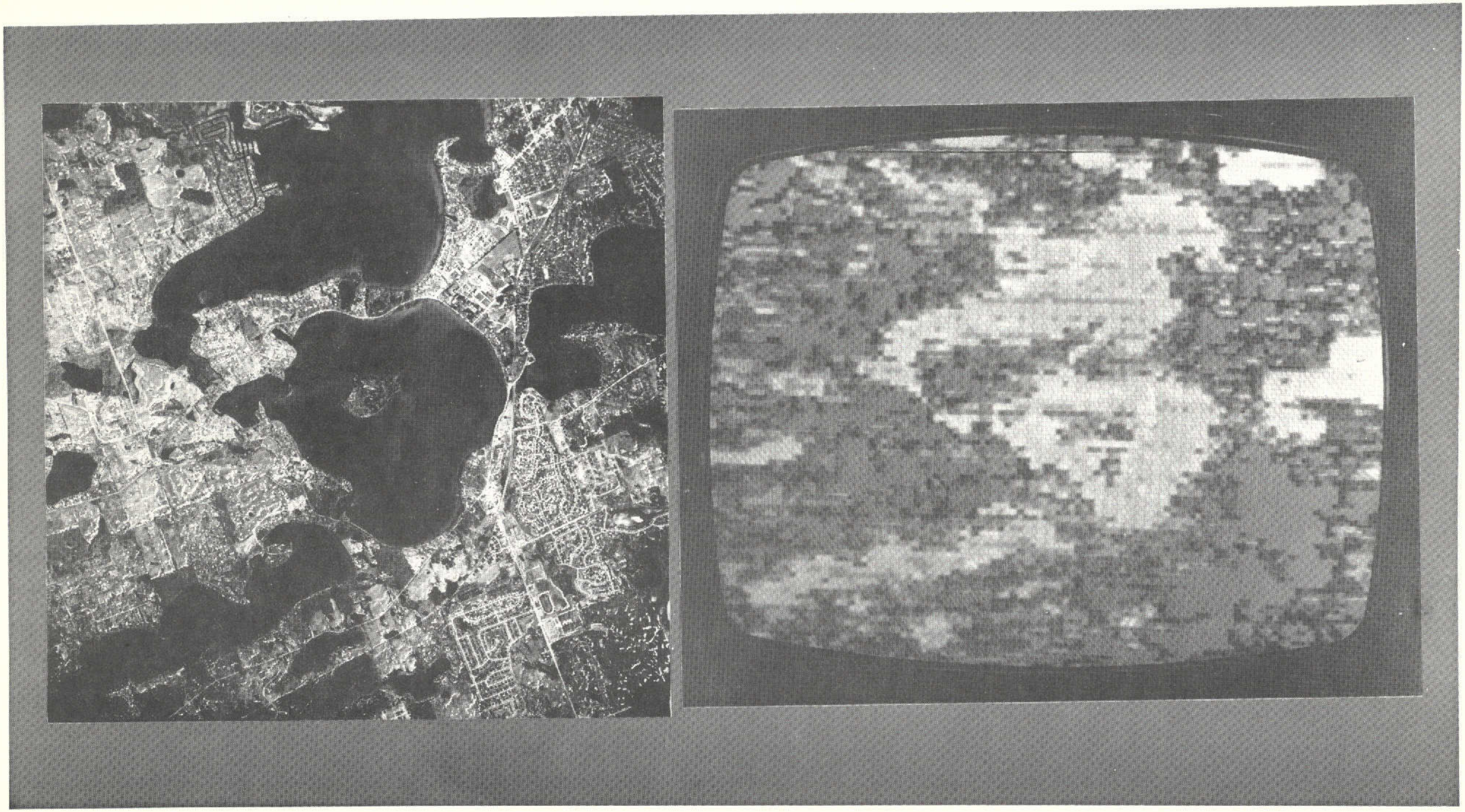

Figure 32 Comparison of Color-Coded TV Display of ERTS Band 4 (ID No. 1247-15474) and Aerial Photograph March 27, 1973.

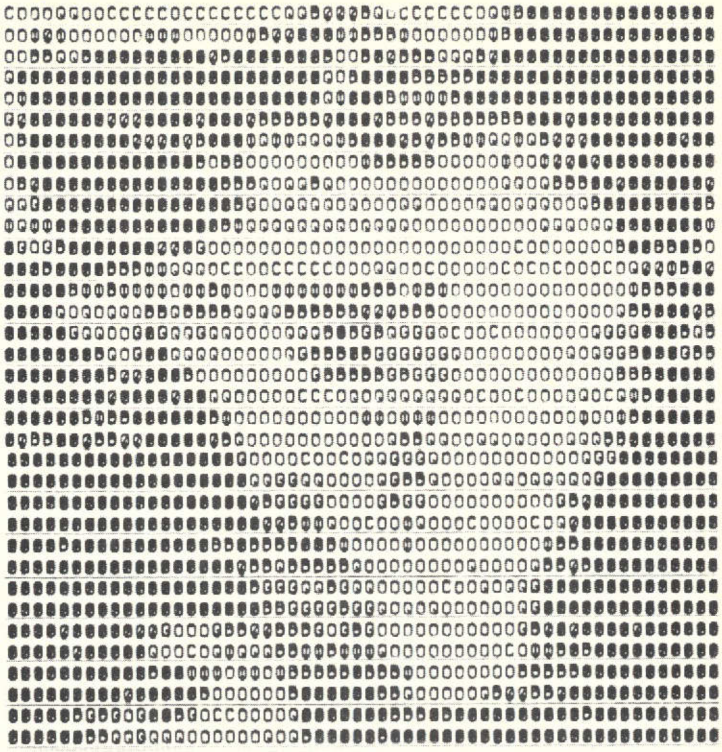

CHARACTER	REFLECTANCE RANGE		
	0.000	-	0.006
.	0.010	-	0.014
/	0.018	-	0.027
C	0.031	-	0.035
O	0.039	-	0.047
Q	0.051	-	0.055
Φ	0.059	-	0.067
G	0.071	-	0.075
B	0.079	-	0.087
[illegible]	0.091	-	0.095
[illegible]	0.099	-	0.100

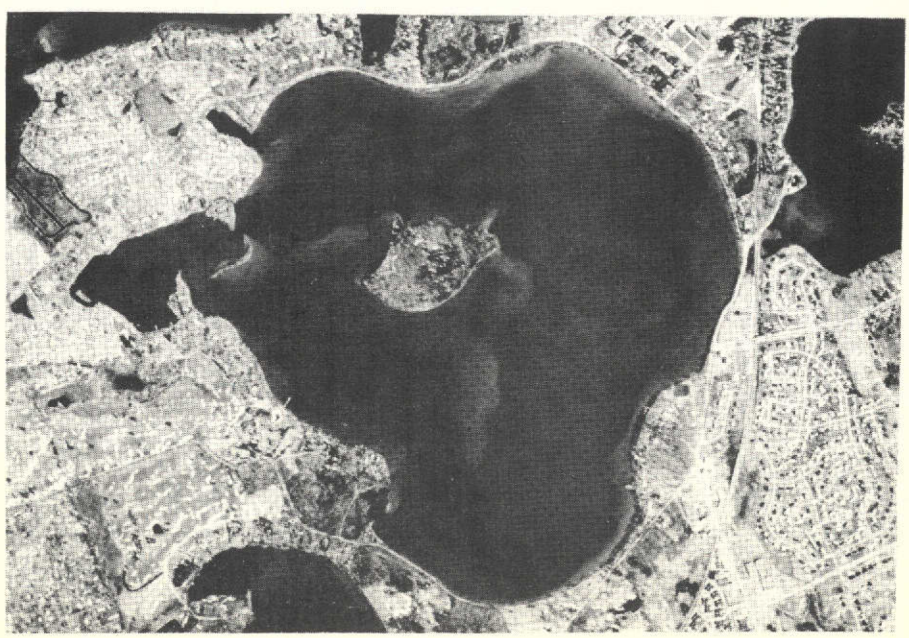

Figure 33 Comparison of ERTS Reflectance Printout from Band 4 March 27, 1973 ID No. 1247-15474, and Aerial Photograph. Orchard Lake.

known lake borders. However, it was necessary to correct the ERTS CCT data for earth rotation and scale in order to produce image overlays for maps and aerial photographs. Land-water boundaries corrected and drawn by a computer-driven plotter at a scale of 1:250,000 are shown in Figure 34.

Repetitive mapping of land-water boundaries would show wetland vegetation encroachments into those lakes with high eutrophication rates caused by increased organic sedimentation in shallow areas.

The water itself in Orchard and Cass Lakes was further classified by decision processing into deep and shallow (bottom visible) categories. Selected areas of known depth (0 – 3 meters) were used for computer "training." Groups of 12 to 40 picture elements representing these training areas were located in a Band 5 printout of the lakes, as shown in Figure 35. Water targets within the whole scene were then classified by computer into deep and shallow categories. The resulting classified image was compared to a photomosaic of this area (Figure 36) in which details of lake bathymetry are visible.

5.4.2 EVALUATION OF DEEP-SHALLOW CLASSIFICATION

Correspondence between the ERTS image and aerial photograph in Figure 36 is generally close, even though the latter was taken five years earlier, possibly under different conditions of lake level, water clarity and bottom vegetation. Allowance also must be made for geometrical distortion of the image, which was not corrected for earth rotation effects. Some apparent discrepancies should be noted. A few shallow areas in Orchard and Cass Lakes were misclassified as deep, perhaps due to dark patches of bottom plants. What resembles shallow water in the lower portion of Otter Lake (air photo) is in fact now a wetland area, which was correctly classified from ERTS. Of course, many bottom details of 1 acre size or less are not resolved in the ERTS image. Nevertheless, even for small lakes (such as 50 acres), ERTS data provides much useful information about lake bathymetry. Mapping lake bottom contours from ERTS on an annual basis would provide important information on changes in sediment deposition and growth patterns of aquatic plants both of which are major indicators of the rate and degree of eutrophication.

A geometrically corrected map of deep and shallow water at 1:250,000 scale is shown in Figure 37.

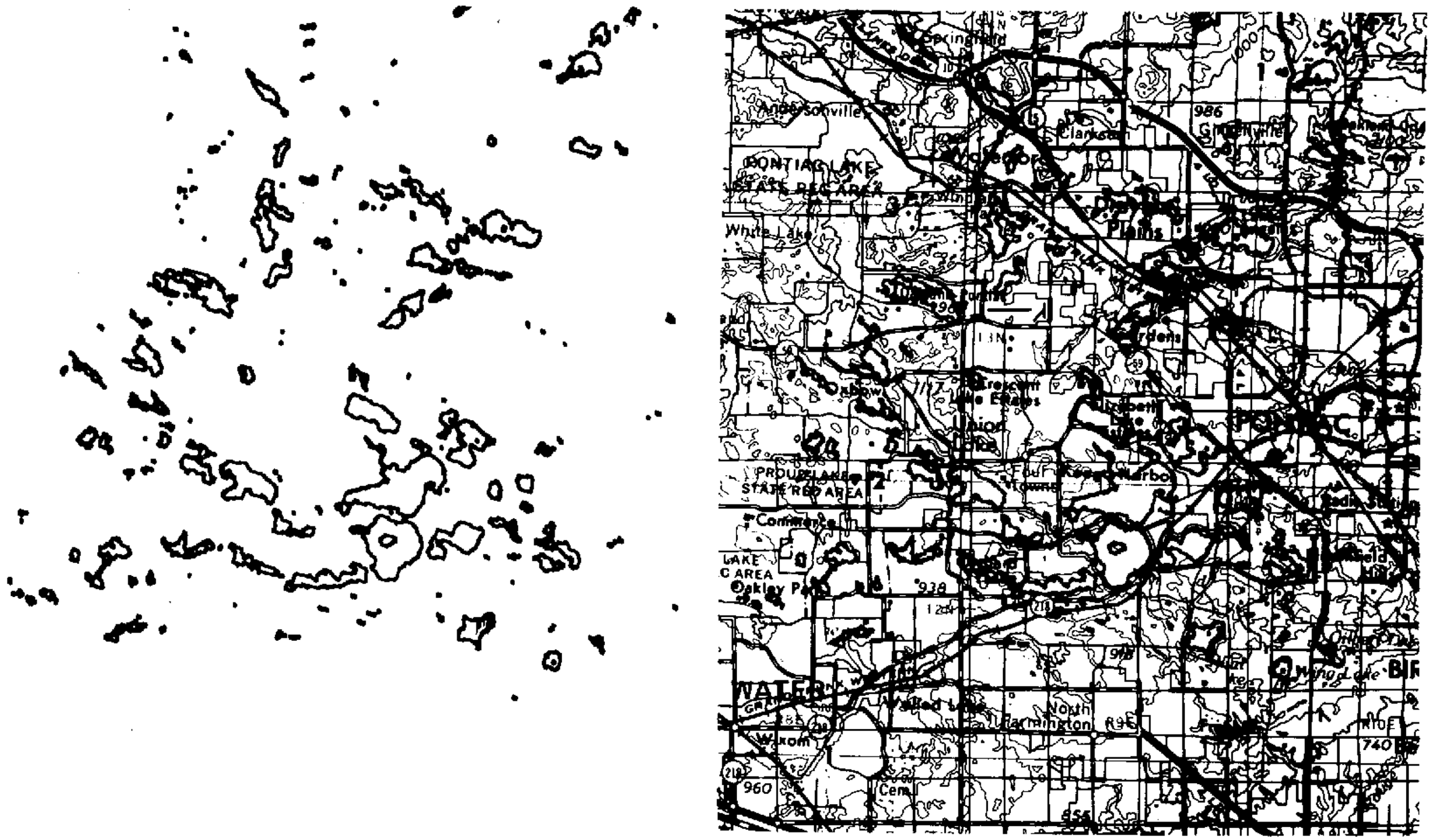

Plotter Overlay of Water Boundaries   Plotter Overlay on AMS 1:250,000 Base Map

Fig. 34 Computer-generated map of water boundaries from ERTS tapes of April 14, 1973 (ID No. 1265-15474)

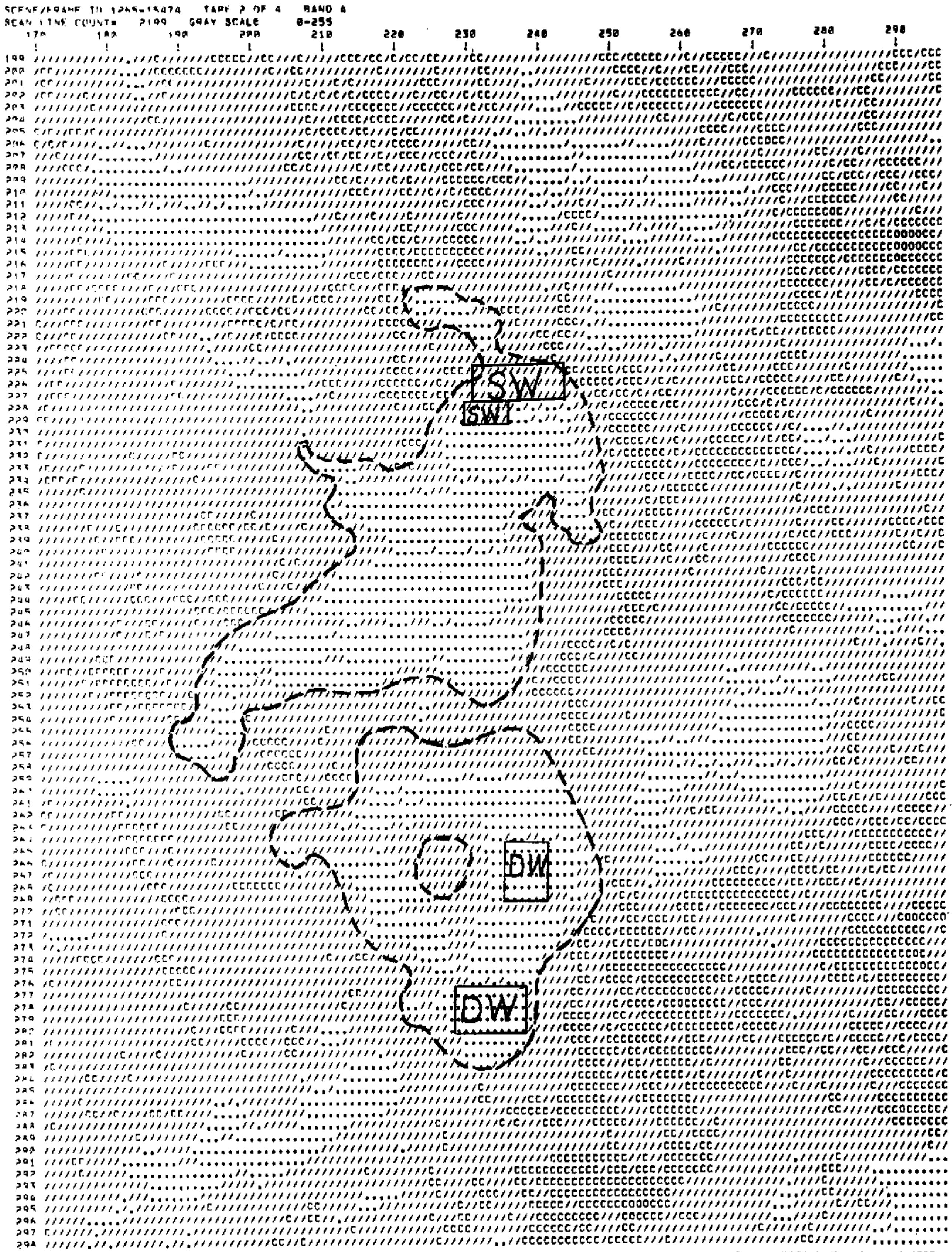

Figure 35 Gray-Scale Printout with Training Sets Annotated from ERTS Band 5, April 14, 1973 (ID No. 1265-15474). Dotted lines are drawn to indicate the approximate land-water boundaries; DW - deep water; SW - shallow water.

Ground Truth Aerial Photo Mosaic
of Orchard and Cass Lakes

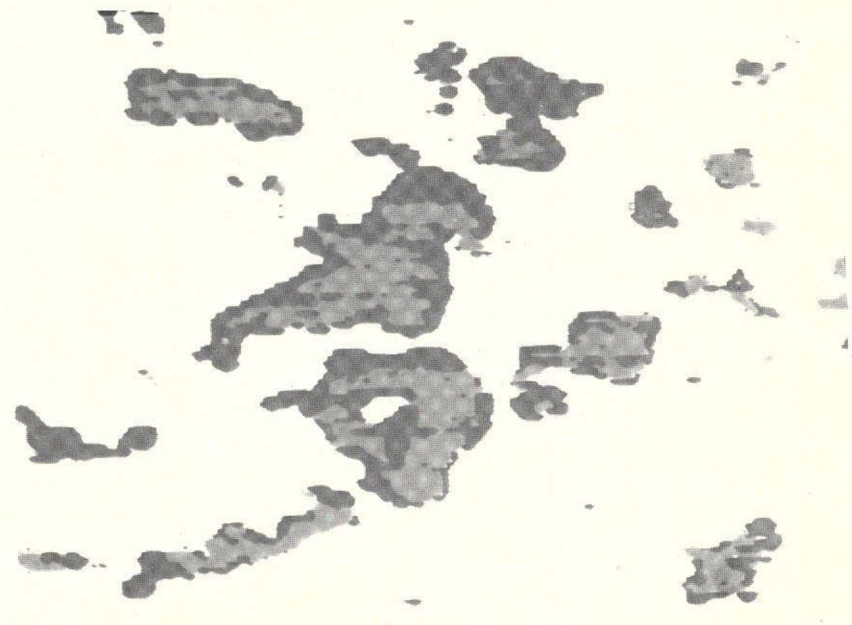

b. ERTS Decision Imagery Showing Deep (Light) and Shallow (Dark) Water

Figure 36 Automatic Classification of Deep and Shallow Water from ERTS Tapes of April 14, 1973 (ID No. 1265-15474).

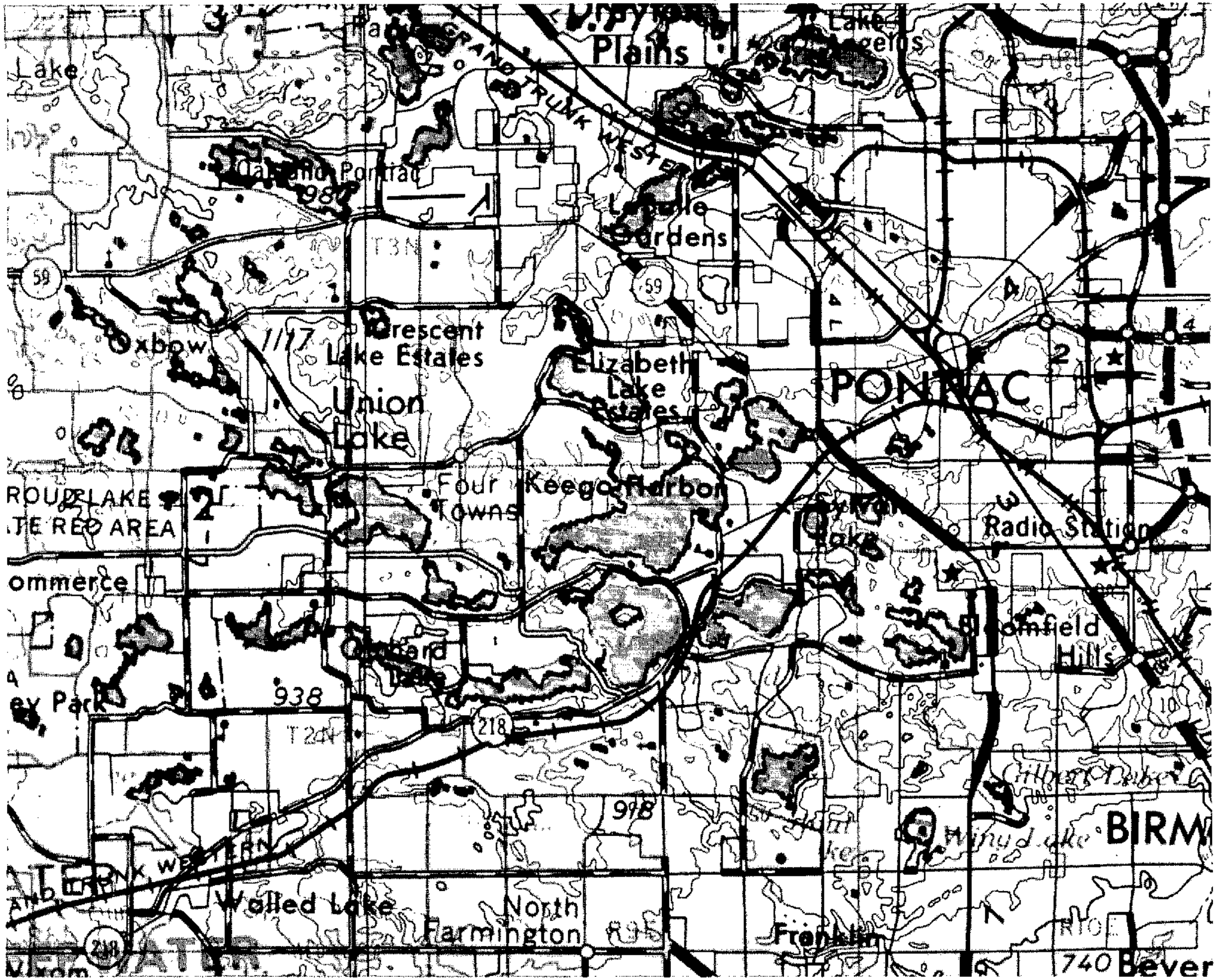

Figure 37 Photograph of ERTS Processed Map Overlay of Test Lakes at 1:250,000 Scale Showing Deep (Light) and Shallow (Dark) Water Categories April 14, 1973.

5.4.3 CLASSIFICATION OF DEEP WATER REFLECTANCE

Portions of the test lakes classified "deep water" were further subjected to canonical analysis and decision processing in an effort to classify the lakes into different deep water categories.

The component of total reflectance of interest here is upwelling or backscattered light. As noted earlier (Section 5.1.3), its magnitude is a function of the concentration of suspended particulate matter, and its color is influenced by the absorption and transmission properties of matter (particles and solutes) in suspension (Jerlov, 1968). Surface (specular) reflectance, which can account for the majority of total reflected light, provides no information about water quality, unless surface scums are present (McNeil and Thomson, 1974). Consequently, minor variations in the quality of diffuse reflectance (upwelling light) tend to be obscured. Yet, when the upwelling light is of sufficient magnitude, its color and intensity can be measured by a multispectral remote sensor, such as that in ERTS.

Our objective in this case was to test the ability of ERTS to discriminate color and intensity differences in the upwelling light from test lakes of varying turbidity, color, etc. Lakes and test dates were selected for comparison on the basis of measured water quality values, as demonstrated in Figures 16 and 17, Section 5.1.1. In principal, those pairs of lakes which are most different with respect to turbidity, etc., on a given date, should be discriminated most easily by ERTS.

As an example, deep water areas in Orchard and Cass Lakes were chosen for computer training sets. Figure 17 shows how the lakes compared in water quality on June 7, 1973. In transparency (Secchi depth), color and turbidity (total particulates) the lakes differed by almost a factor of 2. However, an attempt to classify the lakes into distinct water categories resulted in only a partial separation, as shown in Figure 38. This and subsequent attempts to classify the lakes by deep water reflectance were only partly successful.

On the other hand reflectance values recorded by ERTS and the RPMI varied as would be expected in comparison to water transparency, color and turbidity (Table 5). As turbidity increased and water color varied from green to brown hues, "red" reflectance in band 5 increased, and the band ratios 4/5 decreased. These relationships do not hold as well for certain "brown-water" lakes in the upper peninsula of Michigan, as shown in Table 6. When arranged with the study lakes in a sequence of decreasing transparency (Secchi depth) the northern lakes, particularly Ives, depart somewhat from the progression of higher to lower band 4/5 ratios. Despite its rather low turbidity, Ives Lake water is brown due to organic solutes. This is a typical condition of many

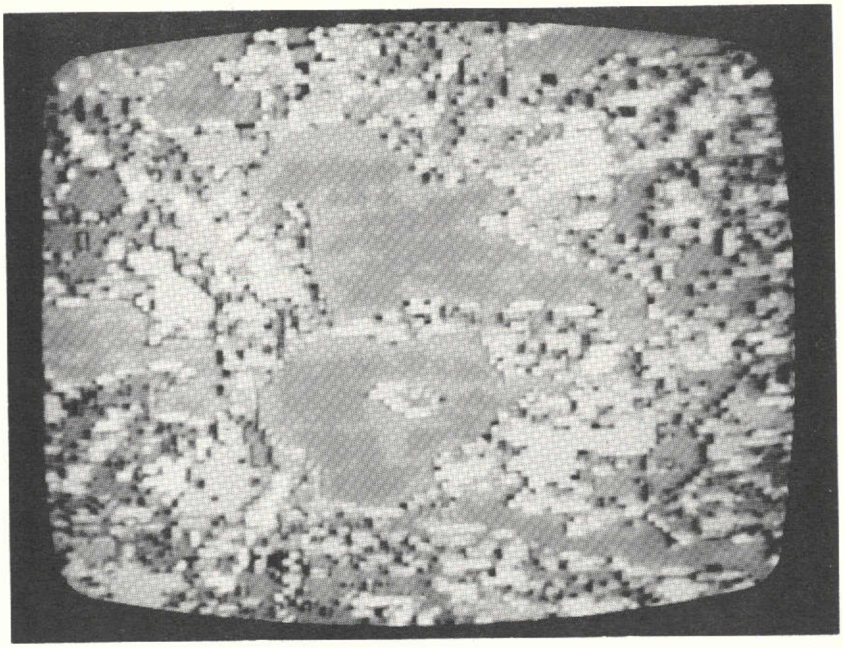

a. Water classified into shallow (light) and deep (dark) categories.

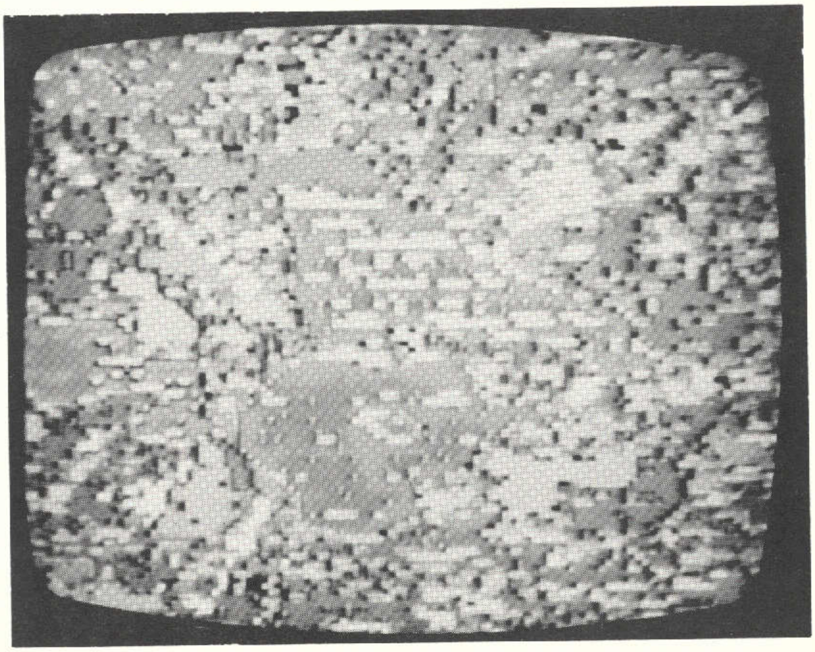

b. Water classification into "Orchard-type" (dark) and "Cass-type" (very light) water categories. Result shows about 80% correct separation.

Figure 38 Classification of Deep Water in Orchard and Cass Lakes on June 7, 1973 ERTS ID No. 1319-15471.

Table 5. Percent Surface Reflectances of Lakes, Recorded by ERTS and RPMI Sensors on 27 March 1973, Compared to Water Transparency and Color on the Same Date.

Lake	Sensor	MSS Band				MSS Band Ratio (4 to 5)	Transparency (Secchi Depth)	Apparent Color (Forel-Ule)	Organic Carbon Mg/ℓ
		4	5	6	7				
Orchard	ERTS	4.00	0.520	0	0	7.69	5 m	10	.81
	RPMI	2.38	0.717	0.218	0	3.32			
Lower Long	ERTS	3.60	1.20	0.270	0.150	3.00	4.0 m	13	.89
	RPMI	1.84	0.997	0.490	-	1.85			
Forest	ERTS	3.30	1.20	0	0	2.75	2.8 m	16-17	1.34
	RPMI	1.34	0.997	0.474	-	1.34			
Island	ERTS	3.97	1.60	0.350	0.370	2.48	1.5 m	15	1.94
	RPMI	1.610	1.010	0.460	0.0767	1.59			

Table 6. Surface Reflectance (%) of Michigan Lakes Recorded Comparison With Water Transparency and Color

Lake	Percent Reflectance In ERTS Bands				Ratio	Transp.	Apparent Color	Suspended Solids
	4	5	6	7	4/5	(Secchi)	(Forel/Ule)	(Mg/ℓ)
Superior	1.39	.36	.23	.24	3.86	14.0	5.5	
Rush	.66	.33	.16	.13	2.00	6.5	9	
Pine	.59	.51	.28	.24	1.16	5.5	12	
Orchard	2.38	.72	.22	-	3.32	5.0	10	.81
South Mountain	.58	.39	.15	.07	1.49	4.5	16	
Lower Long	1.84	1.00	.49	-	1.85	4.0	14	.89
Howe	1.12	.80	.50	.49	1.40	3.7	10	
Ives (20 Aug)	1.29	1.44	1.02	1.22	.90	3.5	19	
Ives* (20 Aug)	.53	.55	.31	.27	.96	3.5	19	
Ives* (21 Aug)	.76	.73	.40	.35	1.04	3.5	19	
Ives* (23 Aug)	.54	.51	.25	.14	1.06	3.5	19	
Forest	1.34	1.00	.47	-	1.34	2.7	16.5	1.34
Island	1.61	1.01	.46	-	1.59	1.7	16	1.94
Kingswood	5.36	4.48	1.73	.75	1.20	[illegible]	17	
Conway	5.61	5.80	3.78	3.82	.97	1.5	16	

*Measured from 2m height, all others measured from 1m height.

acid-bog lakes as well, but is rare among the larger kettle lakes of Oakland County (Humphrys, 1968).

5.4.4 EVALUATION OF DEEP WATER CLASSIFICATION

The investigation shows that ERTS can successfully monitor lake turbidity and color. The relationships established however have not been applied on a broad enough scale of water categories nor under enough different atmospheric conditions to fully quantify the accuracy to which turbidity and color is predicted. The reflectances measured for the study lakes were generally very low (5% maximum in Band 4). More turbid and reflective waters would be expected to yield percent reflectance values that are less degraded by atmospheric "noise" and specular reflectance. However, such lakes would be considerably more eutrophic or contaminated with suspended matter. There is probably less need for regular monitoring of lakes with such manifestly bad water quality. ERTS would be far more useful if it provided early warning of quantitative changes in the quality of lakes that are not yet abnormal.

5.4.5 RPMI DETECTION OF SURFACE PHENOMENA IN ERTS SPECTRAL BANDS

Although surface scums of algae or macrophytes are often cited as evidence of severe enrichment in lakes, these may occur periodically or seasonally on lakes that are not hypereutrophic. The frequency and scale of these blooms are, nevertheless, related to eutrophication states. Such blooms of blue-green algae have been recorded in past years on at least one of the test lakes (Island) but none occurred during the project period. Nevertheless, we conducted RPMI measurements on nearby waters to test the potential of ERTS to detect total or partial coverage of lakes by plant films. Examples of two such phenomena are shown in Figures 39 and 40. The macrophyte (Wolffia) coverage monitored was about 25 – 30% and the algal (Spirogyra) coverage was about 80 – 100%. (In general, blooms may cover up to 100% of a lake's surface.)

In Table 7 are compared the percent reflectances of highly turbid water (no surface scum), the two plant scums, and lawn grass. All were determined using the RPMI. The results show clearly that even a partial surface film causes a substantial increase in infra-red (bands 6 and 7) reflectance over that of turbid water. Although little difference is noted in the band 4/5 ratios, the band 4/6 ratios are dramatically different. It is likely, therefore, that plant scums that represent only a few percent of surface cover would be detectable by ERTS. It is interesting to note also that floating scums of algae are far

A. Algal scum (spirogyra) on Upper Long Lake channel, July 5, 1973. Reflectance measured by RPMI.

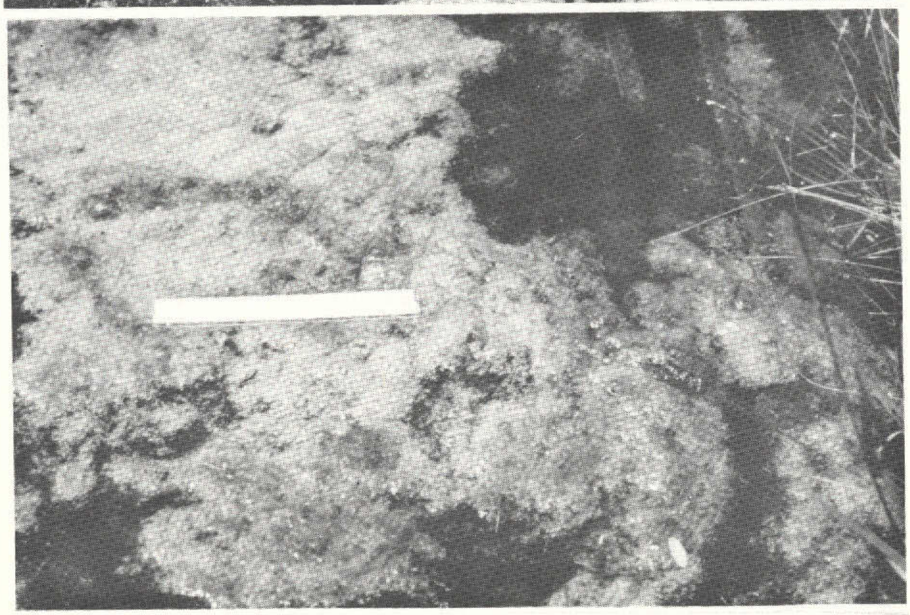

B. Spirogyra mat with trapped oxygen bubbles near shore. Scale is 6 inches.

C. Microscopic view of spirogyra as above. (100x)

Figure 39 Floating Vegetation: Algae

A. Floating Macrophytes (Wolffia) on Dollar Pond near Lower Long Lake, July 5, 1973. Reflectance measured by RPMI.

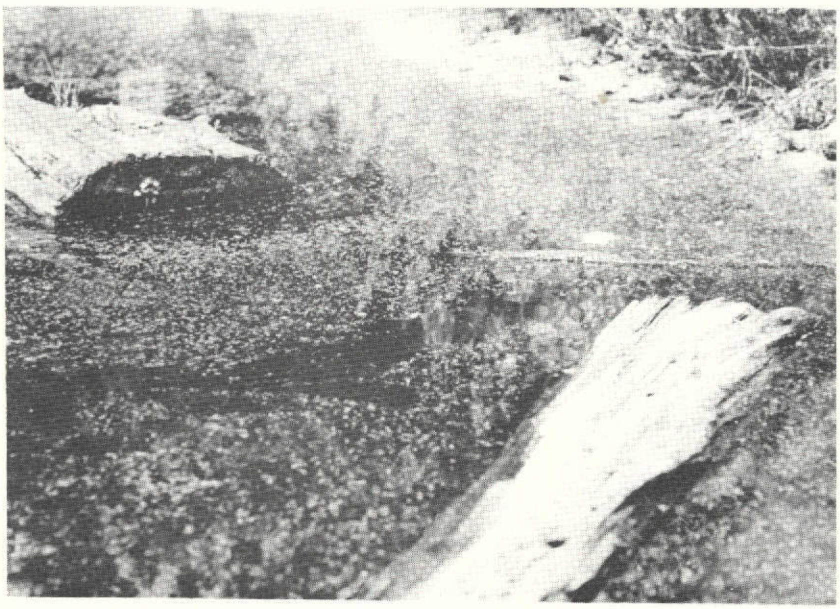

B. Wolffia covering about 30 percent of water surface.

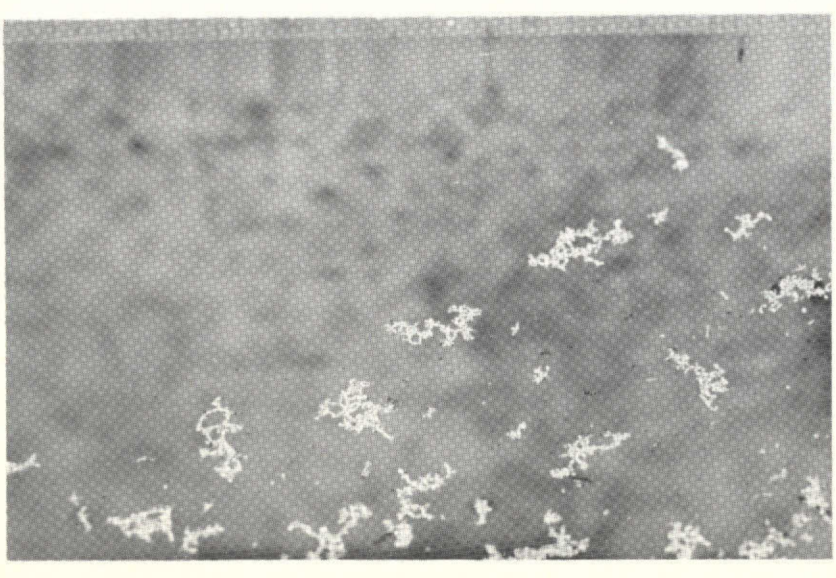

C. Close-up view of Wolffia plants. Approximately 1/2 natural size.

Figure 40 Floating Vegetation: Macrophytes

Table 7. Percent Reflectance* of Water, Floating Vegetation and Grass.

Target	% Surface Cover	ERTS Band				Band Ratios	
		4	5	6	7	4/5	4/6
Highly Turbid Water	0	5.4	4.5	1.7	.75	1.2	3.2
Wolffia sp. (healthy)	25	7	8	10	9	.8	.7
Spirogyra sp. (healthy)	100	15	15	30	34	1	.5
Spirogyra sp. (dying)	100	16	18	30	33	.9	.5
Lawn Grass	100	6	6	37	65	1	.2

* At 1 meter above the target

more reflective than lawn grass in the green-red range (Bands 4 and 5) by virtue of their relatively planar orientation.

The 18-day cycle of ERTS may not be suitable for monitoring transient phenomena such as blooms in lakes. However, if bi-weekly or daily coverage (multiple satellite coverage) becomes available, detection and monitoring of bloom in lakes would be of major importance.

5.5 DETECTION OF LAKE WATERSHED FEATURES IN ERTS BULK IMAGERY

As described earlier, lake and watershed features were examined first in ERTS bulk imagery to establish general limits of detection and resolution. The sensitivity of ERTS to many types of natural and man-made targets is by now well-documented. We can verify that targets which contrast strongly with their surroundings can be detected with somewhat better than 1-acre resolution. However, as is well known, bulk imagery does not afford the necessary precision of target reflectance measurement, machine processing and classification of spectral data and automatic tabulation of target areas, which are all feasible with ERTS CCTs. Computer processing is particularly vital in preparing classified maps of watershed land use as it influences water quality in lakes.

After this study began we realized that, although ERTS detection of certain water quality features (i.e., turbidity and color) might allow us to assess the current trophic condition of a lake, only a consideration of watershed factors would provide some basis for predicting future water quality trends. The anticipation of lake problems resulting from certain types of land development and manipulation is of great interest to planners and managers, since many kinds of land use change are socially, if not physically, irreversible. A historical ignorance of the effects of various land use practices on lake water quality (via drainage) has already had tragic results.

Even now there is still too little good information relating specific land uses to specific water quality situations. Both cause and effect are complicated by many ill-defined variables. However, as these relationships became better defined, the ERTS mapping techniques described here will furnish the quantitative means to monitor land use and cover in the watershed of lakes threatened by eutrophication and hyper-enrichment.

5.6 DECISION PROCESSING OF CCTs TO CLASSIFY WATERSHED LAND USE/COVER

The objective in this phase of the study was to prepare a land use/cover map of part of Oakland County, Michigan, that would include the watersheds of test lakes and many others. The first step was to locate the "training areas" that best typified the land-use categories of interest. These local sites of 50 acres or more were first located in ERTS imagery and recent USDA aerial photographs (1971), and verified by ground truth.

While recognizing that many factors influence the quality of land drainage, we chose the six general types of land-use categories which are listed below in order of their potential to discharge nutrients, especially phosphorus. The codes following the category names correspond to those proposed by Anderson, et al. (1972). While other target categories or combinations thereof might have been chosen as well, the ones listed account for most of the watershed use that affects water quality in the study area. Water categories (deep and shallow) were included to complete the land-use map.

a. Urban, 01. Large commercial areas, major roadways, high density residential areas, and many isolated shopping centers.

b. Extractive Earth, 01-04. Strip mines, gravel pits, construction sites, and other areas of disturbed or bare earth.

c. Tended Grass, 01-09. Golf courses, cemeteries, sod farms, and other areas of cultivated grass which are very green in Michigan in April.

d. Wetlands (nonforested), 06-01. Marshes, bogs, swamps, and low brushy areas.

e. Rangeland (untended grass), 03-01. Natural grasslands, pasture land, dry savannahs, and old fields. Natural grassy areas (rangeland) are normally brownish in Michigan in April. Unharvested crops would probably be included, while plowed fields would be classified as extractive land.

f. Forest Land (trees), 04-03. Mixed hardwood (deciduous) forest. There were no sizable evergreen forests in the study area.

g. Shallow Water, 05. Bottom visible in some ERTS band. In most of the study lakes, shallow water ranged up to 4 meters deep.

h. Deep Water, 05. Waters where bottom contours are not visible in any ERTS band (i.e., over 4 meters).

i. Unclassified. This category includes all targets that do not exceed the probability thresholds established by the investigator.

All of the training areas were located within Oakland County with the exception of wetlands, for which a site farther north in Sanilac County, Michigan, was chosen.

Before producing a decision image from the ERTS CCT, a number of tests were applied to evaluate the computer's ability to produce the desired target classification. The tests included generating classification accuracy tables and viewing the results of processed data, color coded, on a TV monitor.

The classification accuracy table provides one measure of the interpretation accuracy. In this step the canonical coefficients were used in decision processing, but the data processed were limited to ERTS measurements from known areas, i.e., the training set data that were previously edited and stored in a disk file. Processing this data from known targets and keeping an accurate record of the computer decisions permitted the printout in Table 8a to be developed. In the table it can be noted that 96.552 (97%) of the training set measurements from tended grass were correctly classified as tended grass (denoted as Set 1) whereas the remaining 3.448 (3%) of the tended grass measurements were classified as rangeland (denoted as Set 8). It may also be noted in the table that the classification accuracy for all eight categories is 90% or greater.

5.6.1 AREA MEASUREMENT OF WATERSHED CATEGORIES

Once the classification accuracy was acceptable, the CCT was classified into the eight categories. This step resulted in the computer-generated area measurement table shown in Table 8b. This is the type of data product that would be useful for predicting nutrient inputs to lakes, since it defines the amount of land of each category in terms of square kilometers, acres and as a percentage of the total area processed.

It can be seen in Table 8b that forest land (trees), for example, comprised 11% (65,732 acres) of the total 625-square-nautical-mile (581,206-acre) area processed. Total surface water (shallow plus deep) covers 2% of 10,099 acres. It is also apparent that approximately 12% of the area remained unclassified. Most of this unclassified area was determined to be automobile assembly plants (heavy industry) which were characterized by large areas of dark roofs and parking areas. Obtaining similar printouts from additional ERTS overflights would provide additional land-use categories and establish the dynamics of land use within the study area.

5.6.2 CLASSIFICATION OF INDIVIDUAL LAKE WATERSHEDS

Of more practical use is the classification of land use within individual lake watersheds, since this provides a basis for predicting nutrient inputs to

Table 8

a. Classification accuracy table.

Classification Table: 11:02:50

Rejection Level = 0.000000 Percent
Group Biases: Group Bias
4 0.40000

TNG Set	0	1	2	3	4	5	6	7	8
1	0.000	96.552	0.000	0.000	0.000	0.000	0.000	0.000	3.448
2	0.000	0.000	96.552	0.000	0.000	3.448	0.000	0.000	0.000
3	0.000	0.000	0.000	100.000	0.000	0.000	0.000	0.000	0.000
4	0.000	0.769	0.000	0.769	90.000	5.385	0.000	0.000	3.077
5	0.000	0.000	4.706	0.000	1.176	91.765	0.000	0.000	2.353
6	0.000	0.000	0.000	0.000	0.000	0.000	98.182	1.818	0.000
7	0.000	0.000	0.000	0.000	0.000	0.000	0.000	100.000	0.000
8	0.000	1.562	1.562	0.000	0.000	3.125	0.000	0.000	93.750

Program Run Time = 00:00:36

0 Unclassified
1 Tended Grass
2 Forest Land
3 Extractive Earth
4 Urban
5 Wetlands
6 Deep Water
7 Shallow Water
8 Rangeland (Untended Grass)

b. Automatic tabulation of category areas.

ERTS Scene ID - 1265-15474
Date of scene - 14 Apr 73
Center of scene - N43-17/W082-42
Sun coordinates - EL49 degrees
AZ138 degrees

Spacecraft Heading - 191 degrees
Tape Number - 2
Starting Scan Line = 1700
Ending Scan Line = 2340

Category	Percent of Total	Sq. Km.	Acres
Unclassified	12.17	286.30	70,747.48
Tended grass	9.20	216.38	53,468.36
Forest land	11.31	266.01	65,732.55
Extractive earth	1.83	43.03	10,632.10
Urban	15.94	374.83	92,621.77
Wetlands	10.10	237.50	58,688.14
Water, deep	1.01	23.79	5,879.11
Water, shallow	0.73	17.08	4,220.16
Rangeland	37.72	887.14	219,216.36
Totals	100.00	2,352.06	581.206.06

specific lakes. With respect to its effect on water quality, a watershed may be defined in different ways. In the largest sense it includes the whole drainage basin within which all elevation gradients slope toward a lake. The basin would include, by definition, all other lakes "upstream" that discharge seepage, even rarely, to the lake in question. However, by a more functional definition that better applies to lakes in the study area, the watershed is that part of the drainage basin immediately adjacent to the lake. During periods of rain or thaw, this area discharges drainage directly to the lake via surface runoff or storm drains. In these cases the major sources of nutrients are paved surfaces, septic tanks, fertilized lawns, and eroded soils. Waste waters that arrive at the lake after slow percolation through soil or vegetation are generally less enriched, at least by phosphorus (Biggar and Corey, 1969).

Therefore, in mapping watersheds of lakes with diffuse sources of nutrients, emphasis should be given to the narrow zone of land adjacent to and extending back from the water. This zone is defined by this study as being approximately 125 meters wide, or the effective width of two ERTS picture elements. Ordinarily, this zone includes the first rank of waterfront lots, houses, and roads, as well as launching ramps and docking facilities. If warranted, larger areas such as housing developments served by storm drains could be included in the analysis to compute total nutrient flows.

Figure 41a shows a classified printout of Cass Lake (March 27, 1973) on which the lake boundary is indicated. Enclosing this boundary is a polygon which represents the approximate limits of the lake's immediate watershed. (A more detailed polygon could have been drawn to describe the watershed more accurately.) The polygon on the printout was defined by coordinates (scan line and resolution element numbers), which were input to the computer to yield the area measurement table in Figure 41b. The results show that the watershed of Cass Lake is predominantly urban, rangeland and "unclassified"; in most cases the latter category has proved to be extensive areas of asphalt pavement, i.e., also urban. In view of the high degree of urbanization (26%) in this watershed it is not surprising that Cass Lake already shows signs of deteriorating water quality (Figures 16 and 17). This example is given to illustrate the categorizing of land use/cover in a specific watershed.

5.6.3 CORRELATION OF WATERSHED LAND USE/COVER AND WATER QUALITY

As a direct application of this approach to a water quality problem, the watersheds of nine Oakland County lakes were classified by the polygon technique

Figure 41 Editing Land Use From Polygon Around Cass Lake.

a. Categorized Printout of Cass Lake Area Used to Designate Area of Interest to Computer for Land-Use Tabulation, April 14, 1973

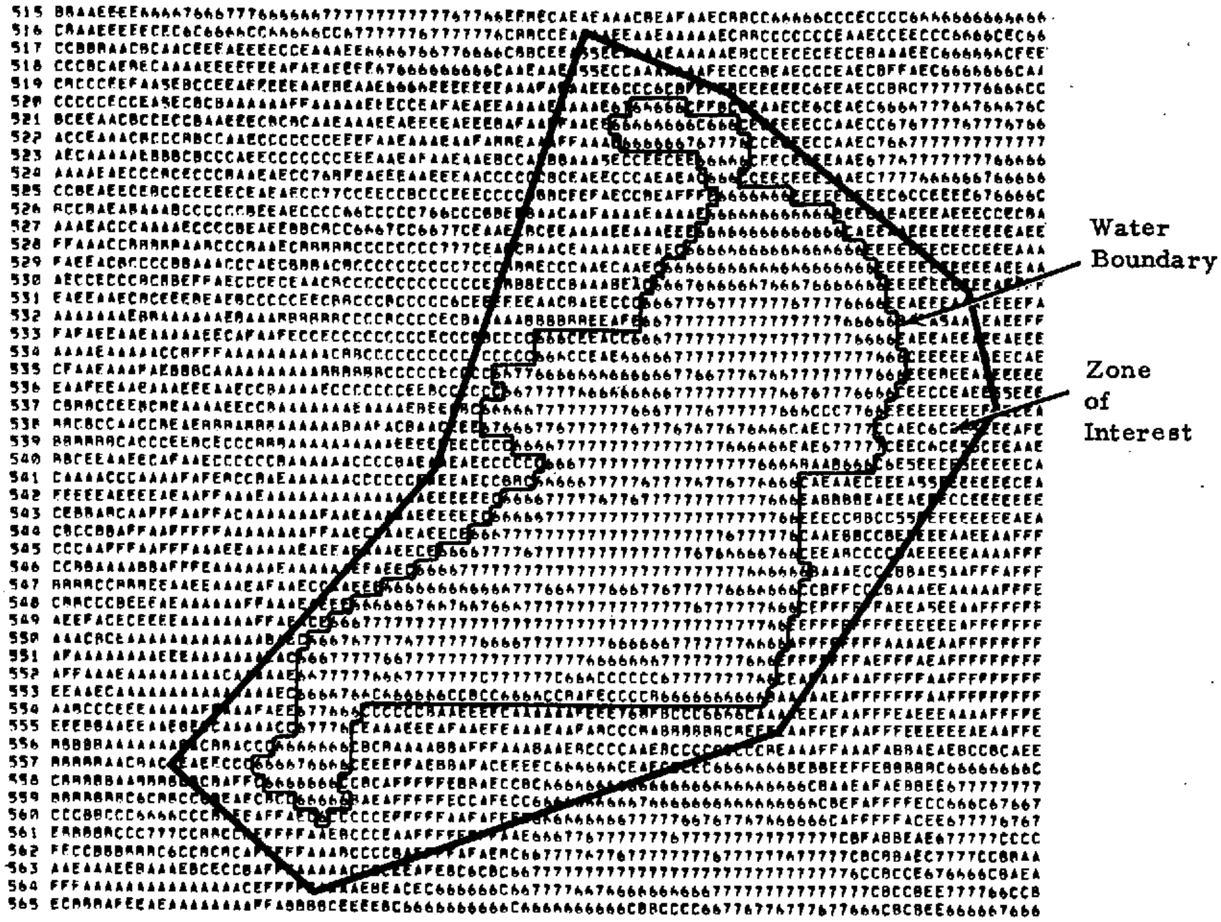

b. Computer Tabulation of Land Use within Polygon Around Cass Lake

Symbol	Category	Percent of Total	Acres	Sq. Km.
O	Unclassified	13.36	281.71	1.14
F	Tended Grass	3.55	74.90	0.30
B	Forest Land	4.72	99.49	0.40
5	Extractive Earth	0.53	11.18	0.05
E	Urban	12.51	263.82	1.07
C	Wetlands	7.90	166.57	0.67
7	Water Deep	24.87	524.29	2.12
6	Water, Shallow	21.58	454.98	1.84
A	Rangeland	10.98	231.40	0.94
	Totals	100.00	2108.35	8.53

and compared to bacterial counts in each lake (Table 10). During summer 1973 the Oakland County Health Department monitored levels of total and fecal coliform bacteria in nearshore areas at several stations on each lake. The counts given in Table 9 are based on ten weekly samples taken between June and September.

Although coliform counts are notoriously variable and sometimes unreliable as a general indicator of waste water pollution, there is apparent here a rough correlation between the average fecal counts and the percentage of "urban" land in the watershed. The correlation is seen better when the urban and unclassified (i.e., also urban) categories are combined as follows:

Lake	E.C. Count (Average)	Urban and Unclassified (%)
Harris/Osmun/Terry	82	65
Sylvan	44	62
Cass	34	47
Orion	33	43
Voorheis	23	26
Elizabeth	17	49
Pine	17	31

The most obvious discrepancy is Elizabeth Lake, which has relatively low counts despite its urbanized watershed. This case would be interesting to examine in detail for evidence that Elizabeth Lake may be more protected from its urban runoff than the others. Coliform counts may not be the best indicators of trophic condition. More conservative factors, such as suspended solids, total phosphorus and chloride, should correlate much better with land use factors in lake watersheds. Unfortunately, no such extensive water quality data were available for the Oakland County lakes.

5.6.4 MAPPING OF WATERSHED CATEGORIES

While the area measurement table was useful here as an inventory of land use/cover within specified boundaries, it was necessary to study printouts of classified data (Figure 41a) or color-coded decision images (Figure 42) to appreciate the distribution of land categories around each lake. In these data products, particularly in the latter, it is readily apparent which categories impact directly on the lake shore and are therefore most important as an immediate source of nutrients in runoff.

TABLE 9. CORRELATION OF LAND-USE AND WATER QUALITY DATA

Lakes	Area Covered by Water sq. km.,	Approximate Percentage of Lakeshore Land in Target Categories							Water Quality Data *				Number of Swimming Areas and Water Rating*		
		Urban	Tended Grass	Bare Earth	Forested Land	Rangeland	Wetlands	Other	Total Coliform Range	Total Coliform Avg.	Fecal Coliform Range	Fecal Coliform Avg.	Safe	Question-able	Unsafe
Harris, Osmun, Terry	.01	43.0	1.0	2.0	3.0	17.0	12.0	22.0	1200-3972	2330	31-210	82	0	6	7
Sylvan	1.35	34.0	3.0	1.0	5.0	13.0	16.0	28.0	538-2371	1051	17-117	44	6	2	1
Elizabeth	1.2	32.0	7.0	0	7.0	25.0	12.0	17.0	333-2333	617	10-33	17	15	1	1
Cass	3.96	23.0	7.0	1.0	9.0	21.0	15.0	24.0	400-2200	736	15-105	34	10	0	2
Orion	.95	21.0	2.0	2.0	8.0	16.0	29.0	22.0	710-1197	851	16-55	33	6	2	0
Pine	1.28	20.0	13.0	0	20.0	24.0	12.0	11.0	491-834	630	13-27	17	10	0	0
Voorheis	0.63	9.0	4.0	1.0	16.0	29.0	24.0	17.0	481-489	485	20-25	23	2	0	0

*As established by the Oakland County Health Department

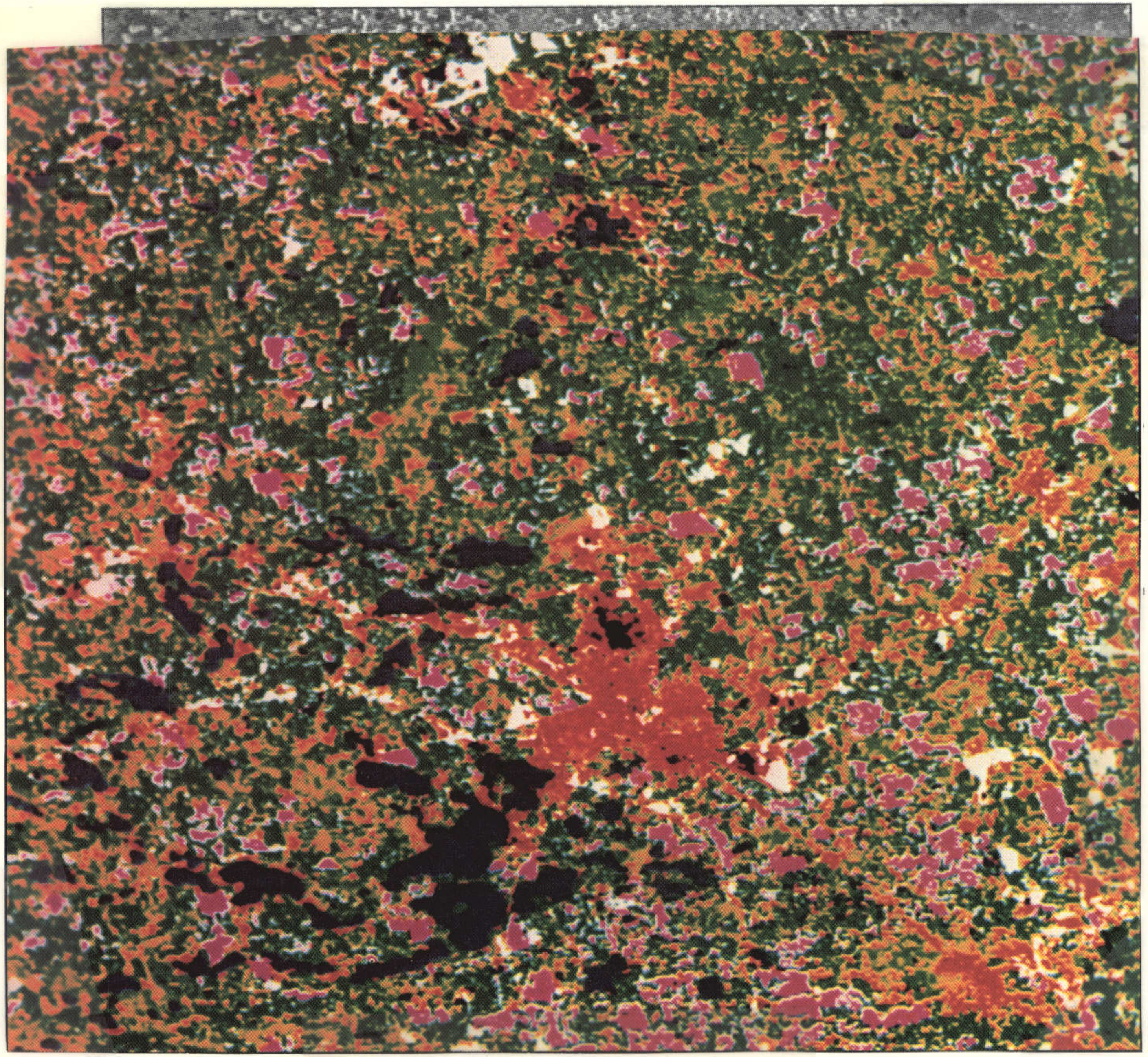

Color Code:

- Red - Urban
- Light Blue - Deep Water
- Dark Blue - Shallow Water
- Yellow - Wetlands
- Dark Green - Grass (untended)
- Light Green - Trees
- Magenta - Grass (tended)
- White - Barren Earth
- Black - Unclassified

Figure 42 Color-Coded Decision Imagery of Land Use in Oakland County Study Area. Derived from ERTS data acquired April 14, 1973 (ID No. 1265-15474).

However, for a more detailed analysis of land-use it was necessary to prepare geometrically correct imagery and overlays from CCTs. The overlays were single-category, color-coded film transparencies generated automatically by a Gerber computer-driven plotter. Standard UTM map overlays were made at scales of 1:250,000 (Figures 43 to 45) and 1:48,000 (Figures 46 to 49). Other "category boundary" overlays (not color coded) were prepared at a scale matching that of aerial photographs -- approximately 1:40,000 (Figure 50).

5.6.5 COMPARISON OF ERTS OVERLAYS WITH MAPS AND AERIAL PHOTOGRAPHY

In Figure 43a, "Water (Deep and Shallow)," the large, roundish lake and its central island are Orchard Lake and Apple Island, respectively. The large lake directly above it is Cass. The same two lakes and others are recognizable at larger scale in Figure 46a, where individual ERTS picture elements are visible as the "stair-step" lake boundaries. Finally, the same lake boundaries in Figure 50 are superimposed on aerial photographs taken by a NASA C-130 on March 27, 1973.

After detailed comparison of these overlays with the base maps and aerial photographs the following comments are appropriate concerning the accuracy of land classifications.

a. At the time of ERTS passage (April 14, 1973), deciduous foliage was sparse. The "forested land" category included chiefly mixed hardwoods. (Few large stands of evergreens occur in southern Michigan.) An example is Apple Island in Orchard Lake (Figure 47). Some older subdivisions in the same area are also classified "forest" rather than "urban" due to their high density of trees.

b. "Tended grass" was readily classified in April (Figures 45a and 48) and included any grassy areas that are fertilized and cultivated: golf courses, lawns, cemeteries, sod farms, etc. New crops emerge later and probably would not have the foliage density to be confused with grass. Some low-density urban areas with numerous lawns are grouped here.

c. "Rangeland" (untended grass) is generally brown in April. As a category it includes old fields, natural range and grassy lowlands.

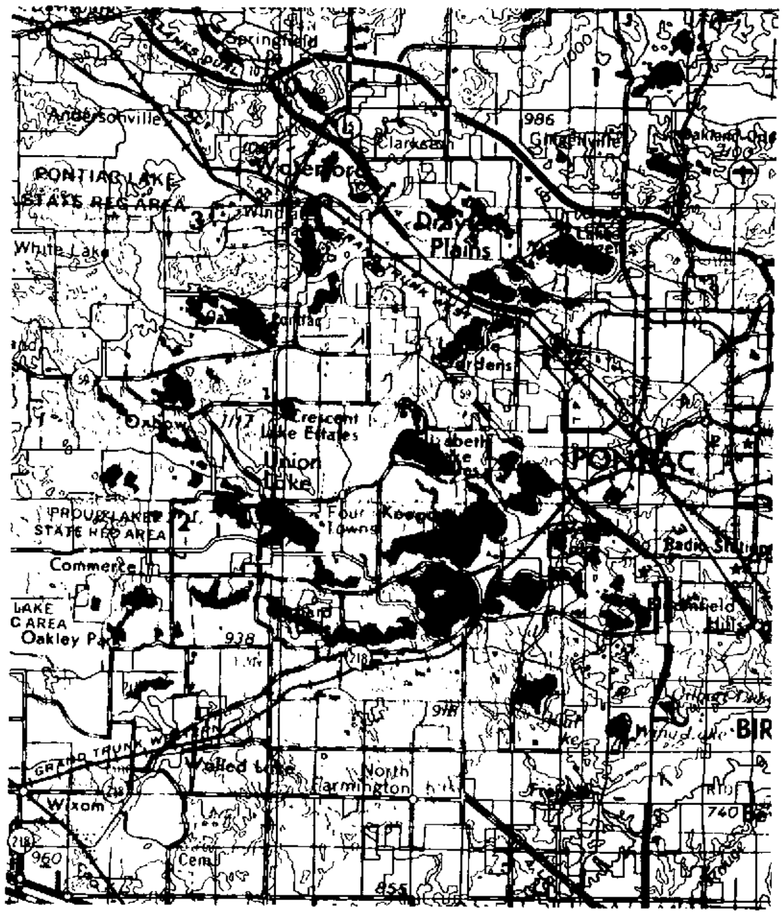

a. Water (Deep and Shallow)

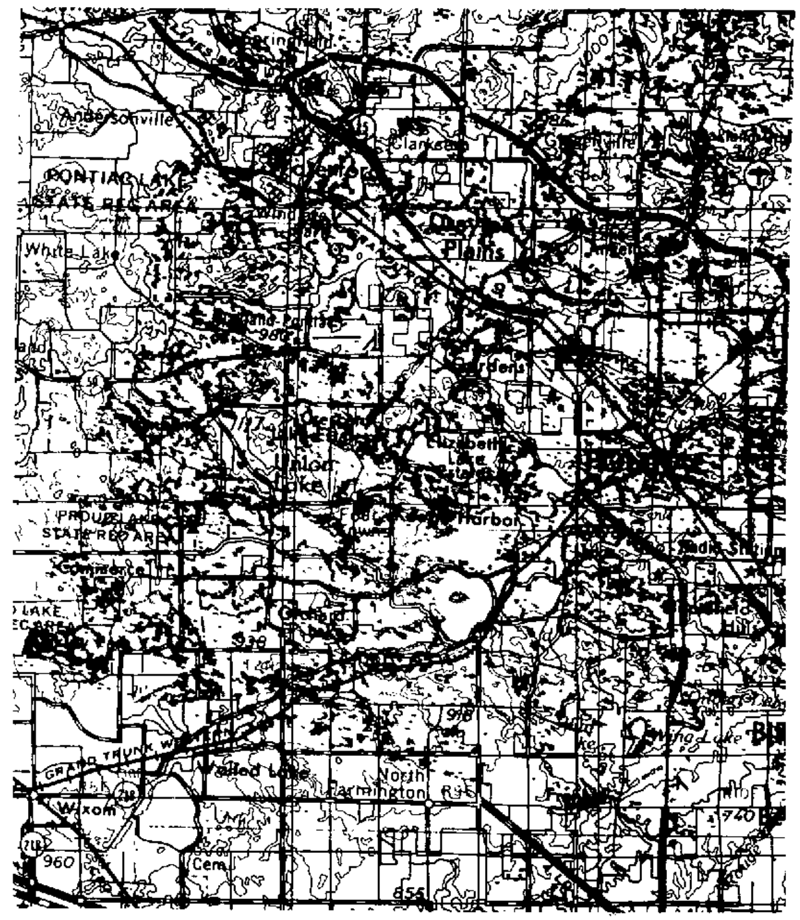

b. Wetlands

Fig. 43 Computer-generated overlays on AMS 1:250, 000 scale map. from ERTS tapes of April 14, 1973 (ID No. 1265-15474)

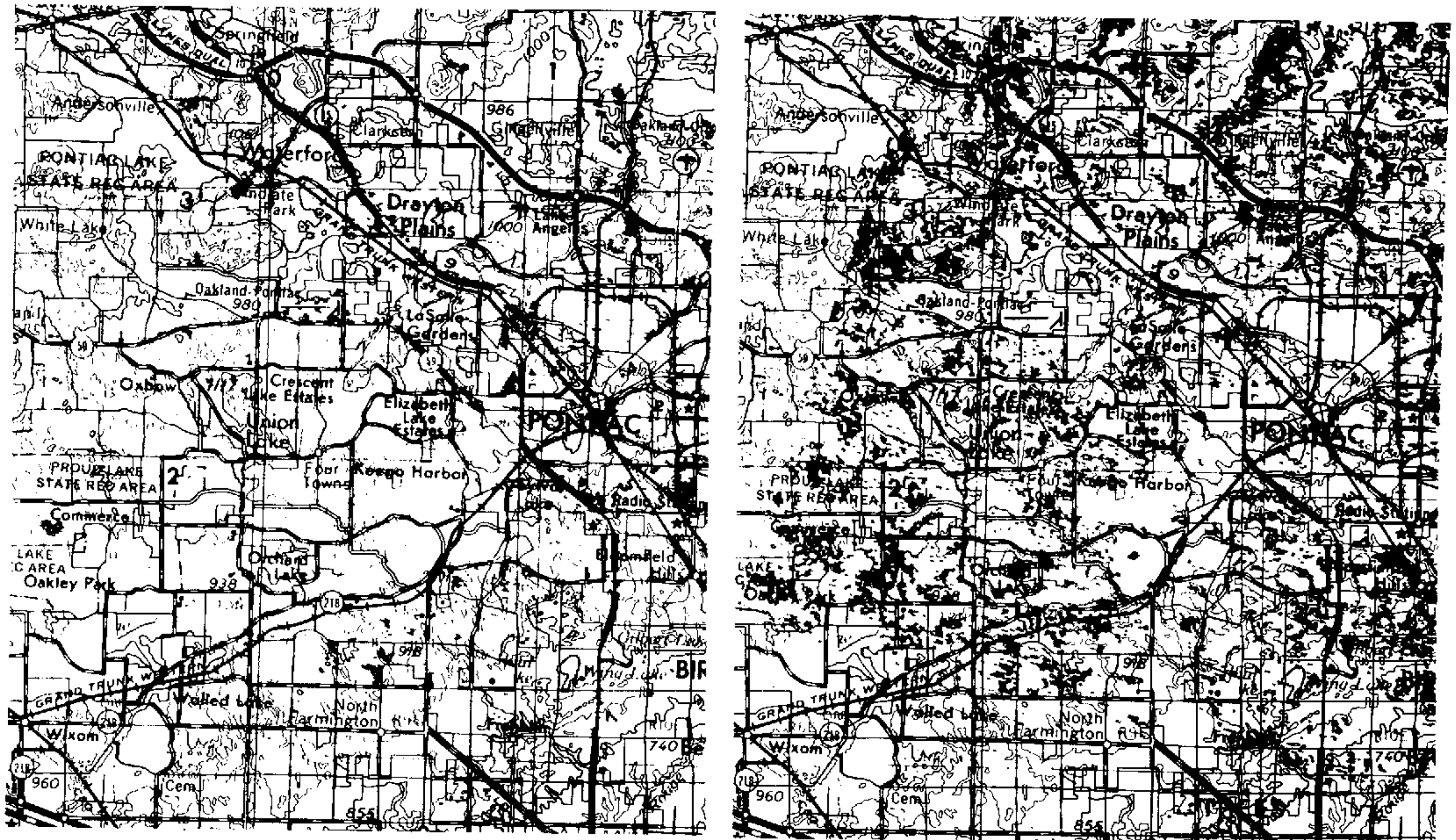

a. Extractive (Bare) Earth

b. Forested Land

Fig. 44 Computer-generated overlays on AMS 1:250,000 scale map from portion of ERTS Tape 2, ID No. 1265-15474 (April 14, 1973).

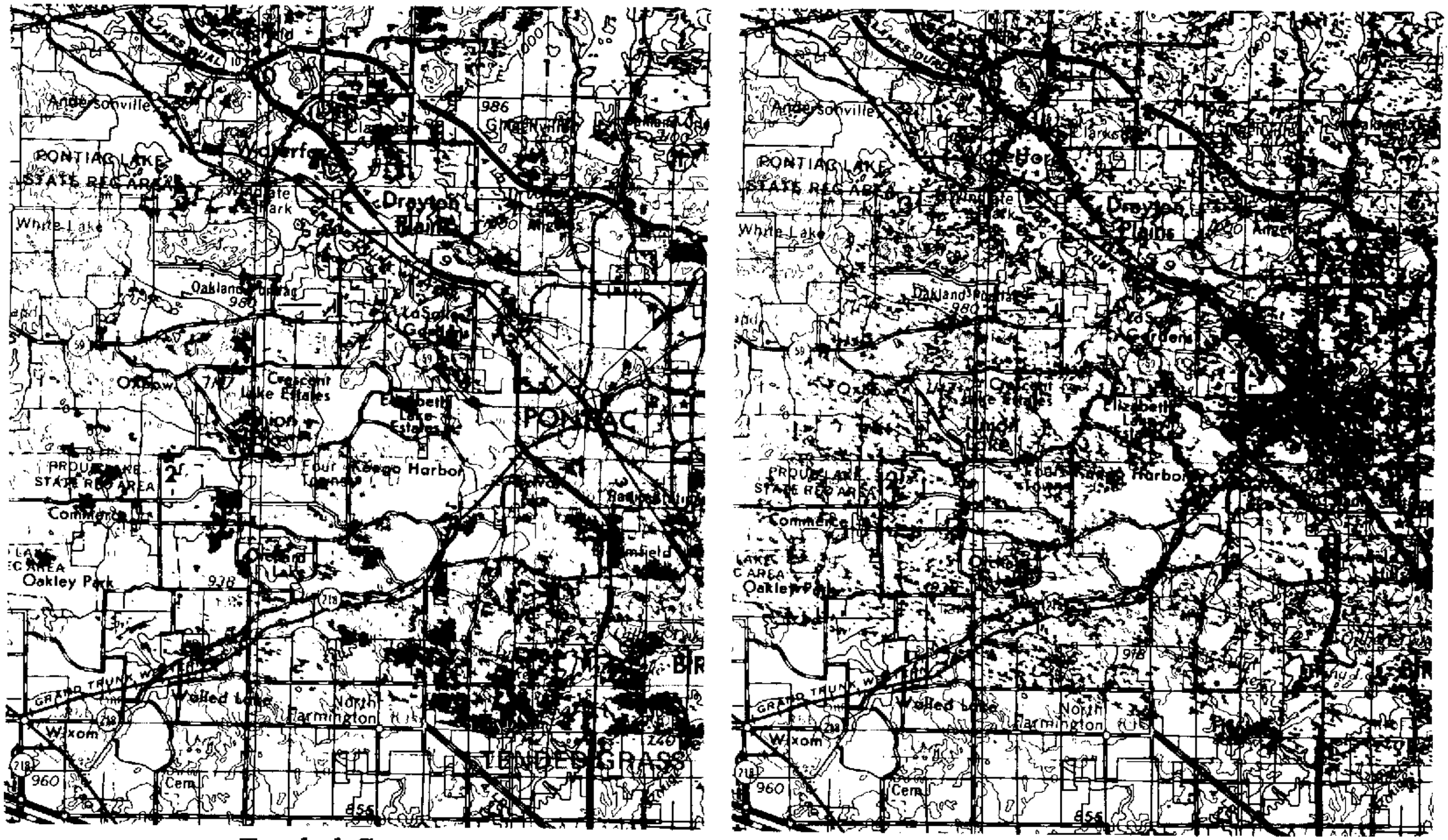

a. Tended Grass b. Urban

Fig. 45 Computer-generated overlays on AMS 1:250,000 scale map from portion of ERTS Tape 2, ID No. 1265-15474 (April 14, 1973).

a. "Unsmoothed" on Vegetation Map

b. "Smoothed" on Land-Use Map

Figure 46 Computer-Generated Map of Water Boundaries on Oakland County 1:48, 000 Scale Maps from Portion of ERTS Tape 2, ID No. 1265-15474 (April 14, 1973).

Figure 47 ERTS Computer-Generated Overlay of Forested Land Boundaries on Oakland County Vegetation Map (Scale 1:48, 000). Map Symbols E, K, M Denote Deciduous Forest. From ERTS Tape 2, ID No. 1265-15474 (April 14, 1973).

C-2

Figure 48 ERTS Computer-Generated Overlay of Tended Grass Boundaries on Oakland County Land-Use Map (Scale 1:48,000). Boundaries Show Recreational and Conservation Map Categories. From ERTS Tape 2, ID No. 1265-15474 (April 14, 1973).

Figure 49 ERTS Computer-Generated Overlay of Extractive Earth Boundaries on Oakland County Land-Use Map (Scale 1:48,000). From ERTS Tape 2, ID No. 1265-15474 (April 14, 1973).

a. Aerial Photograph

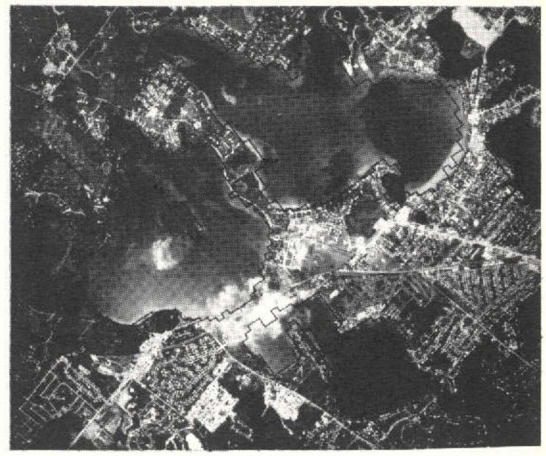

b. Water Boundaries

c. Tended Grass Boundaries

d. Forested Land Boundaries

Figure 50 Computer-Generated Boundaries from ERTS Tapes Overlaying Aerial Photograph. Overlays produced from portion of ERTS tape of April 14, 1973 (ID No. 1265-15474).

d. "Wetlands" are low, brushy areas, predominantly on lake margins or old lake beds. It is doubtful that floating aquatic vegetation would be classified here. In Figure 43b wetlands are seen, for example, around the shore of Apple Island and bordering many lakes.

e. Bare soil or "extractive earth" includes all gravel pits, construction sites and other devegetated areas. Some large asphalt parking areas are classified here as well, perhaps due to a coating of earth or road salt which has modified its normal reflectance (Figures 44a and 49).

f. The training area chosen for the "urban" category was within the city of Pontiac and included industrial, business and high density residential development. All other similarly commercial and residential areas were classified correctly in this category, including the zones of development along major roadways.

g. Areas recorded as "unclassified" later proved to be large expanses of asphalt roof tops, i.e., chiefly automotive assembly plants or other such structures.

It is not possible at this point to express quantitatively the potential of these land categories to discharge nutrients, especially phosphorus, to lakes; clearly, this potential is a function, not only of land use or cover, but also of watershed slope, soil type, rate of runoff, etc. Ground studies beyond the scope of this project are needed to make that kind of assessment. Other factors being equal, however, it is generally true that runoff from "urban" and "extractive earth" categories is richest in nutrients, followed by "tended grass" and "rangeland" (if agricultural). "Forest land" and "wetland" would have the least potential to release nutrients via runoff. These generalities are supported in reviews by Dillon and Kirchner (in press), and Loehr (in press), as cited by Likens and Bormann (1974). Various other studies have indicated that runoff from agricultural land is particularly rich in nitrogen while sewage inputs are high in phosphorus (Biggar and Corey, 1969).

Other sub-categories of land use/cover might have been classified as well, but the main objective here was to refine the procedures for ERTS mapping of <u>any</u> watershed categories of importance to lake water quality.

At map scales of 1:48,000 or more (Figure 46a) the individual ERTS picture elements in the overlay are conspicuous, since they each represent about one acre in area. Consequently, the category boundaries, as plotted automatically, do not conform closely to natural terrain contours, i.e., lake margins. Manual "smoothing" of the plotted lines (by bisecting the elements) makes the discrepancies less distracting, though it does not improve accuracy (Figure 46b).

The base map in this case (Figures 46b, 48 and 49) is a current land use map produced by the Oakland County Planning Commission. While the map classifications of land use are functional and political, as well as physical, these comparisons of ERTS and conventional land use mapping illustrate the point that ERTS overlays are a convenient and inexpensive means of updating such maps, where the larger terrain features are concerned.

Direct comparison of ERTS overlays with contemporary aerial photographs (Figure 50) provides the most information about accuracy of the classification program. At the scale of 1:40,000 the category boundaries in overlays adhere remarkably well to terrain features of the same class. Some exceptions and misclassifications were noted earlier. It should be noted again that the spectral coefficients used here in category recognition (by computer) were merely a first effort. More faithful or detailed classifications of land use/cover undoubtedly would be possible with a more judicious choice of training sets at various times of the year.

Even with only one acre resolution the ERTS data provide abundant detail for thematic mapping purposes in all but the smallest lake watersheds. Judging from the results of this experiment it would be a straightforward next step to generate color-coded map overlays and area tables for selected lake watersheds using a variety of categories of known runoff characteristics. These in concert with the pertinent water quality data would constitute an operational use of ERTS for trophic level monitoring and prediction.

6. NEW TECHNOLOGY

The computer programs and techniques used in this investigation have been under continued development at Bendix for the past 8 to 10 years, primarily using aircraft multispectral scanner data and, more recently, using ERTS MSS and Skylab/EREP-S192 data. Since these procedures have been developed under other programs and are well documented (Rogers, 1974), they are not reported here as new technology.

7. CONCLUSIONS AND RECOMMENDATIONS

7.1 CONCLUSIONS

The investigation has achieved its objectives by demonstrating ERTS potential for monitoring lake eutrophication and land-use in lake watersheds. The watershed maps, updated periodically, would provide the basis for forecasting changes in nutrient inputs and eutrophication rates.

Significant conclusions which can be made by this investigation include the following:

a. Inland lakes of one acre and larger can be detected and mapped by ERTS, particularly in Bands 6 and 7. The shape and orientation of small lakes does not degrade their detection provided the open water is approximately 65 meters wide at its narrowest point.

b. Repetitive mapping of land-water boundaries will show wetland vegetation encroachments into those lakes with high eutrophication rates caused by increased organic sedimentation in shallow areas.

c. Computer processing of ERTS data provides accurate bathymetry maps of lakes showing deep and shallow (i.e., bottom visible) water. Mapping on an annual basis will provide important information on changes in sediment deposition and growth patterns of aquatic plants, both of which are major indicators of the rate and degree of eutrophication.

d. Removal of atmospheric parameters (atmospheric attenuation, and scattering from atmosphere) from ERTS radiance measurements permits the absolute reflectance of lakes to be determined. The atmospheric parameters can be derived from ground measurements with the Radiant Power Measuring Instrument (RPMI) developed by NASA for ERTS ground truth. Direct spot-reflectance measurements of the lakes were obtained with the RPMI for comparison with spacecraft measurements. The reflectance derived from spacecraft data show that: in Band 4, deep water reflectance ranges from 3 to 5.5%; in Band 5, it was 0.3 to 2.3%. Band 6 and Band 7 values were near zero. Shallow water reflectance ranged up to 9% in Band 4.

e. Absolute (%) reflectance, determined from ERTS data for surface waters, can be related directly to the color and light scattering properties of lake water, which in turn are related to trophic conditions. Findings reported here for the six test lakes bear out the expected relationships in a qualitative way. The intensity of reflectance, particularly in Band 5, varies directly with turbidity (and inversely with transparency). The ratio of ERTS Band 4 to 5 (4/5) measurements correlates with suspended matter.

f. Based on results obtained with the RPMI, surface phenomena such as algal scums are readily detectable by ERTS. Detection is noted by a large increase in reflectance measured in Bands 6 and 7 (relative to 4 and 5). More frequent satellite coverage is necessary to make maximum use of this phenomena.

g. Computer classification of deep waters resulted in a partial separation of lakes, based on turbidity, i.e., lakes having a difference of 0.8 and 1.9 mg/liter particulate concentration (dry weight) were mapped into separate deep water categories.

h. Land-use categories mapped by computer techniques from ERTS tapes included wetlands (swamps), rangeland, tended grass, trees, barren earth, and urban areas. Classification accuracy was better than 90% for all categories. In general, it was determined that all of Anderson Level I categories and most Level II categories are readily mapped from ERTS.

i. The application of ERTS CCTs and computer processing techniques permits the generation of map overlays showing land and water categories at a tenth of the cost of conventional mapping techniques. Geometric corrections are applied to the classified ERTS data to produce color-coded map overlays at scales of 1:24,000 to 1:250,000. These geometrically corrected map overlays, one for each target category, are drawn by a pen under computer control. The overlays placed over an AMS map of the same scale immediately provide land/water category locations. A number of new lakes were mapped for the first time.

j. Techniques have been developed for storing and retrieving from a computer data bank the classified land/water data as interpreted from ERTS. The user interacts with the data bank to obtain within lake watersheds the area covered, in square kilometers, by each land-use category. This technique was successfully demonstrated by establishing correlations between watershed land-use.and lake water quality, as indicated by a total and fecal coliform bacteria counts. These computer procedures are basic elements for determining those land-use factors and sources of nutrients that accelerate eutrophication is lakes and reservoirs.

k. The maps and data generated from the ERTS spacecraft can be used to monitor seasonal changes in lake features and in watershed factors that affect eutrophication rates. Repetitive use of these techniques will provide current status of lake eutrophication as well as to serve to alert planners to potential losses in water quality.

7.2 RECOMMENDATIONS

a. A program is recommended that would demonstrate the cost benefits of using ERTS on an operational basis in monitoring and controlling lake eutrophication. ERTS data would provide the basis for computer-generated products including, geometrically correct map overlays showing (a) lakes and ponds classified by trophic state, (b) turbidity patterns in the Great Lakes where each overlay provides suspended particulate concentration, and (c) land-use categories in watersheds. Area measurement tables would also be generated from ERTS tapes. These computer printouts would provide, within the watershed or water mass boundaries, a quantitative measure of the area covered by each category. These ERTS data products should be used to support on-going programs being conducted by agencies, who would in turn provide detailed ground truth on water quality and watershed land use and support the studies and evaluations of the usefulness and cost benefits of the ERTS data products.

b. Ground-level radiometry should also be continued routinely during future ERTS-B investigations. It is important that target reflectances and spectral signatures be expressed in terms of absolute (%) reflectance rather than ERTS radiance or relative digital counts. Further refinement of the atmospheric equations may be needed to derive % reflectance accurately from CCT data. It will also be desirable to accumulate much more information correlating absolute ERTS reflectance measurements to variations of water color, turbidity, etc.

c. Further efforts should also be made to derive CIE expressions for water color directly from ERTS CCT data. These can be verified by and compared to CIE values determined at ground level. Ideally, the same radiometer could be used both for this and the atmospheric corrections. The radiometer should be a rapid-scanning instrument with digital output which covers the spectral range .4 – 1.2 μm. Other expressions for water color (i.e., ERTS band ratios) could be extracted readily from the spectral data recorded by such a radiometer. In summary, there is a clear need to define water color objectively (i.e., by CIE specifications) and to relate this color definition both to trophic indication and to reflectance measurements from multispectral remote sensors.

d. More turbid lake waters should be studied to refine correlations of ERTS band ratios (4/5, 4/6) and percent reflectance in each band, with water turbidity and color. Some portions of the Great Lakes would be better suited by scale and water quality for this experiment. After atmospheric corrections are more refined it should be possible to better classify with ERTS the trophic condition of less turbid inland lakes, like those in Oakland County.

8. REFERENCES CITED

1. American Public Health Association et al., "Standard Methods for the Examination of Water and Waste Water," (13th Ed.), American Public Health Association, New York, 874 pp., 1971.

2. J. Anderson, E. Hardy and J. Roach, "A Land-Use Classification System for Use with Remote Sensor Data," Geological Survey Circular 671, Washington, D.C., 16 pp., 1972.

3. J. W. Biggar and R. B. Corey, "Agricultural Drainage and Eutrophication," pp. 404 - 445, In: Eutrophication: Causes, Consequences and Correctives, National Academy of Sciences, Washington, D.C., 661 pp., 1969.

4. R. H. Blodgett, "Southeastern Michigan: The Land the Glaciers Left Behind," The Explorer, (13(1), pp. 4 - 10, 1971.

5. D. E. Bowker, P. Fleischer, T. A. Gosink, W. J. Hanna and J. C. Ludwick, "Transmissometry and Suspended Matter in Lower Chesapeake Bay: Correlation with ERTS Multispectral Imagery," Proc. American Society of Photogrammetry (Fall Convention, Oct. 2 - 5, 1973), pp. 840 - 847, 1973.

6. P. E. Chase, "Utilization of ERTS-1 Data to Monitor and Classify Eutrophication of Inland Lakes," Interim Report (February 1973), NAS Contract 521810 to Bendix Aerospace Systems Division, Ann Arbor, Michigan, 61 pp., 1973.

7. G. W. Clark, G. C. Ewing and C. J. Lorenzen, "Spectra of Backscattered Light from the Sea Obtained from Aircraft as a Measure of Chlorophyll Concentration," Science, 167:20, pp. 1119 - 1121, 1970.

8. A. E. Coker, A. Higer and C. R. Goodwin, "Detection of Turbidity Dynamics in Tampa Bay, Florida Using Multispectral Imagery from ERTS-1," NASA Symposium on Significant Results Obtained from the ERTS-1 (Mar. 5 - 9, 1973), Washington, D.C., pp. 1715 - 1726, 1973.

9. C. A. Doxiadis, "Emergence and Growth of an Urban Region; the Developing Urban Detroit Area," Vol. 1, Detroit Edison Company, Detroit, 335 pp., 1966.

10. R. H. Dye, D. S. Hanson and C. L. Crawford, "Signature Data Processing Study," Bendix Report BSR 2949, NAS 9-9848, August 1970.

11. Federal Water Pollution Control Administration, Report of the Committee on Water Quality Criteria, U.S. Department of Interior, Washington, D.C., 234 pp., 1968.

12. F. A. Forel, Ficerche fisiche sui laghi d'Insubria, Rend. R. 1st Lombardo, ser. 2.22: 739, 742; 1889.

13. L. C. Gramms and W. C. Boyle, "A Literature Review of Remote Sensing for Water Quality," U. of Wisconsin Remote Sensing Program, Report No. 7, 34 pp., 1971.

14. P. E. Greeson, "Lake Eutrophication - a Natural Process," Water Resources Bulletin, Vol. 5, No. 4, p. 16, 1969.

15. A. Hazen, A New Color Standard for Natural Waters, Amer. Chem. J. 14: pp. 300-310; 1892.

16. L. Hetling, "Occurrence and Transport of Nutrients and Hazardous Substances," (Progress Report) EPA Ecological Research Series, First Annual Reports of the EPA IFXGL Projects, National Environmental Research Center, Corvallis, Oregon, 336 pp., 1973.

17. L. M. Hom, "Aerial Detection of Algae at Clear Lake and Lake Tahoe," Proc. of 3rd Annual Conf., Remote Sensing of Air and Water Pollution, Sacramento, Calif., 1967.

18. Hughs; "Multispectral Scanner System for ERTS – Four-Band System," Report No. HS324-5214, August 1972.

19. C. R. Humphrys (ed.), Oakland County, Michigan; Water Resources, Department of Resource Development, Michigan State University, Lansing, 1968.

20. G. E. Hutchinson, A Treatise on Limnology, Vol. 1 Geography, Physics, and Chemistry, John Wiley and Sons, Inc., New York, 1015 pp., 1957.

21. H. R. James and E. A. Birge, "A Laboratory Study of the Absorption of Light by Lake Waters," Transactions of the Wisconsin Academy of Science, Arts and Letters, 31: pp. 1 - 154, 1938.

22. H. G. Jerlov, "Optical Oceanography," Elsevier Publishing Company, New York, 194 pp., 1968.

23. C. Juday and E. A. Birge, "The Transparency, the Color and the Specific Conductance of the Lake Waters of Northeastern Wisconsin," Trans. Wisc. Acad. 28: pp. 205-259, 1933.

24. V. Klemas, R. Sona, W. M. Treasure and R. Rogers, "Satellite Studies of Turbidity and Circulation in Delaware Bay," Proc. Amer. Soc. of Photogrammetry (Fall Convention, Oct. 2-5, 1973), pp. 848 - 871, 1973.

25. G. E. Likens and F. H. Bormann, "Linkages Between Terrestrial and Aquatic Ecosystems," Bioscience 24 (8), pp. 447-456, 1974.

26. K. M. Mackenthum and W. M. Ingram, "Biological Associated Problems in Freshwater Environments," Fed. Water Poll. Contr. Admin., U.S. Department of Interior, Washington D.C., 287 pp., 1967.

27. W. R. McNeil and K. P. B. Thomson, "Remote Measurement of Water Color and Its Application to Water Quality Surveillance," Proc. 3rd Annual Remote Sensing of Earth Resources Conf., U. of Tennessee Space Institute, Tullahoma (March 25-27, 1974), 30 pp., 1974.

28. Millipore Corporation, Phytoplankton Analysis, Publication AB310, Millipore Corp., Bedford, Massachusetts, 9 pp., 1974.

29. Optical Society of America, The Science of Color, Thomas Y. Crowell Co., New York, 385 pp., 1953.

30. J. W. Oswald, "Remote Sensing Data and Evaluation of Water Quality," Proc. of 3rd Annual Conf., Remote Sensing of Air and Water Pollution, Sacramento, Calif., 1967.

31. M. C. Palmer, "Algae in Water Supplies," U.S. Dept. of Health, Education and Welfare, Public Health Service Division of Water Supply and Pollution Control, Washington D.C., 1962.

32. E. J. Pluhowski, "Remote Sensing of Turbidity Plumes in Lake Ontario," NASA Symposium on Significant Results Obtained from the ERTS-1 (Mar. 5-9, 1973), pp. 837-846, 1973.

33. F. C. Polcyn and I. Sattinger, "Water Depth Determination Using Remote Sensing Techniques," Paper presented at 6th Symp. on Remote Sensing of Environment, U. of Michigan, Ann Arbor, Michigan, 1969.

34. F. C. Polcyn, W. L. Brown and S. P. Steward, "A Method for Calculating Water Depth, Water Attenuation Coefficient and Bottom Reflectance Characteristics," Paper presented at 7th Symp. on Remote Sensing of Environment, U. of Michigan, Ann Arbor, Michigan, 1971.

35. R. H. Rogers, K. Peacock and N. J. Shah, "A Technique for Correcting ERTS Data for Solar and Atmospheric Effects," NASA Earth Resources Survey Program (Abstracts), E74-10489, June 24, 1974, Report NASA-CR-136890, 21 pp., 1974.

36. R. H. Rogers and L. E. Reed, "Automated Land-Use Mapping from Spacecraft Data," Proc. of the 40th Annual Meeting of the American Society of Photogrammetry, St. Louis, Mo., March 1974.

37. R. H. Rogers and V. E. Smith, "Utilization of ERTS-1 Data to Monitor and Classify Eutrophication of Inland Lakes," Interim Report (August 1973), NAS Contract 521810 to Bendix Aerospace Systems Division, Ann Arbor, Michigan, 43 pp., 1973.

38. J. P. Scherz, M. Sydor and J. F. Van Domelen, "Aircraft and Satellite Monitoring of Water Quality in Lake Superior Near Duluth," Paper E-9, 3rd ERTS-1 Symposium, NASA-GSFC, 10-13 December 1973.

39. D. W. Schindler, "Eutrophication and Recovery in Experimental Lakes: Implication for Lake Management," Science, 184(4139) pp. 897-899, 1974.

40. J. D. H. Strickland and T. R. Parsons, "A Practical Handbook of Sea-water Analysis," Bulletin 167, Fisheries Research Board of Canada, Ottawa, 311 pp., 1968.

41. W. Ule, Die Bestimmung der Wasserfarbe in den Seen; Petermanns Mitt. 38: 70-71; 1892.

42. H. L. Yarger, J. R. McCauley, G. W. James and L. M. Magnuson, "Water Turbidity Detection Using ERTS-1 Imagery," NASA Symposium on Significant Results Obtained from the ERTS-1 (Mar. 5-9, 1973), pp. 651-658, 1973.

APPENDIX

A TECHNIQUE FOR CORRECTING ERTS DATA FOR SOLAR AND ATMOSPHERIC EFFECTS

ABSTRACT

A technique is described by which ERTS investigators can obtain and utilize solar and atmospheric parameters to transform spacecraft radiance measurements to absolute target reflectance signatures. A radiant power measuring instrument (RPMI) and its use in determining atmospheric parameters needed for ground truth are discussed. The procedures used and results achieved in processing ERTS CCTs to correct for atmospheric parameters to obtain imagery are reviewed.

INTRODUCTION

The need for target reflectance signatures evolves from the needs of individual Principal Investigators, NASA's requirements to correlate results of a large number of investigators, and the pre-conditions of wide-area extrapolations of ground truth data for automatic data processing techniques. Target reflectance data are needed by all man and machine systems to obtain the unambiguous interpretation of ERTS data. In response to the need for absolute target reflectance signatures, NASA Experiment MMC 655 is evaluating the capabilities of a wide range of techniques for determining and removing solar and atmospheric parameters and effects from ERTS data. Techniques being evaluated include (1) transferring known ground reflectance to spacecraft measurements, (2) using the ground-based Radiant Power Measuring Instrument (RPMI) to measure, directly, the needed solar and atmospheric parameters, (3) using spacecraft data alone (with little or no auxiliary inputs), and (4) using radiation transfer models employing inputs such as surface pressure, ground visibility, temperature, and relative humidity. This paper evaluates the RPMI technique.

ATMOSPHERIC PARAMETERS

The desired reflectance information is difficult to obtain directly from the ERTS sensor radiance measurements because these measurements are a function of unknown solar and atmospheric parameters caused by the intervening atmosphere, and these parameters vary significantly. The radiance, L, sensed by the spacecraft sensor from a given target, depends not only upon the reflectance, ρ, of the target, but also upon the target irradiance, H, and upon the spectral absorption and scattering of the atmosphere between the target and the spacecraft. This atmosphere attenuates the radiance reflected from the target to the spacecraft and adds to the foreground radiance by backscatter of sunlight from the atmosphere, L_A. The composite radiance, L, recorded within an ERTS band for a spacecraft looking vertically is, therefore, related to the desired target reflectance, ρ, and to the solar and atmospheric parameters; H, τ, and L_A; by:

$$L = \frac{\rho}{\pi} H \tau + L_A \qquad (1)$$

where τ is the beam transmittance for one air mass.

The target irradiance, H, has two components; one caused by the direct sun, denoted $H_{SUN} \cos Z$ (in which H_{SUN} is the irradiance on a surface normal to the sun's rays and Z is the solar zenith angle) and a component caused by the sky, denoted H_{SKY}. Expanding H of Equation 1 in terms of the direct sun and sky components and solving the equation for ρ results in

$$\rho = \frac{(L - L_A) \cdot \pi}{\tau \, (H_{SUN} \cos Z + H_{SKY})} \qquad (2)$$

For a remote sensing system looking vertically downward, τ is the atmospheric transmission of one air mass. If m is the number of air masses referenced to the zenith air mass (for which m = 1), the atmospheric transmission through some other value of m is given by τ^m. The direct sun component of target irradiance, H_{SUN}, in Equation 2 can be subdivided as

$$H_{SUN} = H_o \, \tau^m, \qquad (3)$$

in terms of the solar irradiance normal to the sun's rays outside the atmosphere, H_o. Combining Equations 2 and 3, the desired target reflectance, ρ, in terms of ERTS radiance, L, measurements is

$$\rho = \frac{(L - L_A) \cdot \pi}{\tau \, (H_o \, \tau^m \cos Z + H_{SKY})}, \tag{4}$$

where L_A, τ, H_o, m, cos Z, and H_{SKY} are the solar and atmospheric parameters that must be known to accurately compute target reflectance.

Parameters Readily Determined

In the machine processing of ERTS computer compatible tapes (CCTs), the parameters L, H_o, m, and Z of Equation 4 are easily and quickly determined. Target counts, c_i, recorded on ERTS CCTs are transformed to the target radiance, L of Equation 4 by

$$L_i = c_i \, K_i \;\; mw/cm^2 - sr, \tag{5}$$

where i indicates MSS band number and constants K_i are determined as described on Page G-14 of the ERTS Data User Handbook ($K_4 = 0.0195$, $K_5 = 0.0157$, $K_6 = 0.0138$, $K_7 = 0.0730$). The sun zenith angle, Z, is computed from $Z = 90 - \theta_E$, in which the sun elevation angle, θ_E, is also extracted from the ERTS CCT. For sun zenith angles less than 60 degrees, the air mass, m of Equation 4, is given to an accuracy better than 0.25% by m = sec Z. For larger sun angles, a more accurate value is given by Bemporad's formula

$$M = \sec Z - 0.001867 (\sec Z - 1) - 0.002875 (\sec Z - 1)^2 - 0.0008083 (\sec Z - 1)^3. \tag{6}$$

The solar irradiance, H_o, outside the earth's atmosphere is well known and changes less than 6% over a 12-month period. H_o can be determined from NASA-published data (Thekaekara, 1971) or derived from RPMI measurements. Values obtained from RPMI and Dr. Thekaekara's published data for a mean earth-sun distance of 1 astronomical unit (AU), are shown in Table 1.*

If desired, the values specified (for 1 AU) can be corrected for the precise earth-sun distance at the time of ERTS overflight by factors also given in Dr. Thekaekara's report.

The remaining solar and atmospheric parameters needed for Equation 4; L_A, τ, and H_{SKY}; depend on the specific atmosphere within the scene and must be determined by the Principal Investigator at the time of ERTS overflight.

---

*Please refer to back of report for tables, figures, and references.

RADIANT POWER MEASURING INSTRUMENT (RPMI)

One technique for obtaining the remaining atmospheric parameters is to deploy the RPMI shown in Figure 1. This instrument was developed specifically to provide an ERTS investigator with the capability of obtaining the complete set of solar and atmospheric measurements.

The RPMI is a rugged, hand-carried, portable instrument, calibrated to measure both down-welling and reflected radiation within each ERTS MSS band. A foldover handle permits a quick change from wide-angle global or sky irradiance measurements to narrow angle (7.0° circular) radiance measurements from sky and ground targets.

The RPMI's wide dynamic range (1 to 10^6) is tailored to permit measurements to be made over the full range of atmospheric parameters encountered by ERTS. These extremes have been found to include direct beam solar irradiance up to 25 mw/cm^2 in Band 7, sky radiance as low as 0.077 mw/cm^2 - sr in Band 6, and radiance reflected from water surfaces in Bands 6 and 7 as low as 0.02 mw/cm^2 - sr. The RPMI measurements are traceable to an NBS source to an accuracy of 5% absolute and 2% relative from band-to-band. The RPMI calibration is also checked, from time to time, against the NASA Goddard calibration source to ensure uniformity between RPMI and ERTS MSS measurements.

DETERMINATION OF ATMOSPHERIC PARAMETERS

The RPMI is deployed in concert with ERTS overflights to obtain direct measurements, within the four ERTS MSS bands, of (1) global irradiance, H, (2) sky irradiance H_{SKY}, (3) radiance from a narrow solid angle of sky, L_{MEAS} (ϕ), and (4) direct beam-solar irradiance $H_{SUN}(m)$. From these measurements, additional solar and atmospheric parameters, such as beam transmittance, τ; path radiance, L_A; and direct beam-solar irradiance above the atmosphere, H_o, are determined. With these parameters, Equation 4 is applied to transform the ERTS radiance measurements, L, into absolute target reflectance units.

DIRECT BEAM SOLAR IRRADIANCE (H_{SUN})

Direct beam solar irradiance, H_{SUN}, is measured, as shown in Figure 1C, by pointing the instrument directly at the sun with the telescope in place and recording the irradiance at each wavelength.

GLOBAL AND SKY IRRADIANCE

Global irradiance, H, is measured directly in each band as shown in Figure 1B. Additional accuracy in H can be obtained using H_{SUN} (m) and sky irradiance, H_{SKY}, by shadowing the sun and reading global minus direct beam-solar irradiance, and then computing the total target irradiance, using

$$H = H_{SUN} \cos Z + H_{SKY} \qquad (7)$$

The sun angle, Z, may be read from the sun dial on the side of the RPMI after leveling the instrument with its bubble level.

BEAM TRANSMITTANCE (τ)

Beam transmittance, τ, per unit air mass is determined directly from

$$\tau = \left(\frac{H_{SUN}}{H_o}\right)^{\frac{1}{m}} \qquad (8)$$

when the solar irradiance outside the atmosphere, H_o, is known, as in Table 1. The air mass is calculated from the solar zenith angle, using Equation 6.

If solar irradiance outside the atmosphere, H_o, is not known, τ per unit air mass can be determined by making at least two H_{SUN} measurements, denoted $H_{SUN}(m_1)$ and $H_{SUN}(m_2)$, at air masses m_1 and m_2 and computing

$$\tau = \left(\frac{H_{SUN}(m_1)}{H_{SUN}(m_2)}\right)^{\frac{1}{m_1 - m_2}} \qquad (9)$$

If a series of H_{SUN}(m) measurements are made and then plotted on a log scale as a function of air mass, an atmospheric extinction curve similar to that shown in Figure 2 results. By performing a least squares curve fit to the H_{SUN} measurements, greater accuracy in the H_{SUN} values needed for Equation 9 may be derived.

The intercepts of the H_{SUN} lines of Figure 2 with the vertical axis (i.e., m = 0) yields H_o in each ERTS band. These values of H_o can be used in succeeding computations of τ by Equation 8 and as calibration constants to test and recalibrate the RPMI, if necessary, using the sun as a source, at any location in the world.

Beam transmittance, τ, derived from 10 sets of field measurements covering the period January through June of 1973 (Table 2) shows this parameter to range from 70 to 85% in Band 4, from 77 to 90% in Band 5, from 81 to 94% in Band 6, and from 84 to 97% in Band 7.

PATH RADIANCE

The only remaining atmospheric parameter needed to transform ERTS radiance into reflectance is the radiance, L_A, reaching the spacecraft from Rayleigh and aerosol scattering by the atmosphere. As path radiance cannot be measured directly, it must be derived from ground-based sky radiance measurements of the backscatter. The simplest technique is to use the RPMI to measure the sky radiance, $L_{MEAS}(\phi)$, scattered at angle ϕ, as shown in Figure 3, such that ϕ is identical to ϕ, the angle through which radiation is scattered to the spacecraft, and then to correct this measurement for the difference in air masses between the direction of observation and the direction of the spacecraft. This technique provides a straightforward measurement procedure when $Z > 45°$. When L_{MEAS} is recorded at an angle equal to the scattering angle to the ERTS, the path radiance, L_A, seen by ERTS is

$$L_A = L_{MEAS}\left(\frac{1-\tau}{1-\tau^{m_o}}\right), \tag{10}$$

in which m_o is the air mass in the direction of observation (in this case $m_o = \frac{1}{\cos\beta}$) and τ, as previously defined, is the atmospheric transmission per unit air mass. The validity of this formula has been demonstrated by Rogers and Peacock (April 1973) and discussed by Gorden, Harris, and Duntley (1973). Equation 10 is adequate when the atmospheric measurements are made concurrent with the ERTS overflight; (i.e., at a sun angle close to the one at the time of the ERTS flyover).

However, if $Z < 45°$, it is easy to see that $\beta > 90°$ and a simple determination of L_A is not possible. During the summer months, this is frequently the condition at the time of the ERTS overpass. It becomes necessary to make the sky radiance measurements at a time when $Z > 45°$ and to correct for the greater attenuation of the incident sunlight.

A correction factor, T_{ERTS}/T_Z, must be multiplied by Equation 10 to derive the path radiance, L_A, viewed by the spacecraft if the time between the ERTS overpass of the test site and the time of the sky radiance observations is significantly different. An approach for determining this correction factor was reported by Rogers and Peacock (October 1973) and is shown in Figure 3.

Sunlight entering the atmosphere at an angle Z, as shown in Figure 3, is scattered at altitude h in the direction of the observer at point 0. The energy available for scattering depends on the atmospheric extinction coefficient, $\tau_{\infty h}$, measured from outside the atmosphere to altitude h. The attenuation is given by $\exp(-\tau_{\infty h} \cdot m)$. The energy scattered is a function of the scattering coefficient, α_h, at altitude h. Thus, the energy scattered in the direction of the observer from altitude h is proportional to

$$\exp(-\tau_{h\infty} \cdot m) \cdot \alpha_h. \qquad (11)$$

The average attenuation, for all altitudes, before the energy is scattered to the observer is given by

$$T = \frac{\sum_N \exp(-\tau_{h\infty}, \cdot m) \cdot \alpha_h}{N \sum_N \alpha_h}, \qquad (12)$$

in which N defines each atmospheric altitude used in the summation. Use of the value α_h in the equation expresses the importance of each altitude, h, in contributing energy at the observer location point, 0. A normalizing factor is included in the denominator. Values of $\tau_{h\infty}$ and α_h have been tabulated (Valley, 1965). To adjust $\tau_{\infty h}$ from a standard atmosphere to the actual atmospheric conditions at the observer's location, $\tau_{\infty h}$ is multiplied by $\exp(-\tau_{\infty o})/\tau$, in which τ is the measured atmospheric transmission and $\tau_{\infty o}$ is the extinction coefficient for a beam traversing one atmospheric air mass of a standard atmosphere. This is also given by Valley (1965). Variations in T are small, so the error in using a corrected standard rather than a real atmosphere is small.

Thus, a complete formula which gives the sky radiance, L_A, at the time of the ERTS overpass from L_{MEAS} made at another solar zenith angle and air mass is:

$$L_A = L_{MEAS}(\phi) \left[\frac{1 - \tau}{1 - \tau^{m_o}}\right] \frac{T_{ERTS}}{T_Z}, \qquad (13)$$

in which ϕ, the scattering angle to the observer, equals the scattering angle to ERTS, and T_{ERTS} and T_Z are given by Equation 12 for the zenith angles at the time of the ERTS overpass and the time of the L_{MEAS} readings.

The validity of this equation is demonstrated in Figures 4 and 5. Figure 4 shows ground-based sky radiance measurements as a function of the scattering angle for a range of solar air masses. Each of the curves was obtained by pointing the RPMI at the sun and then sweeping it in azimuth and in elevation, taking sky radiance readings at 10° intervals. Alongside each curve, the solar air mass at the time of the observations is given. The curve defined by the open squares, which falls steeply, is for a range of solar air masses, and was produced by recording the zenith sky radiance over a period of several hours. Application of Equation 13 to these data in Figure 4, assuming $T_{ERTS} = 1$, gives the results shown in Figure 5. Except for about ± 5% of scatter, all the points now follow the same line. By selecting L_A from the curve at the scattering angle which exists at the time of ERTS overpass and multiplying this value by T_{ERTS}, the desired value of L_A at the time of the ERTS overpass is determined.

For March, the path radiance was found to be equivalent to that produced by a target having a reflectance of 11% in Band 4, 5% in Band 5, 3% in Band 6, and 1% in Band 7. This radiance error, which varies as shown in Figure 5, is a function of scattering angle (sun angle), to some degree beam transmittance, and average surface reflectance.

GENERATION OF IMAGERY AND DATA CORRECTED FOR ATMOSPHERE

Different approaches for deriving target reflectance from ERTS data are being investigated. The approach that leads to the most accurate reflectance values is the application of Equation 4 and the full set of solar and atmospheric parameters (L_A, H_o, τ, and H_{SKY}). The 27 March 1973 ERTS tape was processed in this manner to produce the color-coded imagery and gray-scaled computer printout of a portion of the ERTS scene shown in Figures 6 and 7. In this case, the color on the TV monitor and the symbol on the computer print-out is directly related to target reflectance. The scenes shown are those of Orchard Lake. The lake is approximately 2.4 km (1.5 miles) on a side and the scene is approximately 4.8 km (3 miles) on a side.

To obtain average reflectance and other statistical information (i.e., average counts, average radiance, standard deviations, etc.) on specific target areas, such as the deep water in Orchard Lake, etc., the gray-scale printout is used as a map to establish the coordinates of the target, using scan-line count and resolution element numbers. These coordinates, input to the computer, define data areas (edits) where the desired statistical computations are performed. Results of computations of average reflectance on deep water areas of six lakes established lake reflectance to be from 3 to 5.5% in Band 4, 0 to 2.3% in Band 5, 0 to 0.5% in Band 6, and 0 to 0.37% in Band 7. Spot reflectance measurements on the same lakes with the RPMI showed similar results.

SUMMARY

Feasibility of the techniques for obtaining and using atmosphere parameters to transform spacecraft data into absolute target reflectance characteristics has been established. The RPMI's wide dynamic range (1×10^6) was found to be essential for obtaining the full set of measurements needed to derive atmospheric parameters.

The field measurements from January through June of 1973 determined the magnitude and range of variations in the beam transmittance, τ, and path radiance, L_A, within the ERTS bands.

REFERENCES

S. Q. Duntley, J. I. Gordon, and J. L. Harris; Applied Optics; June 1973; "Measuring Earth-to-Space Contrast Transmittance from Ground Stations"; pgs 1317-1324.

ERTS Data User Handbook; NASA Document 71SD4249; Revised Sept 1972; pg G-14.

R. H. Rogers and K. Peacock; "Investigation of Techniques for Correcting ERTS Data for Solar and Atmospheric Effects"; NASA-CR-131258, E73-10458; April 1973.

M. P. Thekaekara et al.; NASA Document SP-8005; Revised May 1971.

S. L. Valley, Editor; Handbook of Geophysics and Space Environments; AFCRL; 1965; pgs 7-14 to 7-35.

R. Rogers and K. Peacock; "Machine Processing of ERTS and Ground Truth Data"; Proceedings of Purdue LARS Conference on Machine Processing of Remotely Sensed Data; IEEE Catalog No. 73 CHO 834-26E; pgs 4a-14; Oct 1973.

Table 1. Solar Irradiance Outside Atmosphere, H_o (1AU)

MSS Band	RPMI mW/cm^2	Thekaekara mW/cm^2
4	18.65	17.7
5	15.11	15.15
6	12.33	12.37
7	25.17	24.88

Table 2. Beam Transmittance, τ

MSS Band	Average	Minimum	Maximum	Standard Deviation
4	0.799	0.697	0.856	0.051
5	0.852	0.770	0.901	0.048
6	0.885	0.812	0.940	0.051
7	0.899	0.843	0.975	0.052

Table 3. Atmospheric Parameters

Atmosphere	Date	Air Mass, M	Beam Transmittance, τ				Path Radiance L_A mw/cm^2-sr			
			4	5	6	7	4	5	6	7
A1	9 Feb 1973	2.5	0.856	0.901	0.940	0.975	0.27	0.146	0.093	0.1185
A2	27 Mar 1973	1.49	0.796	0.854	0.884	0.888	0.268	0.127	0.081	0.103
A3	14 Apr 1973	1.33	0.74	0.815	0.875	0.889	0.26	0.165	0.108	0.059
A4	21 May 1973	1.18	0.697	0.770	0.812	0.843	0.4	0.189	0.121	0.154

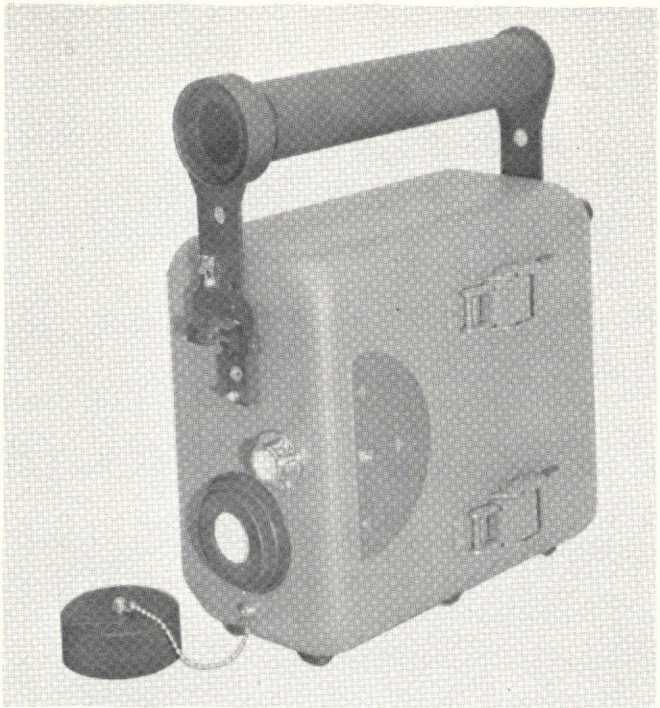

A. RPMI assembled.

B. Global Irradiance (H) – 2π steradian field of view for measuring downwelling (incident) radiation ERTS MSS bands. Bubble level aids this measurement.

Sky Irradiance (H_{SKY}) – Block sun to measure global irradiance minus direct sun component, in every ERTS MSS band. Angle from zenith to sun is also measured in this mode by reading sun's shadow cast on sun dial.

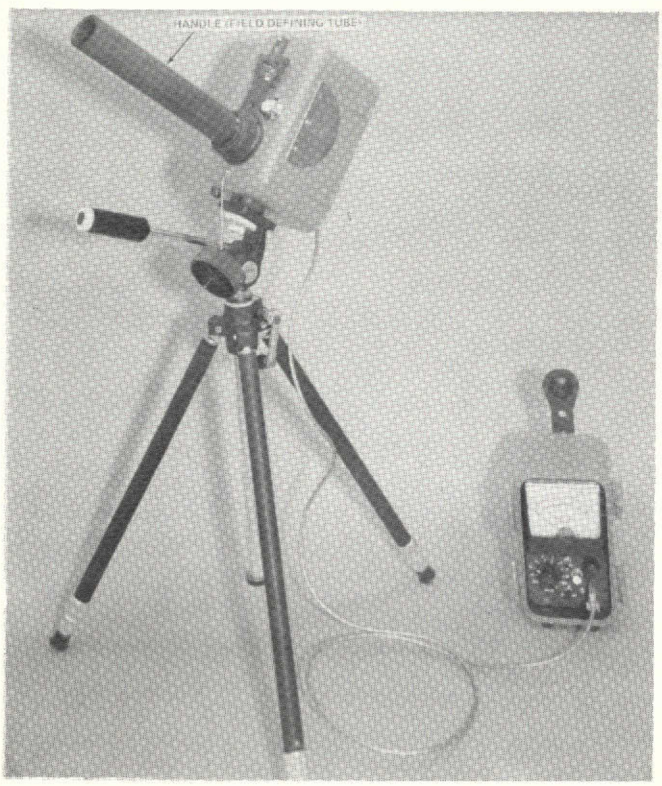

C. Radiance from Narrow Solid Angles of Sky (L_{MEAS}) – Handle serving as field stop permits direct measurements through a 7.0° circular field of view. This mode is also used to measure direct beam solar irradiance, H_{SUN}.

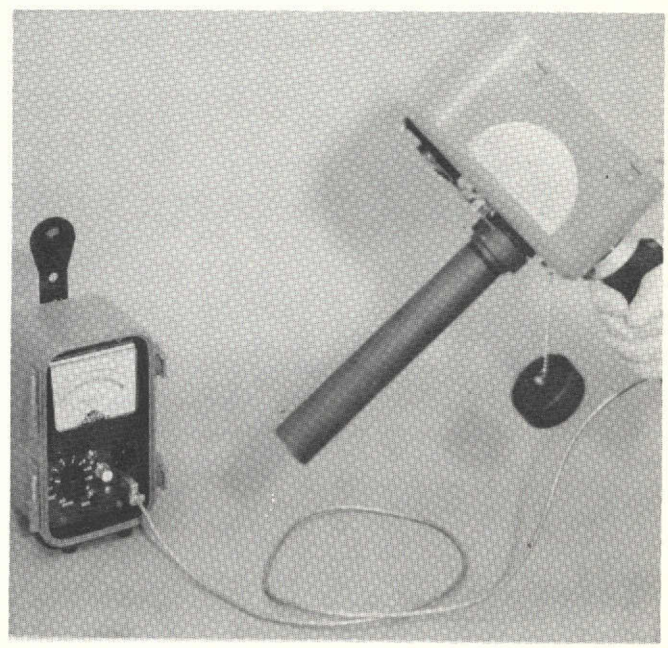

D. Reflected Radiation – Used with small calibration panels and cards to obtain direct measurement of truth site reflectance. Reflectance also immediately derived from ratio of reflected radiance and global irradiance.

11798B-1

Figure 1. Radiant Power Measuring Instrument

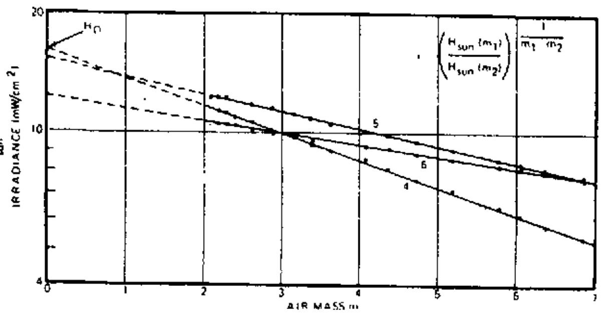

Figure 2. Atmospheric Extinction Curves

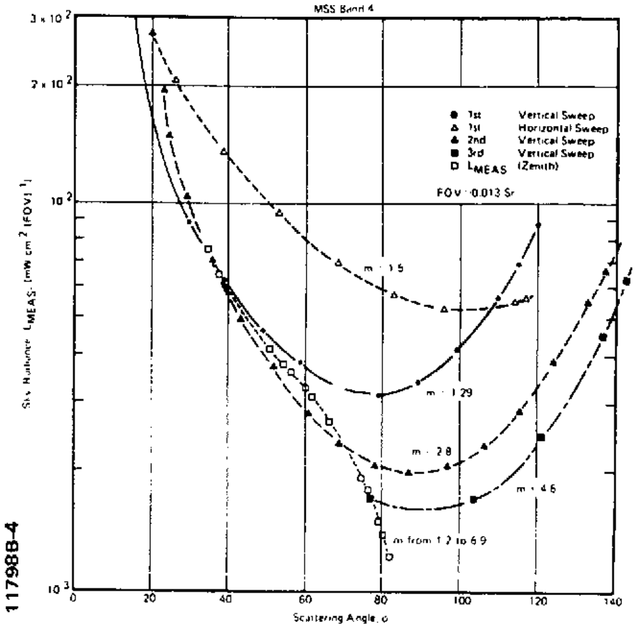

Figure 4. RPMI Sky Radiance Measurements, L_{MEAS}

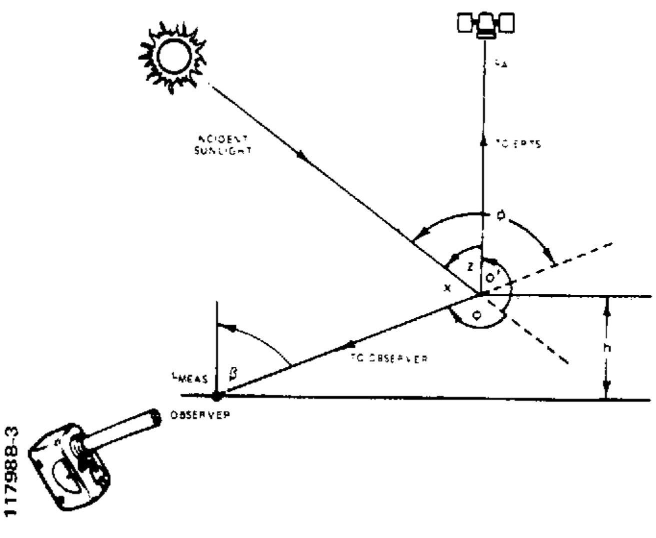

Figure 3. Sky Radiance, L_{MEAS}

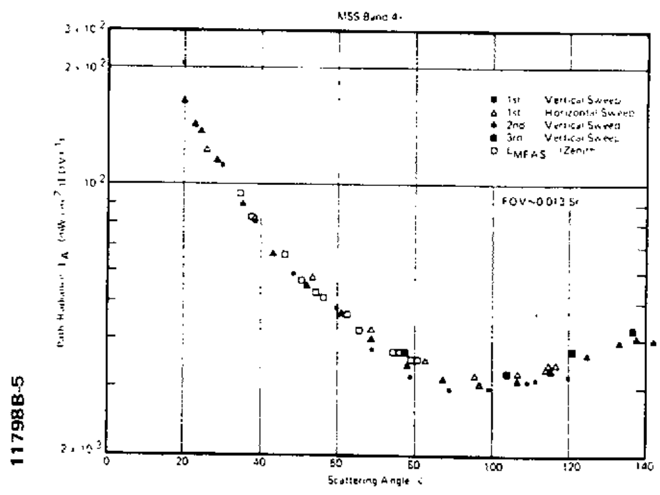

Figure 5. Path Radiance, L_A, from Sky Radiance, L_{MEAS}

ORIGINAL PAGE IS
OF POOR QUALITY

11798B-6

Aerial Photograph

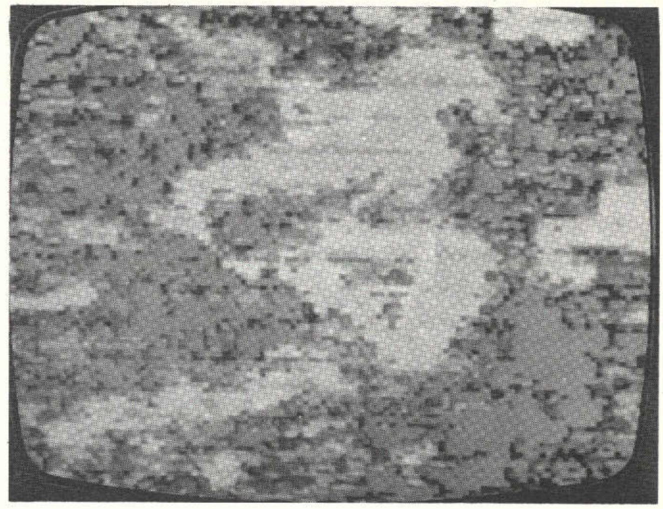

ERTS Band 4 Display

Figure 6. Comparison of Aerial Photograph and Color–Coded TV Reflectance Display

Character	Reflectance Range
	0.000 - 0.006
.	0.010 - 0.014
/	0.018 - 0.027
C	0.031 - 0.035
O	0.039 - 0.047
Q	0.051 - 0.055
Q	0.059 - 0.067
Θ	0.071 - 0.075
B	0.079 - 0.087
Ø	0.091 - 0.095
Ø	0.099 - 0.100

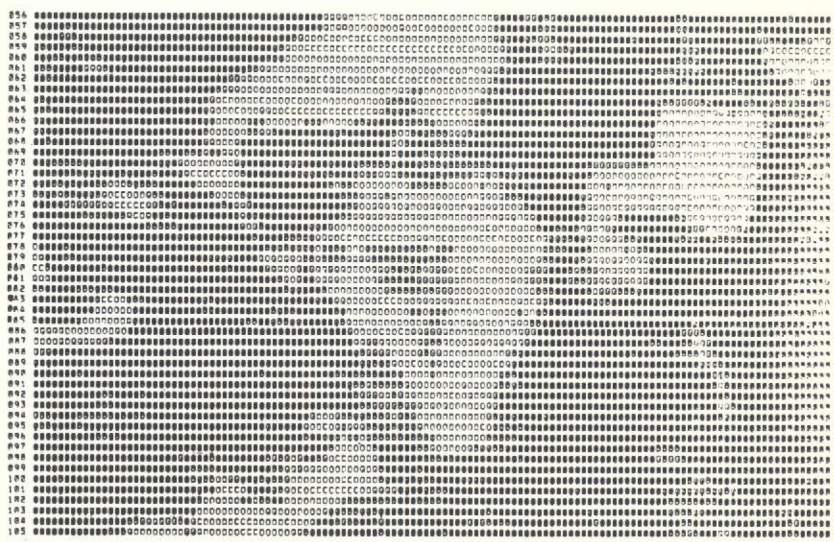

Reflectance Gray Scale Printout
(Band 4)

Figure 7. Reflectance Gray-Scale Printout